DOE/NASA 0336-6
NASA CR - 198466
EDR 17625

## Advanced Turbine Technology

# ATTAP



## Applications Project

## Hybrid Vehicle Turbine Engine

# HVTE-TS

## Technology Support

**1993 - 1994 Annual Report**

**Allison Engine Company**
P.O. Box 420
Indianapolis, Indiana 46206-0420

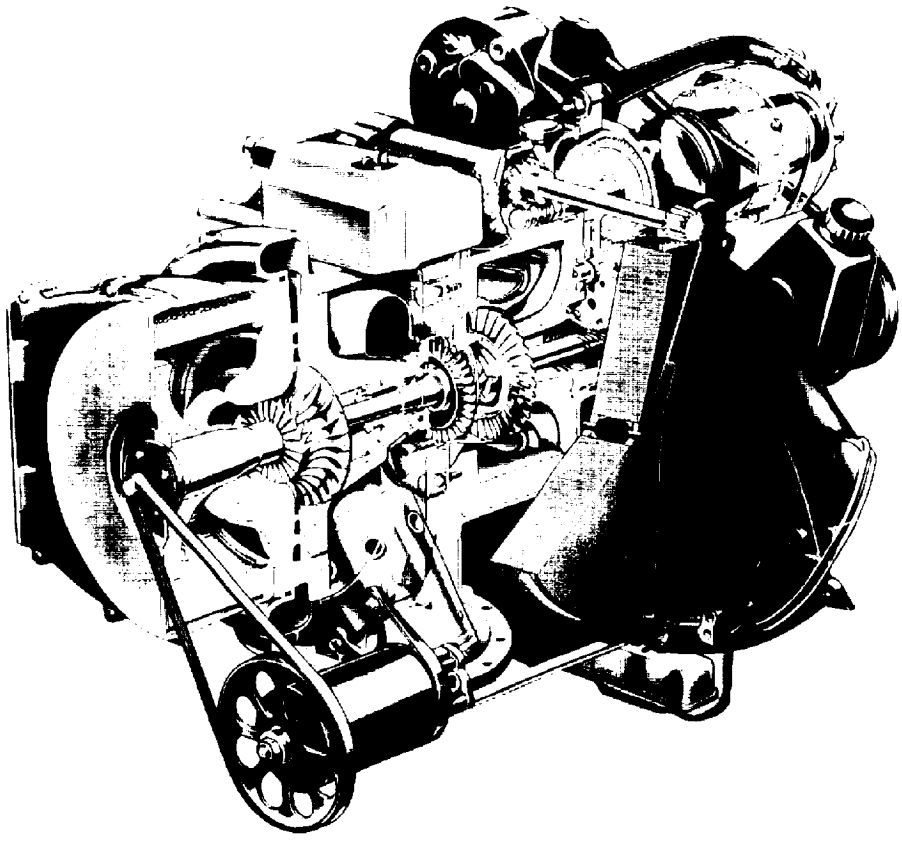

**March 1996**

Prepared for
National Aeronautics
and Space Administration
Lewis Research Center
Cleveland, Ohio 44135
Under Contract DEN 3-336

For U.S. Department of Energy
Conservation and Renewable Energy
Office of Vehicle and Engine R&D
Washington, D.C. 20545
Under Interagency Agreement DE-AI01-90CE50300

## NOTICE

# FOREWORD

This report presents a summary of technical work accomplished on the Advanced Turbine Technology Applications Project (ATTAP) for calendar year 1993 and for the Hybrid Vehicle Turbine Engine — Technology Support (HVTE-TS) Project during calendar year 1994. Work was performed under National Aeronautics and Space Administration (NASA) contract DEN3-336 for both projects, with the HVTE-TS project being a contract modification of the existing ATTAP to reflect the new thrust of the technology development. The report is arranged per the original work breakdown structure (WBS). Only WBS elements with activity in 1993-1994 are reported herein.

This technology project is funded by the U.S. Department of Energy, Conservation and Renewable Energy, Office of Transportation Technologies, Propulsion Systems, Advanced Propulsion Division. Project management and technical direction are provided by the NASA Lewis Research Center (LeRC), Aeronautics Directorate, Propulsion Systems Division, Advanced Propulsion Applications Office.

The overall intent of the ATTAP is to bring the automotive gas turbine engine to a technology state at which industry can make commercialization decisions. Key to this goal is the development and demonstration of structural ceramic component technology as the critical high risk/high payoff element in this type of engine, and such ceramic technology is the prime focus. Automotive gas turbine attractions include the following potential advantages:

- significantly increased fuel economy
- ability to meet Federal emission standards with untreated exhaust
- ability to operate on a wide range of alternate fuels
- inherently smooth, low vibration operation

Allison Engine Company (Allison) addressed the ATTAP, and continues with the HVTE-TS with a team drawing upon:

- Allison's extensive ceramic design, analysis, and materials data base and expertise
- previous activities with General Motors Corporation (GM):
  - substantial experience, design, and test capabilities
  - automotive gas turbine technology and hardware
  - test vehicle resources
- the infrastructure of expertise and resources in place in the American ceramics industry
- the working relationships between the ceramic industry and Allison
- the unique capabilities and resources at universities and national laboratories, such as:
  - High Temperature Materials Laboratory (HTML) at Oak Ridge National Laboratory (ORNL)

In this arrangement, Allison serves as prime contractor. Major ceramics industry development subcontractors during 1993-1994 included Schuller International; Corning, Inc.; AlliedSignal Ceramic Components (ASCC); Ceramics Process Systems (CPS); Norton Advanced Ceramics (NAC); and Kyocera Industrial Ceramics Corporation.

## TABLE OF CONTENTS

## TABLE OF CONTENTS (cont)

## LIST OF ILLUSTRATIONS

## LIST OF ILLUSTRATIONS (cont)

## LIST OF ILLUSTRATIONS (cont)

## LIST OF TABLES

## SUMMARY


ATTAP/HVTE-TS activities during 1993 and 1994 included the redirection of technology development focus; the relocation of project assets from the GM Tech Center to Allison; test-bed engine design and development; ceramic component design; materials and component characterization; ceramic component development and fabrication; ceramic component rig testing; and test-bed engine fabrication and testing.

The ATTAP technology focus was redirected and broadened to include key technologies needed for advanced gas turbine electric generator sets such as those under development in the Hybrid Vehicle Propulsion System Program (Hybrid). The application of the technology was redirected from a prime power role to a hybrid propulsion system role, where the turbine power plant drives a high speed alternator for electrical power generation. Within this time frame, the Allison Gas Turbine Division of GM was sold, becoming the Allison Engine Company. Concurrently, GM automotive gas turbine assets were transferred to Allison Engine Company and relocated from the General Motors Technical Center (GM Tech Center) in Warren, MI to Allison in Indianapolis, IN.

Test-bed engine design and development continued with the analysis of and design modifications to the poppet valve premixing combustor. The need for the design modifications, identified through previous testing, was undertaken to correct overheating of the combustor from impingement of hot gas flow. Additional work was also accomplished in the area of control logic for the poppet valve combustor.

Ceramic and associated ceramic/metal component design activities included a continuing effort to design a gasifier turbine rotor to meet the requirements for performance, mechanical strength, reliability, and dimensional accuracy.

Allison materials characterization efforts have yielded additional information on two material systems: Norton Advanced Ceramics' NT230 siliconized SiC and Ceramics Process Systems' SRS201 Sialon. Gasifier turbine rotors were used in the component characterization of the CPS material. Analysis of failures in other components yielded data on Norton NT154, Norton NT164, Norton NT230, and Kyocera SN252 material systems.

Ceramic component process development and fabrication continued with several ceramic component subcontractors, including Schuller International, for insulation systems and processes; Corning, Incorporated, for extruded regenerator materials and processes; and several suppliers of structural ceramics components, such as AlliedSignal Ceramic Components, Ceramics Process Systems, and Norton Advanced Ceramics. Toward the end of this reporting period, Kyocera was also identified as a potential source of structural ceramics and was contracted to begin work in the development program.

Component rig activities were focused on transferring the component testing capability from the GM Tech Center. The activities consisted of two major efforts. Efforts were first, the movement of the test rigs to Indianapolis, and second, the establishment of the test capability within the available facilities at Allison. Construction of test cell facilities, providing the necessary control systems and instrumentation, providing the necessary safety equipment, and installing the necessary support systems for air, cooling, exhaust, and fuel proved to be a major undertaking during the period. Installation was begun, or plans were made, for the combustor rig, the hot gasifier rig, the regenerator disk performance rig, the regenerator transient durability rig, and the regenerator cold flow seal leakage rig.

Test-bed engine fabrication, testing, and development activities continued to verify improvements in ceramic component technology permiting the achievement of both program performance and durability goals. Several engines, dynamometers, and a variety of component parts were also moved from the GM Tech Center to Allison, and fabrication of a test cell for the AGT-5 engine was begun.

Engine and hot rig test hours were accumulated in 1993-1994 as summarized in Table I below.


*Table I.*
*Total test hours.*

| | Pre-1993 | 1993-1994 | Cumulative |
|---|---|---|---|
| Engine hours | 1867 | 241 | 2108 |
| Hot rig hours | 2023 | 362 | 2385 |
| Total hours | 3890 | 603 | 4493 |

## INTRODUCTION

This is the sixth of a series of reports documenting work performed on the ATTAP/HVTE-TS. This is a combined report to cover work performed in both 1993 and 1994. Work in 1993 was conducted by a team directed by Allison, with significant activities at both the then Allison Gas Turbine Division in Indianapolis and at GM's Advanced Engineering Staff (AES) at the GM Technical Center, as well as at the several domestic suppliers who are under development subcontracts. Work in 1994, because of GM's divestiture of the Allison Gas Turbine Division, was directed and performed by the new Allison Engine Company using the same domestic ceramic suppliers as in the preceding efforts. The U. S. Department of Energy (DoE) sponsored the work, which was managed and technically directed by NASA-Lewis Research Center under contract DEN3-336.

## GOALS AND OBJECTIVES

ATTAP was intended to advance the technological readiness of an automotive ceramic gas turbine engine. ATTAP aimed to develop and demonstrate structural ceramics having the potential for competitive automotive engine life cycle cost and for operating for 3500 hours (automotive engine life) in a turbine engine environment at temperatures up to 1371°C (2500°F). Project objectives were the following:

- enhance the development of analytical tools for ceramic component design using the evolving ceramic properties data base
- establish improved processes for fabricating advanced ceramic components
- develop improved procedures for testing ceramic components
- evaluate ceramic component reliability and durability in an engine environment

In the continuing program in 1994, objectives of the HVTE-TS program are the same as those of the ATTAP, with additional focus as follows:

- develop four key technologies to a level so a commercialization decision can be made on:
  - structural ceramic materials and processes
  - low emissions combustion systems
  - regenerators and seal systems
  - insulation systems and processes
- to make this technology applicable to the automotive gas turbine engines that form the basis of hybrid automotive propulsion systems consisting of combined batteries, electric drives, and on-board power generators

The relationship of the HVTE-TS project to the Hybrid Electric Vehicle (HEV) project is graphically depicted in Figure 1. Both the HEV and HVTE-TS projects draw upon the significant technology base established by ATTAP. As the key technologies are developed, the results of the technologies in materials, components, and manufacturing processes will be incorporated into the hybrid projects at various milestone stages of the program. Ultimately, the Hybrid program, with the support from HVTE-TS, will lead to a solid basis for a commercialization decision within a reasonable time frame.

## PROGRAM SCHEDULE AND CONTENT

Figure 2 shows the scheduled activities in the ATTAP. Materials assessment occurred at the initiation of ATTAP and resulted in the targeting of ceramic component technology goals and the identification of materials, processes, and manufacturers to address those goals. The materials assessment was updated in Year 3 and again in Year 5, at which time the state of the art was reassessed for each component and required technology improvements were defined. The identification and evaluation of materials, processes, and manufacturers were ongoing, continuous activities in ATTAP, and promising candidates were integrated into the program as merited. Similarly, those technologies and/or ceramic component suppliers that did not productively evolve to address program goals were deleted from the ATTAP effort. A similar approach is being continued with the HVTE-TS program, as shown in Figure 3.

Looking forward, the HVTE-TS program phases are matched to the various generations of Hybrid engines as they evolve in that program. Additional emphasis is being placed upon development of alternate suppliers for components, systems, and manufacturing processes to attain automotive volumes.

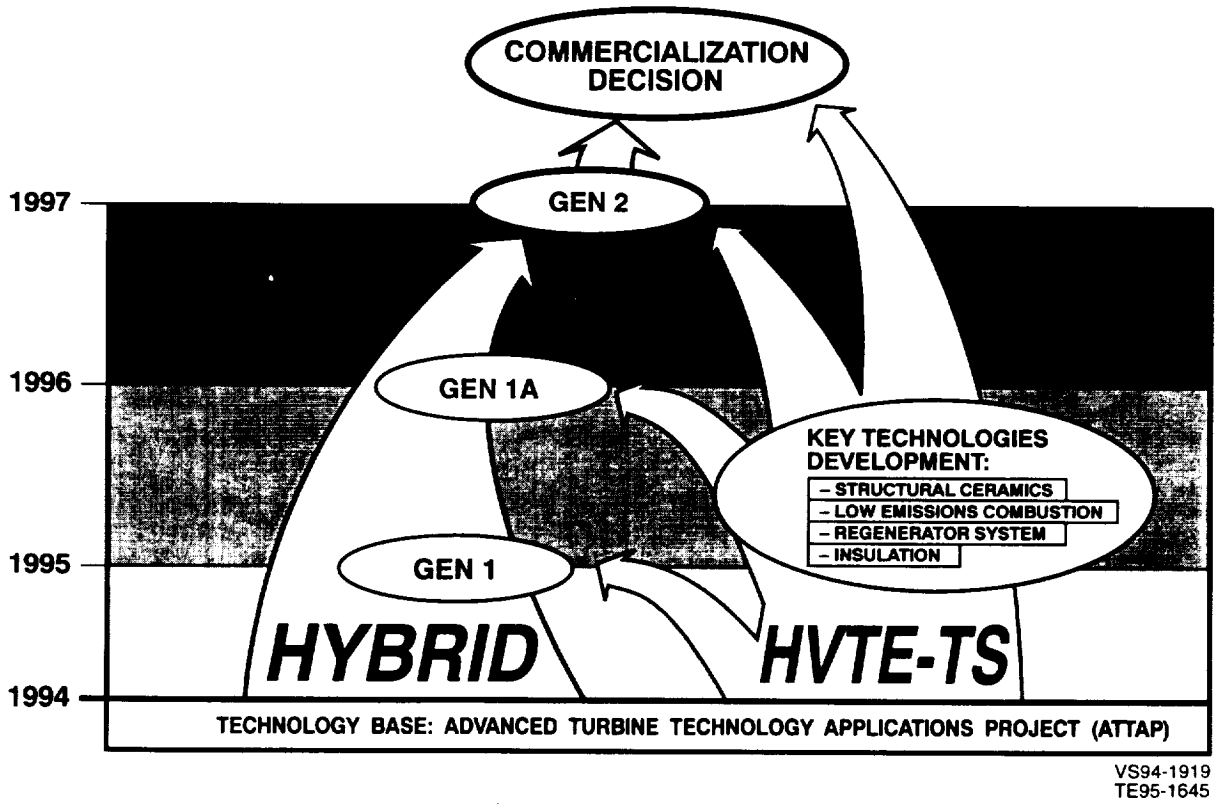


*Figure 1. HVTE-TS relationship to Hybrid turbine APU development.*

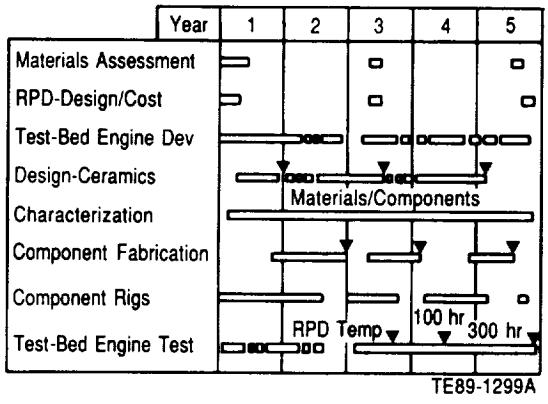


*Figure 2. ATTAP schedule.*

A reference powertrain design (RPD) was established during the ATTAP and included preliminary design of a powertrain system to meet performance, cost, and reliability design goals. The RPD, as revised through the ATTAP, reflects current ceramic technology and goals, and is being carried through the HVTE-TS program. The initial Hybrid engines will operate at somewhat lower temperatures than the original RPD goals; however, for this technology program, it was decided to continue development with the original 1371°C (2500°F) turbine inlet temperature (TIT) goals. This will provide growth margins for future Hybrid configurations.

Test-bed engine development, shown as an intermittent activity during ATTAP, included efforts aimed at ensuring the availability and functionality of the AGT-5 gas turbine engine as the test-bed for the high temperature ceramic components. Engine development was not a primary focus of ATTAP, but those activities recognized the need to continue the evolution of the engine in order to handle additional power and thermal loads. The AGT-5 engine also served as a test-bed for design changes resulting from the integration of high temperature flow paths. The engine will continue to be used in this role in the HVTE-TS program.

Central to the logic of Allison's approach to ATTAP/HVTE-TS is the iterative component development cycle. The cycle, as illustrated in Figure 4, includes the design/fabrication/ characterization/rig test/engine test sequence of activities. The development cycle reflects the anticipated improvements in ceramic materials and associated component processing technologies and the incorporation of laboratory

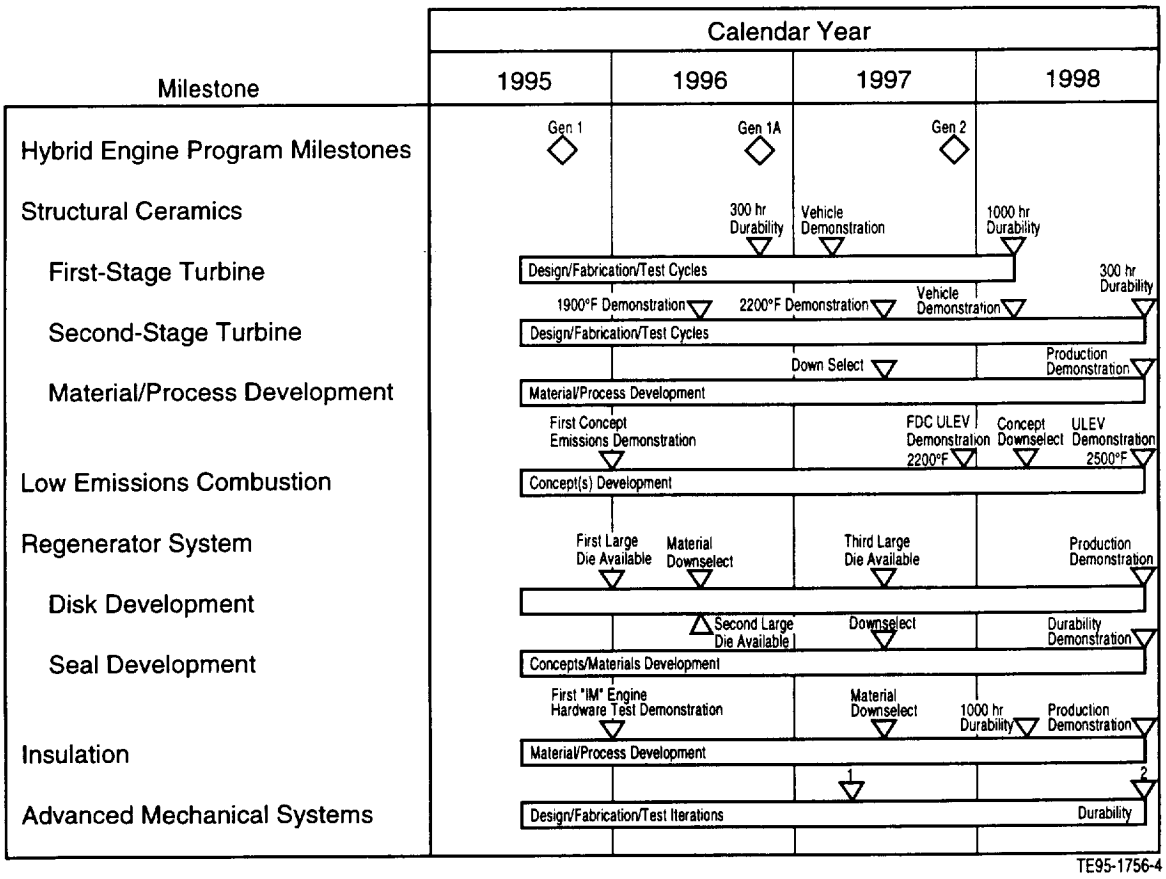


*Figure 3. HVTE-TS schedule (time phased to Hybrid program objectives).*

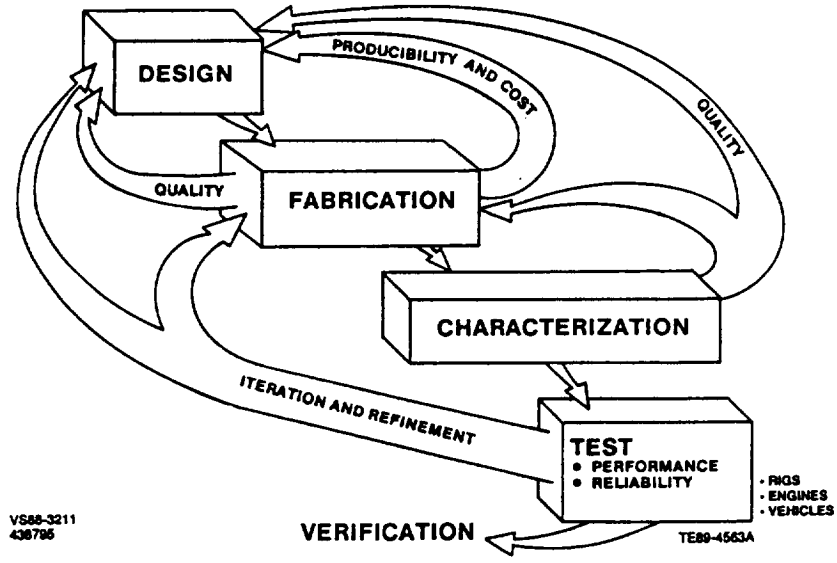


*Figure 4. Ceramic component development cycle.*

characterization data and rig/engine test results into succeeding designs.

The initial design activity featured the then-current monolithic ceramic technology in the design of the gasifier turbine stage of the AGT-5 engine for 1371°C (2500°F) TIT plus other required hot flow-path pieces. The second design phase incorporated toughened monolithic materials, used in the same gasifier stage components. The third phase incorporated advanced (e.g., from ORNL's Ceramic Technology for Advanced Heat Engines [CTAHE] project) materials and processes as they became available. Succeeding design phases include other necessary ceramic components in the high-temperature test-bed engine, notably power turbine flow-path pieces. Additionally, as new material systems are developed at major ceramic suppliers, and manufacturing techniques and processes are developed, components from these programs will be incorporated into the design cycle as part of the HVTE-TS program, ultimately yielding component capability and process validation that can be transferred to application in Hybrid program components.

Component fabrication includes those process development activities by ceramic suppliers resulting in the fabrication of engine-usable components. Characterization involves the laboratory activities, at both Allison and outside suppliers, that measure and define the various properties and qualities of ceramic materials in either test bar form or in actual components. Examples are microstructural evaluation and measurements of density, strength, oxidation resistance, toughness, etc. Included are the development and application of nondestructive evaluation (NDE) techniques.

Component rig activities include the development of rigs for component verification and testing (e.g., hot gasifier turbine rigs) as well as the actual testing activities. Test-bed engine testing includes the test activities associated with test-bed engine development plus the verification and development testing of the ceramic components. Each component development cycle (Figure 4) begins with design, followed by component fabrication, characterization, rig testing, and finally engine testing. The rigorous development process is iterative between the users and the ceramic supplier community, and ensures developing an understanding of the behavior of components in service and in continuous identification of areas for improvement.

## TEST-BED ENGINE

Figure 5 shows the automotive gas turbine engine being used as the ceramic component development test-bed for ATTAP/HVTE-TS. This GM-developed engine, the AGT-5, is a two-shaft, regenerative configuration with axial-flow gasifier and power turbines. The engine produces approximately 110 horsepower (hp) at its original full-power TIT of 1038°C (1900°F).

The emissions and alternate fuels goals are considered achievable based on demonstrated GM experience. For example, the AGT100 engine's (from the AGT project) combustion system has displayed laboratory steady-state emissions of oxides of nitrogen ($NO_X$), carbon monoxide (CO), and unburned hydrocarbons (UHC) well within the Federal Emissions Standards using diesel fuel, jet fuel, and methanol. Although such systems have demonstrated the potential for low emission/alternate fuel gas turbine combustion, much work remains before achieving a fully-functional system suitable for automotive applications. Such efforts were originally outside the scope of ATTAP, but the development of components, processes, and technologies in the HVTE-TS program will be incorporated into engines expected to be applied to the Hybrid program.

## FOUR KEY TECHNOLOGIES

During the ATTAP, emphasis was placed upon ceramic component technology as develop-

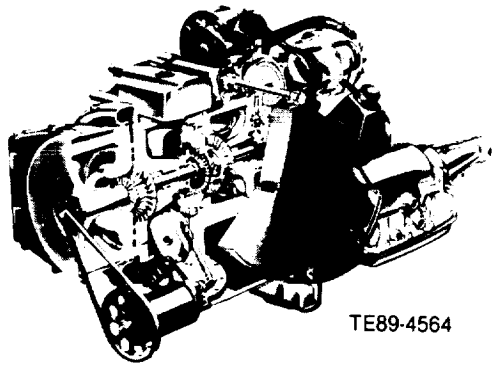


*Figure 5. ATTAP/HVTE-TS test-bed engine — AGT-5.*

ment/demonstration targets. The critical development components were selected because their functional success was critical to the viability of the ceramic automotive turbine engine, and each required further technological development to be reliable, durable, and cost effective in the automotive engine. The components included:

- gasifier turbine rotor
- gasifier turbine vanes
- gasifier turbine scroll
- regenerator disks
- thermal insulation

With the new thrust of the HVTE-TS project to support of the Hybrid Propulsion System, the project is now structured to develop critical technologies to support a production feasibility demonstration in four years. The technology requirements of an advanced turbine driven on-board generator unit is dependent upon (Figure 6):

- structural ceramic materials and processes
- low emissions combustion systems
- regenerators and seal systems
- insulation systems and processes

Development of these four key technologies is based upon the broad range of experience gained during the AGT project and the ATTAP, and will be continued through the HVTE-TS program.


VS94-2126
TE95-1646

*Figure 6. Four key technologies.*

# I. ENGINE/POWERTRAIN DESIGN AND DEVELOPMENT, ANALYSIS, AND MATERIALS ASSESSMENT

## 1.4 TEST-BED ENGINE DESIGN AND DEVELOPMENT

### 1.4.1.2 Mechanical Design - Regenerator Seals

Two major requirements, cost and performance, drove the design of the regenerator. A critical aspect of the regenerator system is the design of the sealing system. The seal system consists of the primary seal directly contacting the rotating disk and a secondary seal bridging between the block or cover and the primary seal platform. The secondary seal allows the primary seal to move axially to compensate for wear, disk out-of-flatness, or misalignment. All parts of the seal system must function properly together as a system in order to provide effective regenerator seals, and thus have good overall engine performance. Leakage through the regenerator seals is a particularly strong performance driver because these leaks are essentially losses directly overboard from compressor discharge.

The secondary seal can be designed in one of three basic configurations. As shown in Figure 1.4.1-1, the leaf attached to the primary seal platform is the "attached leaf" design. The leaf attached to the block or cover is the "reverse leaf" design. A third approach is the secondary L-seal. This type of seal demonstrated substantially lower leakage than the reversed leaf. This seal slides in a groove in the cover or block, and is not rigidly attached to either member. The three different seal designs are presented schematically in Figure 1.4.1-1. The L-seal design reduced seal system part count by approximately 87% relative to the reversed leaf design. It is substantially lower in cost than either alternative as well. For these reasons, the L-seal was adapted as the baseline secondary seal for engine design and development.

Corners and joints are always difficult to seal, and the L-seal provides no exception. A straight cross arm, offset from the disk diameter can be used. By accommodating the difference in mass flows between the air and exhaust sides of the

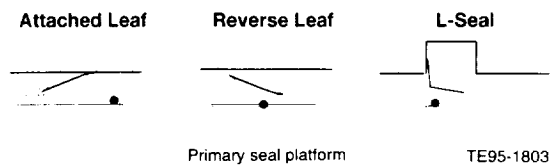


*Figure 1.4.1-1. A secondary L-seal was selected for the engine regenerator development based on good results at General Motors - Advanced Engineering.*

regenerator through adjusting area ratios, a slight performance gain is realized. The disadvantage of this approach is that with a straight cross arm, the seal rim segments, air, and exhaust sides are not symmetric. This problem can be addressed by using a boomerang-shaped cross arm. This provides both the proper area ratio and allows the rim segments to be symmetric. Unfortunately, this also increases the complexity of the cross arm and has the further disadvantage of requiring an additional corner in the L-seal and possibly an extra joint as well.

**1.4.1.2.1 Seal System Design.** Leakage flow across the seal cross arm consists of a differential pressure term, from air side to exhaust side, and a physical transport term caused by the disk rotation. This gives rise to vastly different seal pressure loads as the cross arm is traversed from end to end. This effect has been known for many years, and in fact an analytical treatment is available in technical literature. These loads can be managed by providing grooves in the cross arm to either load or unload particular regions of the cross arm. By changing grooving and secondary seal location it is possible to maintain a fairly uniform loading from end to end. The possible exceptions are the hub area and the location where the cross arm and rim join. In addition to simple force balance, it is also desirable to maintain a moment balance on the cross arm.

The combination of requirements still allows for a large set of potential solutions. It is not possible to evaluate them all, particularly when several different operating conditions and several different regenerator sizes must be considered. It was noted, however, this was a classic optimization problem. Allison developed a computer code, derived from methodology in the technical literature, that would determine optimum L-seal location based on a set of input conditions and

constraints. For example, a given set of operating conditions and cross arm physical shapes are input into the program. Variables considered for optimization must include the constraints, e.g., constraints on the L-seals must be confined to certain areas on the cross arm, must be straight, must be a certain distance apart, must maintain either both force and moment balance or just force or just moment, must maintain a certain average loading, etc. These constraints could be applied either individually or in any combination. The code would perform the analysis and provide as an output both the location of the secondary L-seals and the required groove pattern to meet the constraints, if possible.

The code made it possible to conduct an extensive optimization of the L-seal/regenerator system. The result of all this analysis was a straight 1-inch wide cross arm centered on the hub. Note the small performance gain allowed by providing optimum area ratio was traded away in favor of a simple symmetric seal design in order to gain lower manufacturing cost.

The detailed process is not required for the rim sections of the seal; therefore, only the differential pressure term is active. This leads to one pressure distribution operative everywhere around the rim, with the possible exception of the cross arm-rims joint. Optimization consists primarily of finding a secondary seal location yielding good loading at all differential pressure conditions.

An extensive series of optimization experiments yielded the final physical dimensions of the L-seals. The one area judged to be deficient in the design was the spring elements, which used a helically wound metal strip as a spring device to energize the L-seal/seal platform, and in order for this type of spring to deflect, it must move axially. Friction prevents this motion, so the spring was effectively coil bound. Additionally, this type spring cannot provide axial travel to allow for sufficient wear of the seal platform.

**1.4.1.2.2 Springs.** In order for the seal system to work properly, it must be preloaded axially to ensure the sealing surfaces remain in contact with the regenerator disk. With the reversed or attached leaf designs, this function can be provided by the secondary seals themselves. The L-seal requires another member, however, that loads the L simultaneously against both the seal platform and the inside of the seal groove. This flexible element must be able to apply a uniform load along the entire L and should be able to provide a nearly constant force over the full required axial travel range. Allison designed several alternative approaches:

- a finger spring minimizing the action of the attached or reversed leaf design
- a continuous canted coil spring
- a spring platform using a combination of leaf and helical springs to load the seals

Stress calculations performed on the L-seals indicated they were capable of approximately 0.075 inches of axial travel before the stress in the corner became too high. All of the listed springs were capable of providing at least this level of deflection. The spring platform idea was judged to be too expensive relative to the others, and did not proceed past the preliminary design stage.

The finger springs are shown in Figure 1.4.1-2. The concept is simple. The spring was designed to be slightly wider than the seal groove. In combination with the loop on the end of each finger, the L-seal would impart a radial preload against the seal groove. Axial compression would simultaneously provide an axial preload. The fingers were 0.1 in. wide on a 0.25 in. pitch, allowing the springs to be interlaced down the hot cross arm to activate both L-seals. The springs can also be easily bent into an arc to accommodate the D-shape of the L-seal. It was recognized from the start that these springs might be difficult to manufacture and install. On the other hand, they provide the necessary axial travel and preload in both directions.

The canted coil spring was proposed as an alternate design. This is a patented spring design manufactured by Bal Seal, Inc., and the spring and installation are show in Figure 1.4.1-3. Even though it is helically wound, the canted coil spring differs from a conventional helical spring as the shape of the coils is elliptical and each coil is slanted about the ellipse major axis relative to the coil axis. When a radial load is applied to the coil normal to the major axis, the coil slants

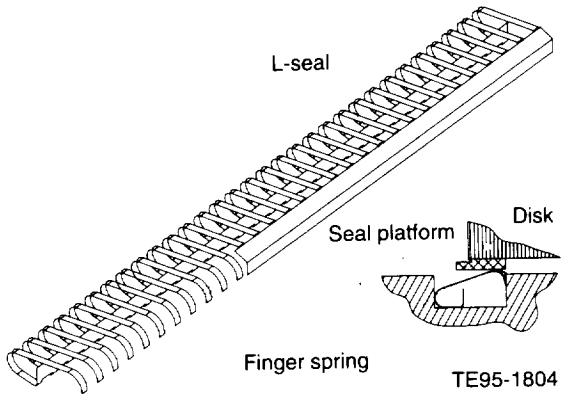


*Figure 1.4.1-2. A finger spring fabricated from sheet metal was designed to act as a helper spring for the L-seal.*

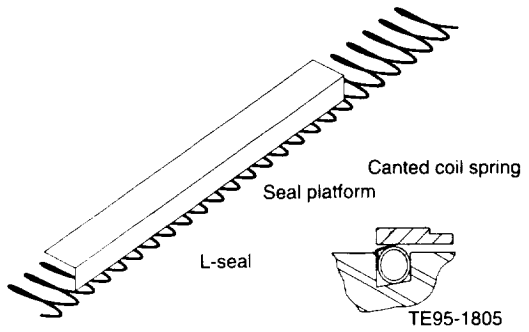


*Figure 1.4.1-3. The unique canted coil spring provides a simple, inexpensive means of providing nearly uniform loading to the secondary L-seal.*

over further. There is no need for the coil to move axially, and therefore, the coil bound problem is eliminated. Rather large deflections, up to 45% of the initial spring height, can be accommodated by this spring. This is exceptional and allows an overall compact design. The force deflection curve for the spring is relatively constant over approximately 80% of the usable spring deflection. The coils are more closely spaced than the fingers on the finger springs and the tight spacing provides for nearly uniform loading of the L-seal. The spring, manufactured in long, continuous lengths, is easily installed and can be manufactured in a variety of high temperature capable materials such as René 41.

**1.4.1.2.3 Materials.** Manufactured carbon-graphite material has been used successfully for the regenerator seal platform rims. It can also be used for the cold side cross arm, but is not suitable for the hot cross arm due to the high temperatures encountered at this location on the engine. The hot cross arm consists of a metal substrate with a plasma-sprayed wear face coating. The coating used is best described as barely adequate at the maximum anticipated running temperatures. In order to produce the required cost reductions and improved performance, other coatings and application processes must be developed.

There have been several other changes in available regenerator seal materials. During the reporting period, suppliers ceased manufacture of the preferred carbon-graphite material. On an experimental basis, carbon-carbon composite material was substituted for carbon-graphite. Higher temperature capable polyimides have become available that may be suitable for use on the regenerator cold side.

The Tribology Division of Argonne National Laboratory was enlisted to expedite the material development aspects of the regenerator seal system. Argonne will characterize the friction and wear properties of various alternative carbon-graphite and some selected carbon-carbon composite materials. The major part of Argonne's work will be identifying alternate materials and fabrication techniques for the hot cross arm. In order to support Argonne in this effort, Allison refurbished and shipped to Argonne a friction and wear test rig. A dead-weighted gimbal mounting fixture loads three 1 in. diameter test buttons against a 6 in. diameter rotating disk. This entire apparatus is contained inside a furnace that allows the disk and test buttons to be heated to typical regenerator cross arm operating temperatures. The test rig has been previously used by Allison to develop nickel oxide/calcium fluoride wear coatings. Argonne will add a state-of-the-art control and data acquisition system to facilitate their work on improved wear face materials.

### 1.4.1.3 Regenerator Drive System

There is no plan to drive the regenerators from development engine turbomachinery directly; therefore, in order to rotate the disks, an auxiliary power source is required. This has the advantage that the regenerator speed can be controlled independently from the engine speed.

Allison has selected a constant rotational speed producing a maximum speed at the rim well within current Allison experience of 100 ft/min. Because the pressure distribution across the regenerator is a function of both disk rotation speed and differential pressure, selection of a constant speed simplifies design of the cross arm by reducing the variation in loading with engine operating condition.

Several options, each approach having its advantages and drawbacks, were considered for the drive system. Two alternatives were considered initially:

- a pinion and ring gear affixed to the outside diameter (OD) of the regenerator disk, driven by an external motor
- a direct electric drive using the regenerator disk as a motor armature.

For the direct electric drive, a switched reluctance motor was proposed, requiring only a magnetically permeable armature mounted on the OD of the disk similar to the ring gear for the gear drive. This approach has the additional advantage, with some additional control capability, of being able to levitate the disk, therefore eliminating the need for a hub in the disk or spindle. Initial cost estimates indicated this approach was very attractive as well. Unfortunately, initial preliminary designs showed the motor was extremely inefficient, operating at only 15% efficiency. A different type motor was required to boost efficiency into the acceptable range greater than 85%. The required development program did not meet the development schedule requirements, so this option was deferred.

The gear drive system has the advantages of proven design and acceptable efficiency. On the other hand, it has more parts. Since both the ring gear and pinion must operate unlubricated at relatively high temperatures, there is the potential for high wear on gear teeth. The current Allison design for the development engines consists of two 12 volt gear motors, one for each regenerator disk. The ring gear is mounted to the regenerator disk using RTV adhesive. Both gear and pinion are made from through-hardened 440C stainless.

Two different gear tooth designs are being developed. The first uses a modified involute geometry while the second has a special cycloidal tooth form. The purpose of the cycloidal design is to reduce sliding during the tooth action in an attempt to reduce wear. Several coatings to provide wear resistance are also being explored. The current version of the regenerator system, drive, seals, etc, is shown in cross section in Figure 1.4.1-4.

1 - L SECONDARY SEAL AND SPRING
2 - PRIMARY SEAL PLATFORM
3 - PINION SHAFT SEAL
4 - PINION SHAFT
5 - RING GEAR
6 - ADAPTOR RING
7 - RTV ADHESIVE BEAD
8 - REGENERATOR DISK

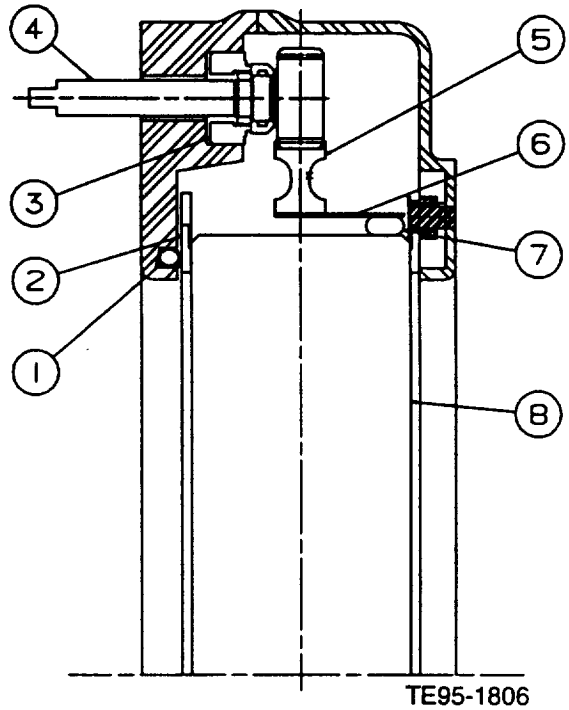


*Figure 1.4.1-4. One potential regenerator system incorporates L-seals and a mechanical pinion and ring gear drive system.*

## 1.4.2 Combustion Systems

Analysis of a design modification to the poppet valve premixing combustor (Figure 1.4.2-1a) was initiated during the reporting period. A need for this modification was identified during poppet valve combustor testing (see Section V). A narrow ring of zirconia thermal barrier coating (TBC) spalled off the combustor inner liner immediately downstream of the valve seat. The thermal barrier bondcoat was exceeding its thermal limit in this region. This was attributed to an increased convective heat transfer coefficient resulting from flow impingement normal to the surface of the inner liner. The fuel/air mixture exiting the fuel preparation zone was attaching to the surface of the valve seat and impinging on the inner liner. Results of flow modeling of this phenomenon are shown in Figure 1.4.2-2a.

A combustor modification called the extended valve seat design (Figure 1.4.2-1b) was proposed to eliminate impingement on the inner liner. This involved changing the contour of the valve seat so flow exited it in a direction nearly parallel to the surface of the inner liner (depicted in Figure 1.4.2-2b); however, heat transfer analysis of the proposed modification indicated a different approach should be taken. Although the metal inner liner would run cooler, the temperature of the ceramic valve seat would increase.

Results of the heat transfer analysis are shown in Figure 1.4.2-3. Axial conduction is the primary means of cooling the valve seat. By extending the length of the valve seat, its downstream end was predicted to run 14°C (26°F) hotter. When the baseline valve seat was tested, beads of silicon exuded to the surface of the part. Rather than modify the combustor in a way that would worsen this condition, it was decided to evaluate a different modification called the enhanced backside cooling design (Figure 1.4.2-1c). In this design, the valve seat is shortened and the flow path between the inner and outer liners is curved inward to increase backside convective cooling of the inner liner. With this arrangement, the valve seat peak temperature will be reduced and flow impingement on the inner liner will not occur. Analysis of this configuration will take place in 1995. The temperature profiles expected with this new design are compared to the original baseline in Figure 1.4.2-3.

## 1.4.4 Engine Systems Integration

*Poppet Valve Control Logic.* In 1993, several tests of the poppet valve low emissions combustor were performed in an AGT-5 engine on a dynamometer stand. These tests are described in Section V of this report. The poppet valve combustor is a variable geometry premixing combustor, so some means was necessary for controlling the axial position of the poppet valve and switching fuel between the start and main fuel nozzles. Positioning of the valve was accomplished semiautomatically by a linear actuator and its associated controller. Positioning was semiautomatic in the sense that the linear actuator controller was not interfaced with the engine control microprocessor. The poppet valve was placed in the idle speed position during a start sequence. Steady-state test points were set by making slow changes to engine speed and valve position. Fuel transfer between the start and main nozzles was accomplished by solenoid valves. Following a start sequence and a short warm-up period, fuel transfer was accomplished by opening the main nozzle solenoid, delaying for one or two seconds, then closing the start nozzle solenoid. Air was used to blow fuel out of the start nozzle and subsequently cool the start nozzle.

In the longer term, variable geometry control and fuel scheduling will be automated and integrated into the engine control to permit transient testing. Variable geometry positions will be selected to maintain constant flame temperature in the reaction zone of the combustor. This is accomplished with an open-loop algorithm that monitors engine air flow, fuel flow, and combustor inlet temperature. A rapidly responding linear actuator with its own controller will deliver a position corresponding to an analog voltage command from the engine control microprocessor. During a start sequence, fuel must be staged between start and main fuel nozzles. When combustor inlet temperature reaches a specified level, the engine controller will transfer fuel in the same sequence as described above.

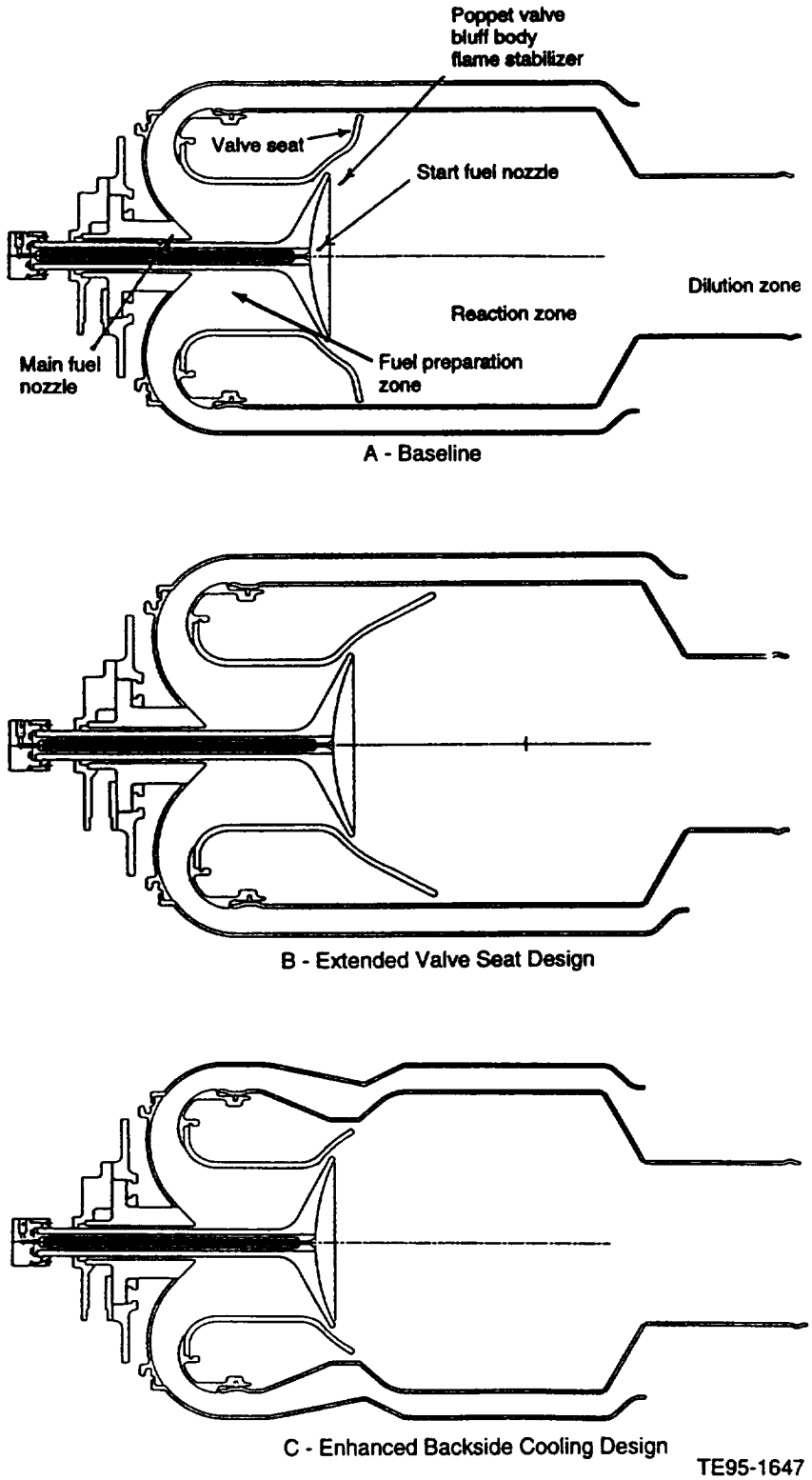


*Figure 1.4.2-1. Poppet valve premixing combustor, baseline design, and proposed modifications.*

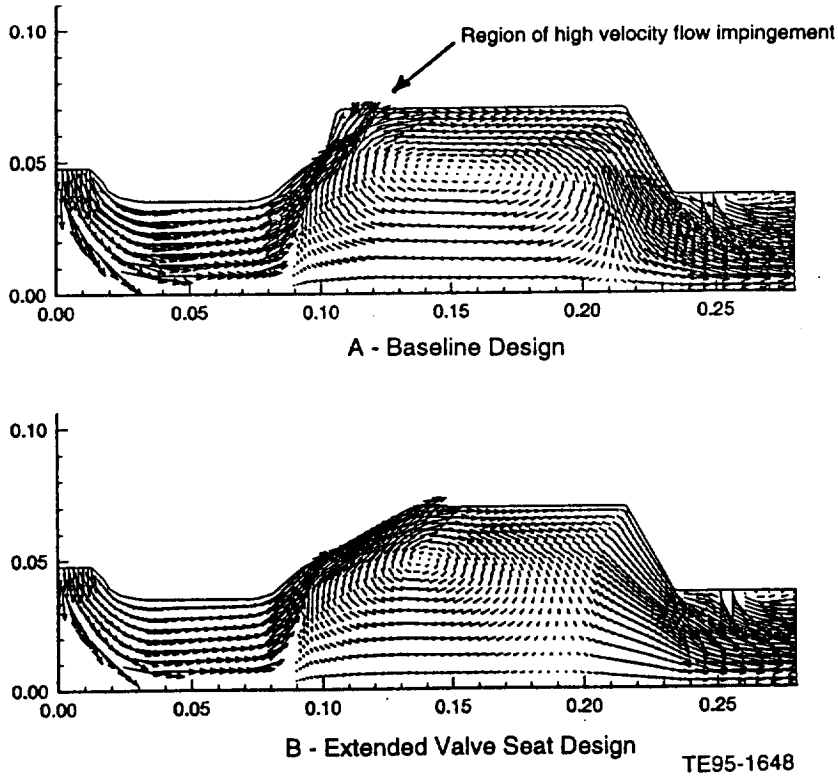


*Figure 1.4.2-2. Poppet valve combustor cold flow velocity vectors, baseline design, and extended valve seat modification.*

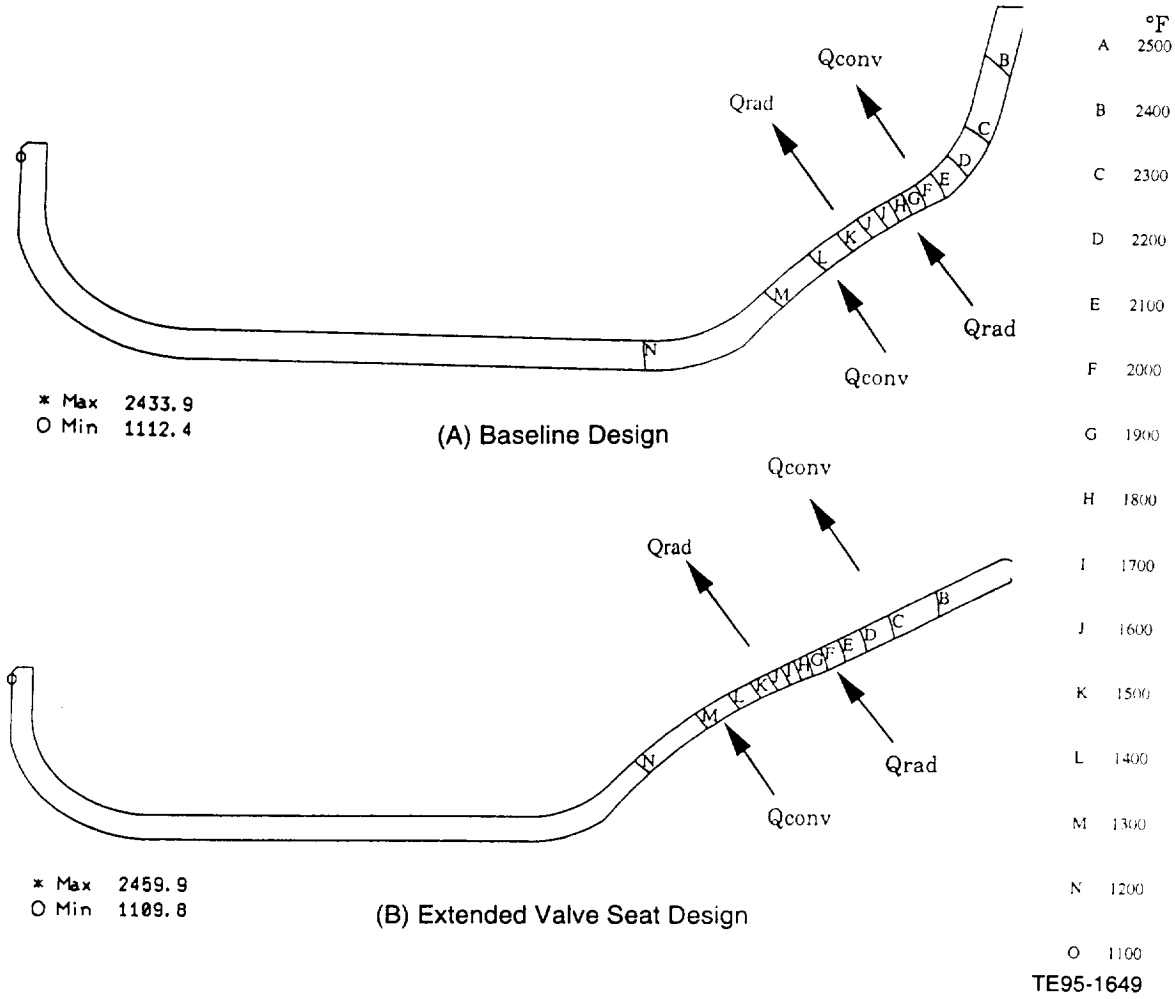


*Figure 1.4.2-3. Predicted temperatures of baseline and extended valve seat configurations.*

# II. CERAMIC COMPONENT DESIGN

## 2.1 DESIGN ACTIVITIES

### 2.1.3 Gasifier Turbine Rotor

#### 2.1.3.1 Objective/Approach

This activity is focused on designing structural ceramic rotors for the gasifier turbine that meet performance, mechanical strength, probability of survival (POS), and dimensional criteria for operating in the AGT-5, regenerator hot rig(s), and test-bed engine(s) at RPD conditions. Efforts include the analytic assessment of the structural reliability (statistical basis) of gasifier rotor designs considering various ceramic material systems. The rotor design reliability goal is 0.9797. Critical points in the engine operating cycle are analyzed, including 1370°C (2500°F) RIT maximum power steady-state and a cold start to maximum power transient.

#### 2.1.3.2 Accomplishments/Results

- Completed the design and analysis of a subscale 20-bladed gasifier rotor for use in the regenerator hot rig.
- Both Norton's NT154 and CPS's SRS201 materials were assessed and found acceptable for the application.
- The stress levels are the same for the subscale and full-scale 20-bladed rotors.

#### 2.1.3.3 Discussion

The regenerator hot rig is much like the AGT-5 hot rig but smaller. The rig has a compressor, burner, turbine, and two regenerator disks. A ceramic turbine rotor is needed to withstand the TIT needed to achieve the 1800°F regenerator inlet temperature of the 2500°F RPD engine cycle. The purpose of the rotor is to produce hot gas for the regenerator; therefore, high thermodynamic efficiency is not required. To speed the development time, the AGT-5 airfoil was simply scaled down and the shaft speed scaled up to achieve the same flow conditions. The airfoil and rotor hub stresses are identical to the successful full-size AGT-5 gasifier rotor. Figure 2.1.3-1 compares the full-scale and subscale NT154 cold spin stress fields. The cold start transient is the mechanical design point for rotors because the high transient thermal gradients result in the minimum POS for any operating condition. Figure 2.1.3-2 shows the predicted worst case transient temperatures for the NT154 AGT-5 rotor. The same temperature profile was used for subscale NT154 and SRS201 subscale rotors because the two materials' thermal properties are similar. Figure 2.1.3-3 shows the similarity in stress and POS results for the full and subscale NT154 under transient conditions. Figure 2.1.3-4 shows the subscale 20-bladed SRS201 gasifier rotor stresses for cold spin and worst case transient conditions. The transient POS of 0.8748 for the SRS201 rotor is low, but is reasonable for a development program.

CPS delivered proof tested SRS201 subscale 20-bladed gasifier rotors that have not yet been tested in the regenerator hot rig.

### 2.1.4 Ceramic Rotary Regenerator System Design

The overall goal of the ceramic regenerator design was to analyze, design, and develop a rotary regenerator disk system for an automotive application.

#### 2.1.4.1 Regenerator Performance

**2.1.4.1.1 Objective/Approach.** The main objective of the regenerator performance analysis was to optimize the many design variables to achieve maximum performance of a ceramic disk. Performance prediction algorithms were also developed to support engine cycle analysis, which permitted numerous trade studies. The approach was to update or develop computer codes that could accurately evaluate the many design variables and also rely on Allison's previous regenerator experience coupled with current manufacturing practices.

**2.1.4.1.2 Accomplishments/Results.**

- A FORTRAN routine has been updated to complete numerous trade studies to optimize disk performance.

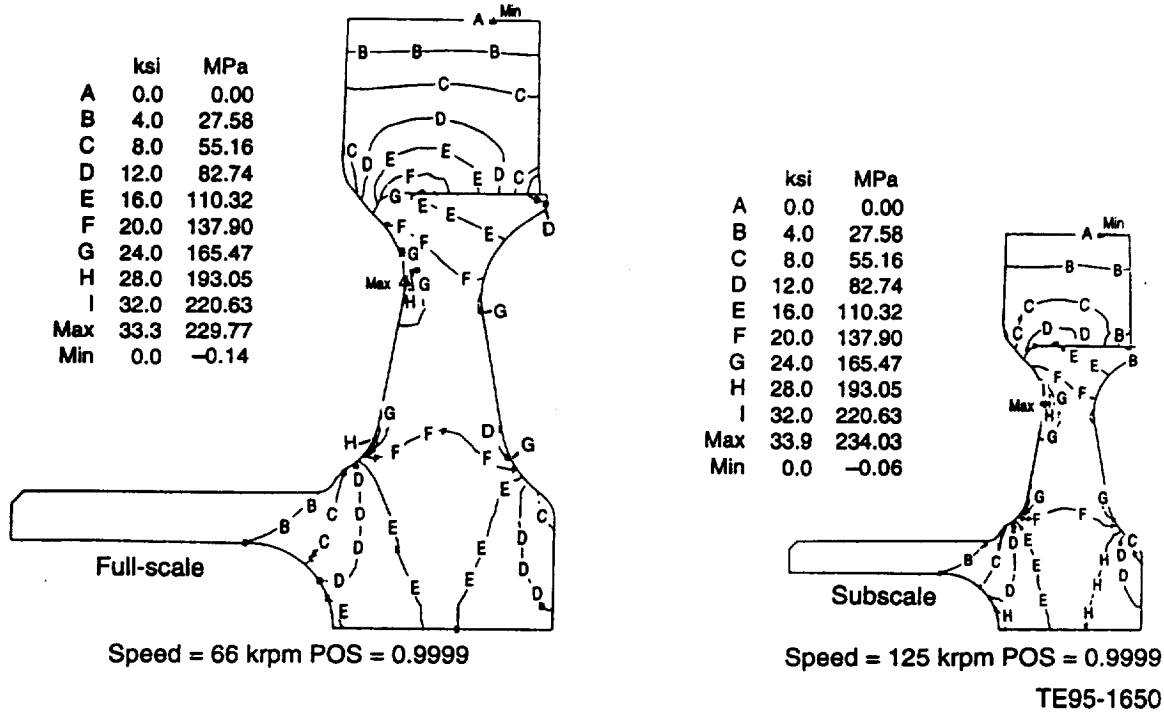


*Figure 2.1.3-1. Stress comparison of full-scale and subscale NT154 20-bladed gasifier rotors under cold spin conditions.*

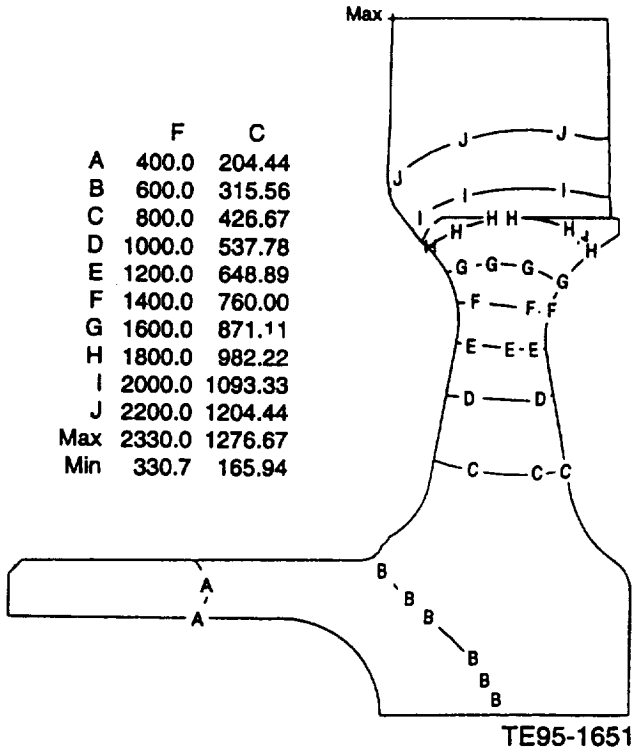


*Figure 2.1.3-2. Predicted worst case transient temperatures for the full-scale NT154 20-bladed gasifier rotor.*

- A detailed heat transfer analysis of the ceramic regenerator disk was completed to determine the three-dimensional temperature distribution within a disk.
- A transient disk performance FORTRAN routine was developed to aid in the analysis of the engine cycle trade studies.
- A complete regenerator disk system design was completed, using cost effective manufacturing techniques and maximizing engine cycle performance.

**2.1.4.1.3 Discussion.** Regenerator performance is influenced by a wide range of independent variables; maximum performance is only achieved when a total system optimization is completed. System optimization goes beyond traditional regenerator measures of performance, such as effectiveness and pressure drop, and extends to performance of the entire engine. The criteria for optimization is the change in engine power (HP) and change in engine specific fuel consumption (SFC) relative to a baseline configuration. The change in HP and SFC analysis includes not only the disk thermal effectiveness, disk pressure drop, and seal leakage (when appropriate), but also includes an engine

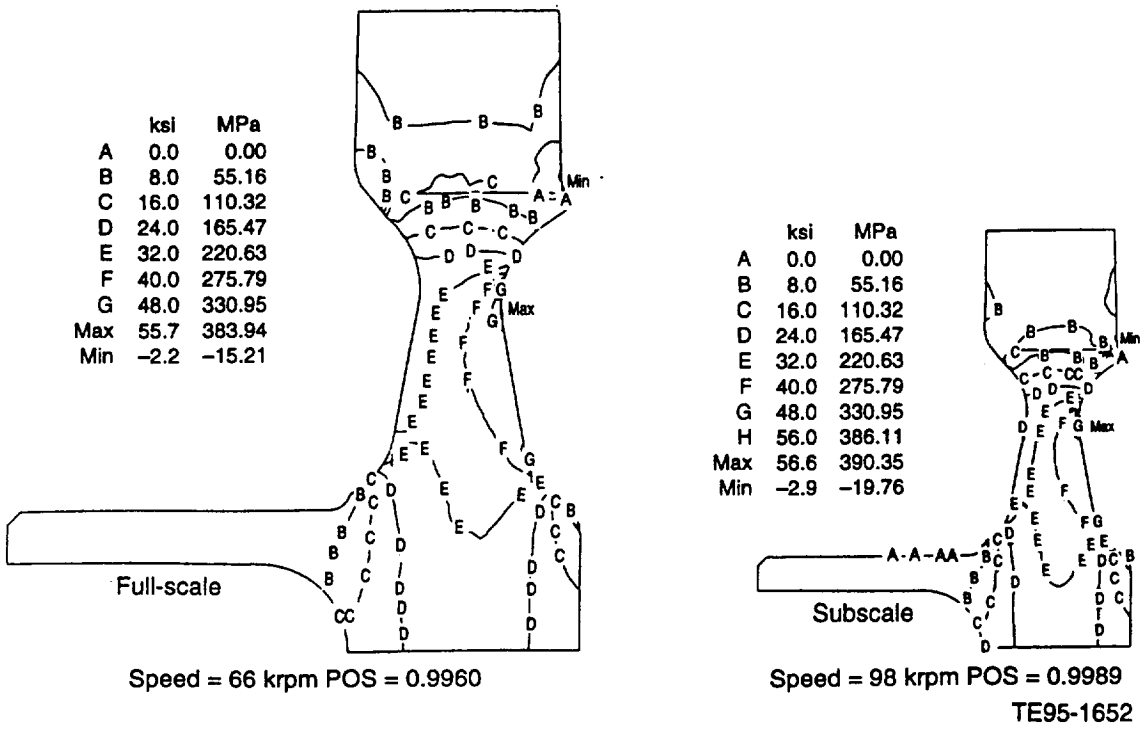


*Figure 2.1.3-3. Stress comparison of full-scale and subscale NT154 20-bladed gasifier rotors under worst case transient conditions.*

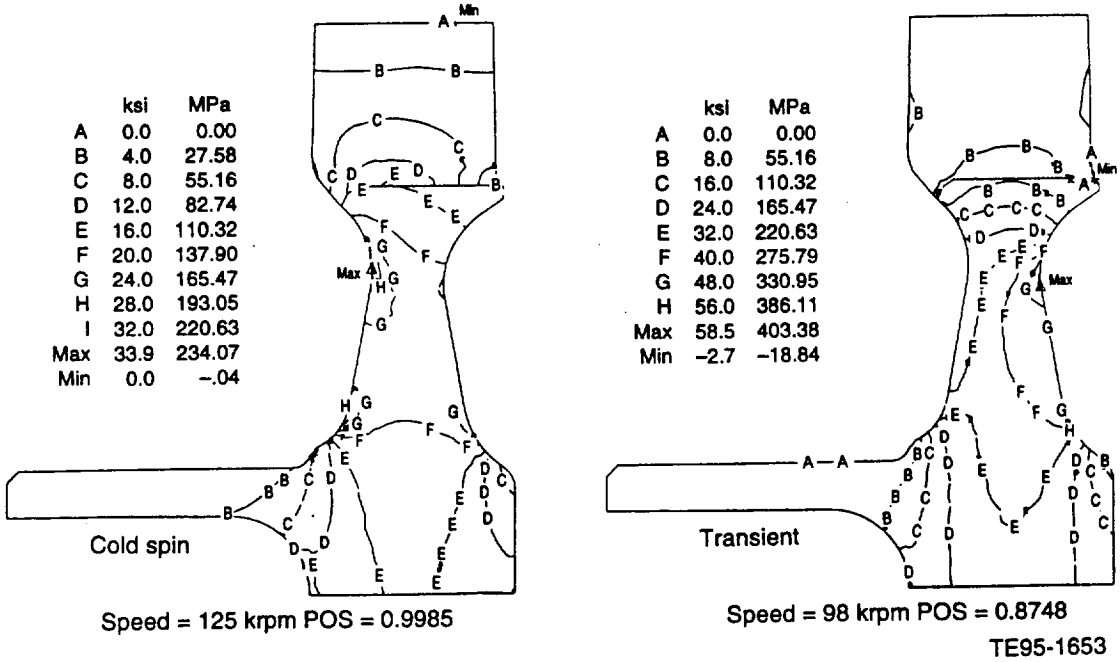


*Figure 2.1.3-4. Subscale 20-bladed SRS201 gasifier rotor stresses for cold spin and worst case transient conditions.*

cycle. The assumed engine cycle has an effect on the absolute results,but this is minimized by comparing percent changes of HP and SFC. The change in HP is most sensitive to the pressure drop of the disk, while the change in SFC is most sensitive to the effectiveness. This is important because many variables have an inverse effect on pressure drop and effectiveness. As an example, if the disk thickness is increased, the effectiveness increases; the pressure drop also increases, which generally is beneficial to SFC but detrimental to HP. Therefore, this criteria provides a true optimization and/or compromise of the regenerator system performance when considering the many independent variables.

The independent variables can be grouped into three categories: microproperties of the disk, macroproperties of the disk, and properties of the disk/seal system. The microproperties of the disk include the disk material properties (density, specific heat, and thermal conductivity) and the matrix properties (cell shape, wall thickness, and cell density). Material properties of the two candidates, lithium aluminum silicate (LAS) and magnesium aluminum silicate (MAS), were provide by the disk supplier and were not considered a variable in the optimization. The matrix properties were optimized in a study prior to 1993 to establish the matrix geometry. This study included both triangular and rectangular cell structures and was not constrained by current manufacturing limits. It is recognized that the only cost effective manufacturing process for a disk is the extrusion process, which is the current manufacturing technique for automotive catalytic converter substrates. The best compromise geometry for a disk is a 2-to-1 rectangular cell structure, 0.005 inch thick walls, and 1100 cells per square inch cell density. These properties are an incremental stretch for the current manufacturing limits of extrusion technology, but they are attainable. The engine cycle used in this optimization was established for the AGT-5. The cycle differs from the currently used cycle, but not enough to significantly change the results.

The macroproperties of the disk include the disk diameter, disk thickness, hub diameter, and rim fill diameter. The latter two properties were designed so no reduction in open flow area was required, which benefits disk performance. The hub diameter was designed so the hub does not extend beyond the cross arm seal width, and therefore, no potential heat transfer area is sacrificed at the hub. Rim filler is material impregnated into the matrix at the outer diameter to prevent the communication of pressures from one side of the disk to the other. This is required when the passages at the outer diameter of the disk are not aligned with the axis of the disk (referred to as cell slant). Cell slant is prevalent in disks manufactured by the wrapped process. The use of extruded disks, which do not have significant cell slant, removed the need for rim filler. With no rim filler, the open flow area is bounded only by the rim seal, the largest possible outer diameter; therefore, the latter two macroproperties have been designed to maximize disk performance.

Disk diameters and thicknesses are very important properties and must be selected through the use of an optimization study. To accomplish this optimization study, a matrix of diameters and thicknesses were used to calculate the HP and SFC of the current engine cycle. These results were converted to the optimization criteria with the RPD disk being the baseline size. The results are shown in Figure 2.1.4-1. This figure illustrates that increasing the diameter of the disk is beneficial for HP and SFC. Figure 2.1.4-1 also demonstrates the law of diminishing return with regard to diameter; the performance benefit from a 70% to 80% increase in diameter is much greater than the gain from a 100% to 110% increase in diameter. As stated before, the disk thickness is a compromise between HP and SFC and demonstrates the law of diminishing return. The range of dimensions used in Figure 2.1.4-1 was not constrained by manufacturing or installation concerns, but for an engine selection these would become important. For example, current extrusion technology does limit the diameter for a one-piece disk extrusion. This extrusion limit would have to be considered during regenerator sizing to ensure the cost advantages of extrusion could be utilized. Even though rotary regenerators are very compact heat exchangers, the space claim for most engine installations requires the diameter and/or the thickness to be constrained.

The properties of the disk/seal system affecting disk performance are the disk revolution speed (rpm), gas-to-air ratio, seal widths, and flow distribution. A similar study to the diameter/

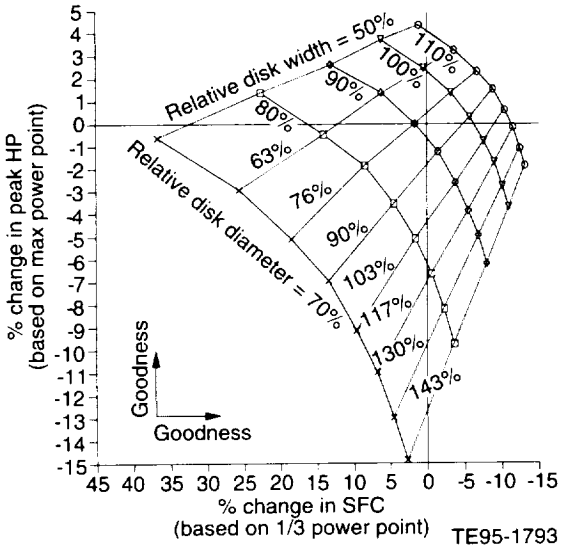


*Figure 2.1.4-1. Disk diameter and thickness optimization.*

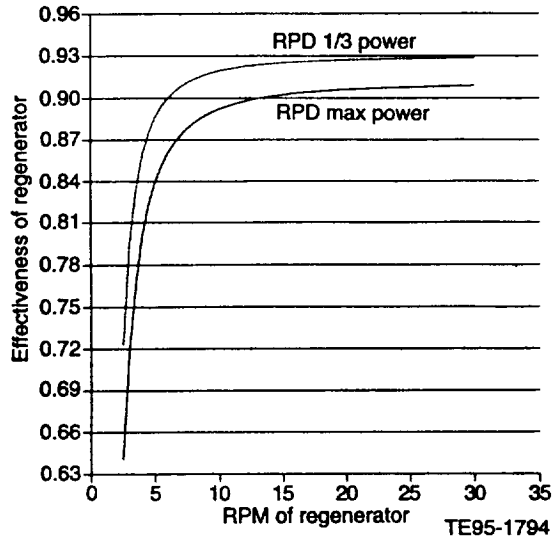


*Figure 2.1.4-2. Effectiveness versus regenerator rpm.*

thickness study shown in Figure 2.1.4-1 was completed for the disk rpm and gas-to-air ratio. The revolutions per minute of the disk has a minimum acceptable value of 8 to 10 rpm, as illustrated in Figure 2.1.4-2, below which the effectiveness is severely reduced. Once above this lower limit, the effectiveness asymptotically approaches a maximum value. The upper practical limit on the rpm is controlled by seal leakage and seal wear. The HP and SFC optimization study for rpm, which included the effects of seal leakage, demonstrated that a rotational speed of 30 rpm gave the best trade off between HP and SFC. The surface speed produced was lower than previous experience with larger disks, and led to the conclusion that seal wear should be the same or even lower than obtained in previous experience.

The gas-to-air ratio (G/A) is the disk frontal area on the gas side divided by the disk frontal area on the air side; the cross arm seal separates these two areas. Figure 2.1.4-3 illustrates the gas and air frontal areas for a variety of cross arm seal shapes. Previous analysis has indicated that a G/A ratio near 1.2 provided the optimum balance between HP and SFC, and this was confirmed. The effectiveness of the disk is maximized near a G/A ratio of 1.0, but the pressure drop on the gas side, the highest and most critical, is significantly reduced with a G/A ratio greater than 1.0. The drawback to a G/A ratio greater than 1.0 is that the cross arm seal cannot be symmetric, as shown in the second row of Figure 2.1.4-3, and therefore requires a more complex and costly seal design. A straight cross arm seal was considered the only viable seal shape from a cost standpoint, but this requires the seal to be offset to obtain a G/A ratio greater than 1.0. Sketch 4 in Figure 2.1.4-3 represents the offset configuration. The offset seal and other unsymmetric seal configurations could not be analyzed with the standard regenerator performance model, so a new heat transfer model was developed. This new model determines the three-dimensional temperature distribution within the disk. Using the new thermal model, the offset seal evaluation demonstrated any benefits from using a G/A ratio near 1.2 was negated by a distorted temperature pattern. Figure 2.1.4-4 illustrates the distorted disk temperature pattern on the hot face of the disk. This temperature distortion reduced the effectiveness from approximately 92% to 81%. To accommodate a straight cross arm, the cross arm should be symmetric about the center of the disk, resulting in a G/A ratio of 1.0. This final design of a symmetric straight cross arm seems simplistic and uncreative, but was actually arrived at only after a comprehensive study.

The performance of the regenerator disk is not the only design criteria considered when seal widths are determined, but performance concerns are important. As the seal widths are increased, the leakage is reduced and the open flow area of the disk is also reduced. Leakage

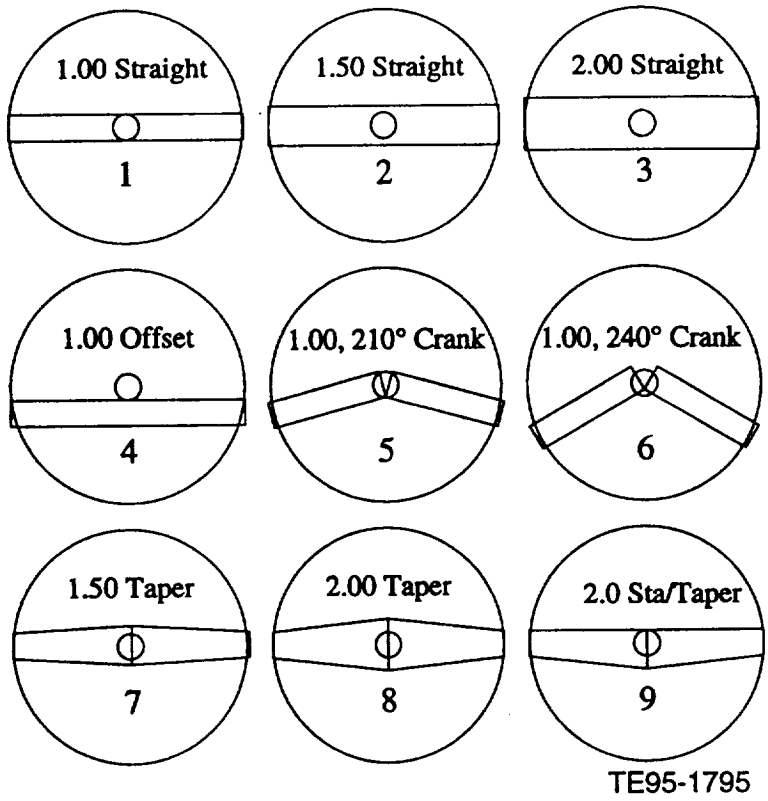


*Figure 2.1.4-3. Potential cross arm seal shapes.*

reductions improve engine performance, but a reduced flow area reduces regenerator, and therefore engine, performance. This trade-off was completed using the change in HP and SFC analysis previously applied.

The last variable affecting regenerator performance is the flow distribution on both the air and gas sides. Previous experience identified the flow distribution as a very important consideration. All of the current performance predictions have been completed assuming a uniform flow distribution. This assumption is made for two reasons: one, if the flow paths on both the air and gas sides are designed properly, the flow should be approximately uniform and two, the flow distribution is unique to every engine and specifics of the current engine are not yet known. The new disk temperature distribution model has the capability to analytically evaluate nonuniform distributions of flow and temperature, but this capability has not been explored because the flow and temperature distributions are not known at the present time. Further work will be completed on the flow distribution's effects on performance when some characteristic distributions have been determined.

The last performance issue addressed was the transient performance of the regenerator disk. Many important design considerations occur in a transient period, fuel burn, peak temperatures, and exhaust emissions during engine start-up; acceleration response; deceleration response; and engine shutdown. These considerations cannot be addressed with a steady-state analysis; the regenerator disk represents a considerable thermal inertia to the engine cycle. Some experimental transient regenerator results have been recorded in previous programs, but the transient behavior is difficult to accurately measure. Theoretical studies have also been completed on the transient response of regenerators, but all of the research found at Allison and in the open literature have severe limitations. The first limitation was the assumption that steady-state operation was followed by a step change in only one parameter until steady-state conditions were again achieved. The second limitation was that only one or two of the seven

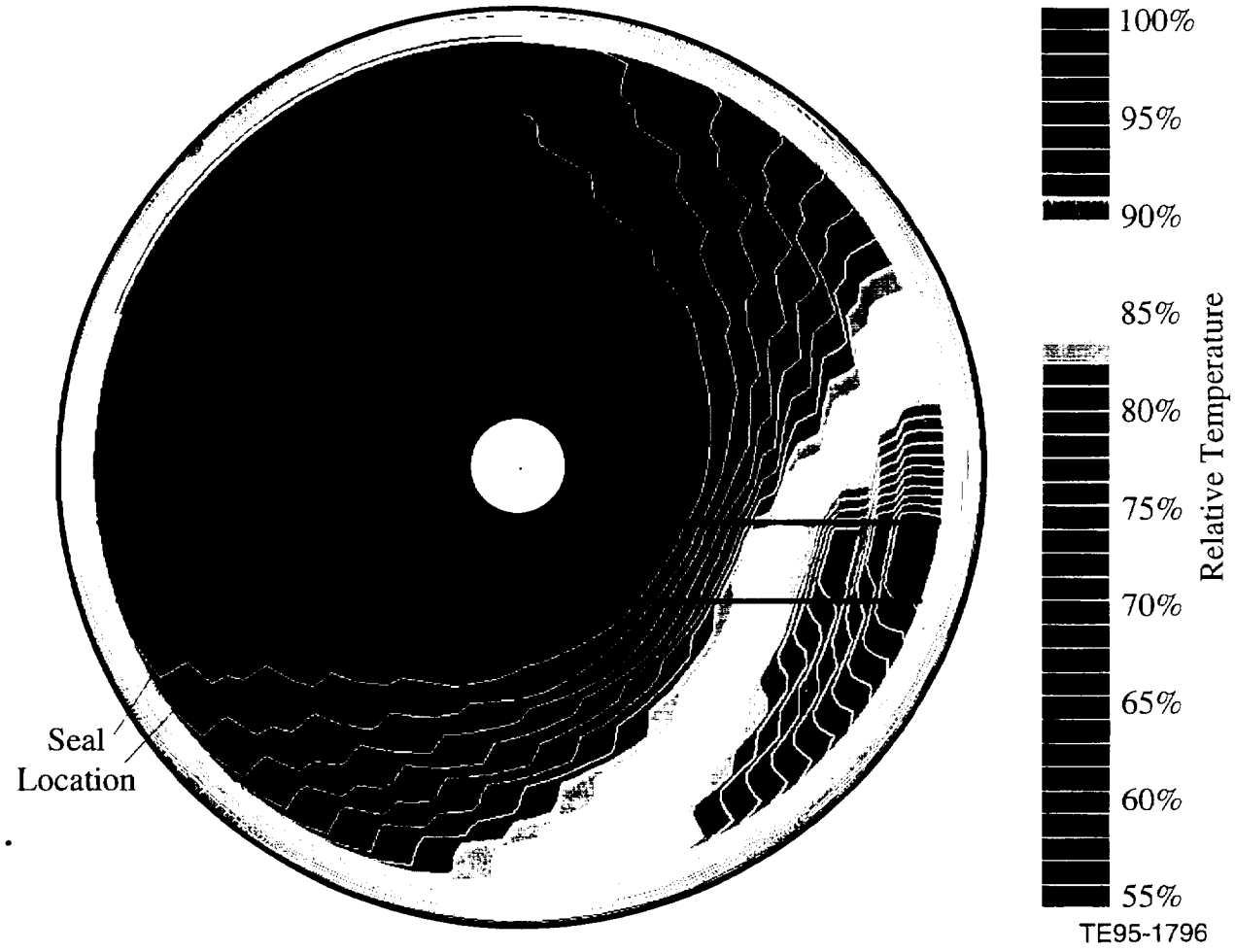


*Figure 2.1.4-4. Hot face temperature distribution with offset cross arm seal.*

independent variables could be varied simultaneously as a function of time. The seven independent variables are the flow, pressure, and temperature on both the air and gas sides and the disk rpm. In actual engine operation, all seven variables could change simultaneously and at each sequential time step the parameters vary. The first limitation could be overcome by using the principle of superposition, but the second limitation is a fundamental restriction of the analysis technique.

To overcome these limitations, a new transient model was developed allowing complete variability of the seven independent variables. This model was based on the steady-state solution but was governed by a lumped thermal capacitance analysis. To verify the integrity of this new model, test data and the other transient models were used for comparison. A good correlation was established and the transient model was incorporated into a transient engine cycle analysis. This analysis demonstrated the need to quickly reduce the power output to zero, which is sometimes referred to as a load dump. The load dump must be achieved without allowing the engine rotor to overspeed. The fuel is cut off, but the regenerator recycles heat and keeps the turbine inlet temperature (burner inlet) high. Therefore the transient behavior of the regenerator is very important to this and some other engine operating conditions.

## 2.1.4.2 Regenerator Disk Mechanical Design

**2.1.4.2.1 Objective/Approach.** The main objective of the regenerator disk mechanical design was to analyze and develop the support and drive methods of the disk. Both support and drive shape the disk design in the areas of the outer diameter and the inner diameter. The goal was to develop a cost effective approach satisfying the functional requirements. The approach was to develop the design tools and methodologies required to evaluate the many possible configurations.

**2.1.4.2.2 Accomplishments/Results.**

- A variety of low cost hub designs were formulated and analyzed.
- A study was completed on the attachment of a ceramic disk to a metallic ring gear.
- A three-dimensional force/moment equilibrium analysis was completed and developed into a computer program.
- A cost effective design was completed to support and drive the regenerator disk.

**2.1.4.2.3 Discussion.** The regenerator disk must be supported in both the radial and axial directions to ensure uninhibited circumferential motion. The radial support can be either at the inner diameter in the form of a centered hub bearing, or it can be at the outer diameter in the form of guide rollers. Allison's previous experience has been with a centered hub bearing, but other manufacturers in the industry have used guide rollers. The trade-off between these two approaches is complicated and neither one has an obvious advantage. A third, but undeveloped and untested approach, is to use the direct electric drive as a magnetic bearing. In discussions with an electric motor supplier, who could design and provide the direct electric drive, it was noted that the additional hardware to add a magnetic bearing feature were minimal. The whole concept of the direct electric drive and this magnetic bearing feature should be pursued in the future, but it is not considered a viable approach at the present time. The decision was made to use the centered hub bearing approach because of its past success and known design methodology.

The major challenge of the centered hub bearing for the current automotive application is the development a cost effective hub/bearing design. Previous disk designs relied upon intricate machining of a solid ceramic hub and then a second firing of the disk to insert this solid hub. Both of these features are costly and do not lend themselves to mass production, so alternative disk hub designs were formulated. Avoidance of complex ceramic machining could be accomplished by transferring the bearing retaining features (snap rings) from the disk hub to the spindle shaft, as illustrated in Figure 2.1.4-5. This minimizes the hub final machining to only the bearing surface. Also shown in Figure 2.1.4-5 is the previous barrel shaped bearing, which allowed the disk to be misaligned with respect the shaft. After an analysis of the potential misalignment, resulting from axial movement of the disk seals, it was determined the disk could only move approximately 1 deg. It was concluded that much of this misalignment could be accommodated in the bearing clearances; the moment potentially imposed on the disk would be small. Therefore, the straight cylindrical bearing with a shaft shoulder and a shaft mounted snap ring is a simple yet effective bearing design.

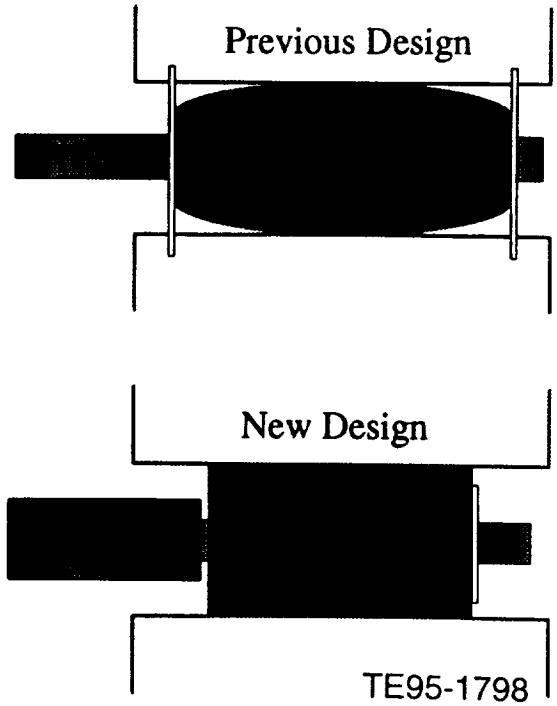


*Figure 2.1.4-5. Hub bearing design changes.*

The other key feature of the centered hub bearing approach is the ceramic hub forming the bearing surface. The current practice of using a separate slip cast solid ceramic hub is cost prohibitive because it is joined to the disk with a foam cement. The foam cement must be fired in a separate process, a costly additional step. Cold setting cements not requiring firing exist, but do not have the strength and other properties of the foam cement. Therefore, a design study was completed to develop a more cost effective approach. Many ideas were considered to address the functional problems. The two fundamental difficulties are the differential thermal expansions of the materials and the low strength of the ceramics. Figure 2.1.4-6 illustrates a few of the ideas considered. Since the hub design details involve the disk manufacturer, many discussions were held to assess the cost effectiveness of the designs. A design has not yet been selected since a comprehensive evaluation of the many candidate designs has not been completed. Plans are in place to fabricate several of the designs and subject them to loads experienced in engine operation. In conclusion, some good candidates exist for a low cost hub, but a final design has not yet been selected.

The differential thermal expansion at the outer diameter of the disk and ring gear is an important design issue. The classic problem of attaching a low expansion ceramic to a relatively high expansion metal is complicated by the extreme temperatures of a regenerator disk. Many designs have successfully been used in the industry to solve this problem, but many required extensive development. Allison has used a room temperature vulcanizing (RTV) elastomer for all of its ceramic regenerator disk applications and this has proven to be a robust design. The major concern when using RTV is the limiting temperature. A previous study was conducted at Allison on the thermal degradation of a commercial RTV and included both time of exposure and temperature. The results demonstrated that the RTV has a limiting temperature between 600°F and 700°F. An obvious but important design feature of RTV attachment is that the RTV is located in the lowest temperature region, the cold edge of the disk. The two design variables controling the temperature of the cold edge of the disk are the disk thickness and the rim seal thickness. In heat transfer terms,

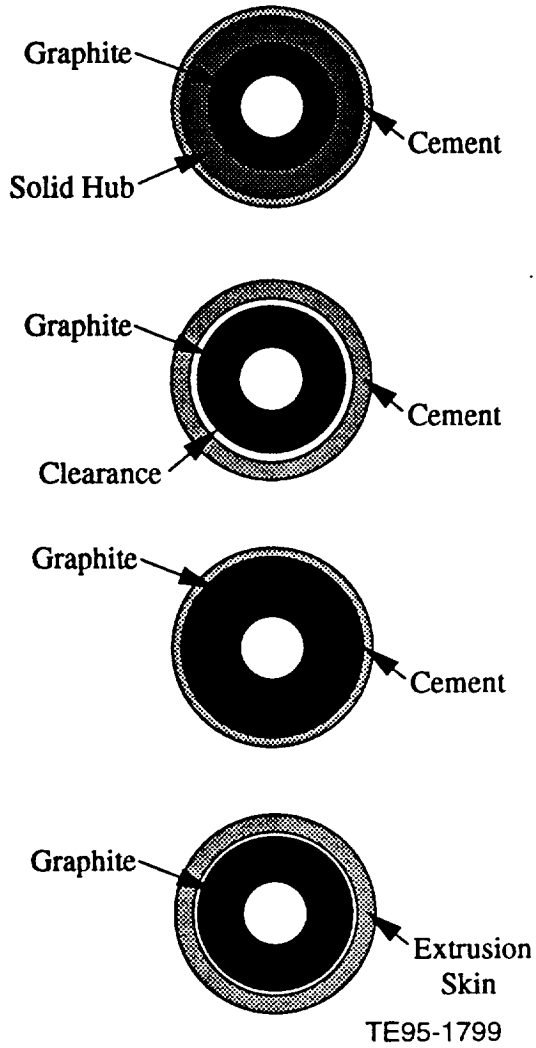


*Figure 2.1.4-6. Low cost hub designs.*

the disk thickness controls the axial conduction and the rim seal thickness controls the radial conduction. The cycle conditions impose a given temperature difference on a disk, but the thickness of the disk controls the axial gradient (i.e., °F/in.). A thinner disk will have a higher axial gradient and, therefore, the average temperature under the RTV will be higher. The rim seal thickness also has an important effect on cold edge temperatures because it controls the proximity of the cooling and heating air flows. As illustrated in Figure 2.1.4-7, the seal thickness has a major effect on the cold edge temperature at small thicknesses because the heating due to axial conduction is countered by the cooling by radial conduction. Once the seal thickness is above 0.5 inch, the axial conduction is dominant and the effect of seal thickness is minimal. This

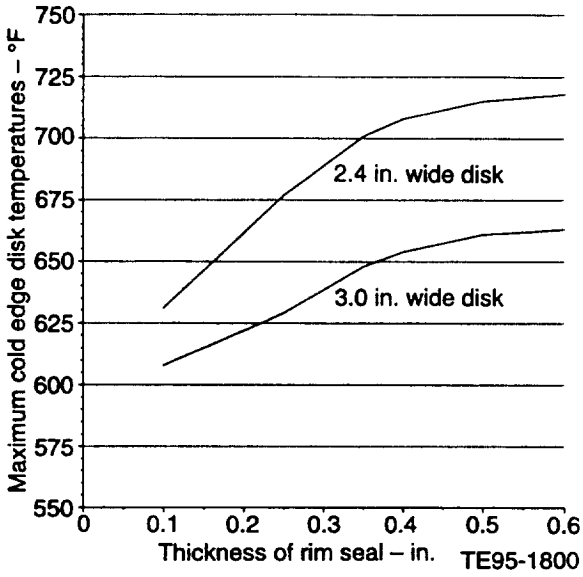


*Figure 2.1.4-7. Maximum cold edge disk temperatures.*

study was used to ensure the temperature of the RTV attachment area is within the acceptable limits for RTV. These results and many other design considerations were used to select the disk thickness and seal width thickness.

The last mechanical design issue for the disk was the development and use of a force equilibrium analysis. This analysis was completed to predict the external loads on the disk, including axial, radial, and circumferential loads. The loading information will also be used in a future disk stress analysis. Figure 2.1.4-8 illustrates all of the major loads on the disk. A FORTRAN routine was developed to solve force and moment balance equations to satisfy equilibrium. The unbalanced radial loads are transmitted through the center bearing, and the circumferential forces (torques) are balanced by the drive gear. The axial force balance, however, is not straightforward. The disk is not rigidly constrained in the axial direction and a force equilibrium is only achieved when two or more rim and/or cross arm seals bottom-out and transmit load to the housing. The difficulty is that prior to the analysis, it is not known which seals will bottom-out as the disk misaligns with respect to the shaft and moves axially. For example, the disk could rotate under the loads and bottom-out two opposite face rim seals, or the disk could be pushed axially and bottom-out the rim and cross arm seal on one face. There are more than

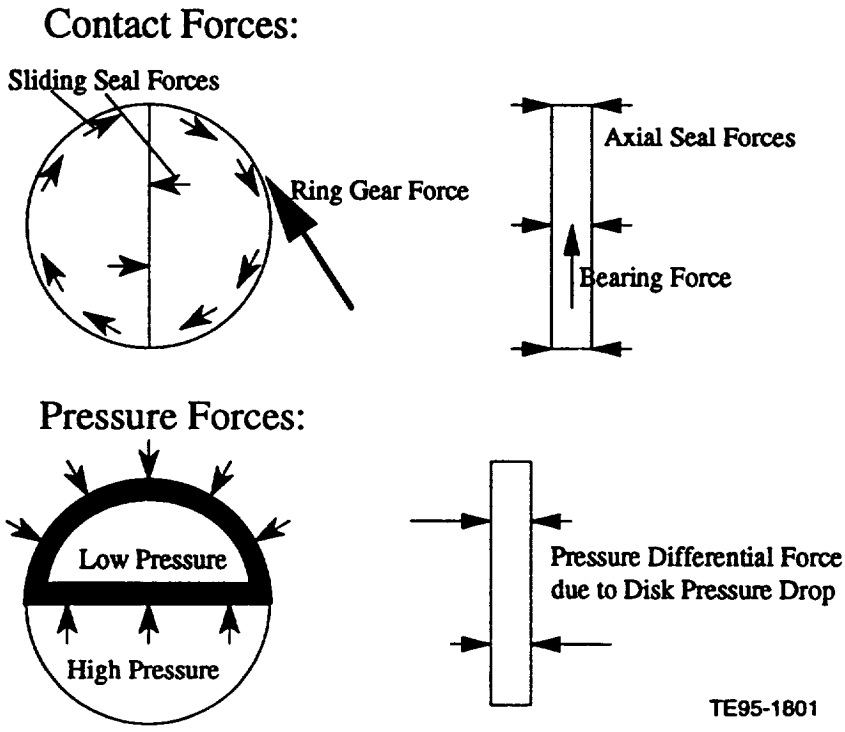


*Figure 2.1.4-8. Contact and pressure loads on disk.*

six possible movement scenarios the disk could assume. All of these must be checked to establish the one physically possible scenario. In most cases, the disk is pushed axially due to the pressure loads and the cold rim and cross arm seals are bottomed-out. The other difficulty is that most forces are coupled to forces in other directions. For example, an axial seal force produces a shear load on the disk face, affecting the disk torque, then affecting the gear tangential and radial force, then affecting the bearing forces, then affecting the torque, etc. Therefore this coupled system is solved using an iterative technique. After these and other analysis difficulties were resolved, a useful tool was available to predict the loads, torques, and disk position.

One important use of the disk force equilibrium analysis is the selection of the circumferential-gear drive location. The circumferential location of the gear drive has a major influence on the bearing loads at the center hub. The tangential gear load, which produces torque, must be reacted through the center bearing along with the disk weight, seal loads, etc. At some circumferential locations, the tangential gear load partially cancels out the weight and other loads, but at other circumferential locations it adds to the out-of-balance force. This is illustrated in Figure 2.1.4-9 by a plot of the radial bearing load as a function of the circumferential location of the drive pinion. The figure demonstrates that the

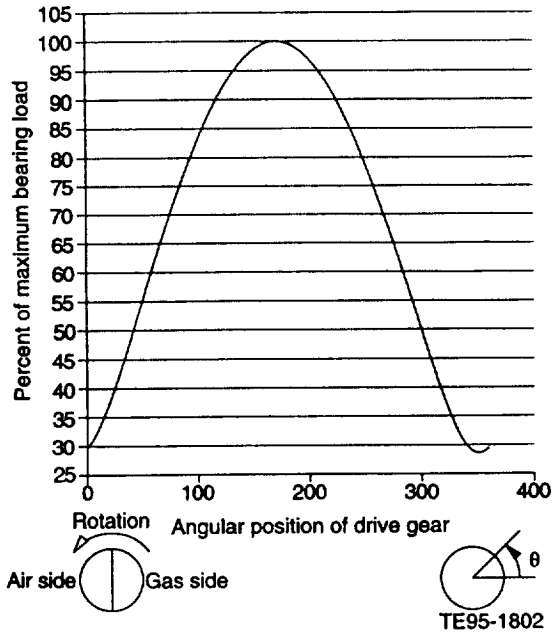


*Figure 2.1.4-9. Plot of the radial bearing load as a function of circumferential location on the drive pinion.*

drive gear should be near the 0 deg. positions to minimize the bearing loads. Attempts should be made to locate the drive gear near this optimum location, but for practical packaging reasons, it usually cannot be located exactly at the minimum load location.

# III. MATERIALS CHARACTERIZATION AND CERAMIC COMPONENT FABRICATION

This section describes the ongoing ceramic material and component fabrication, characterization, and development activities that are a key focus of ATTAP and HVTE-TS. The ceramic materials subsection documents the results of characterization and qualification of ceramic materials and components being developed for advanced gas turbine engine applications, including the characterization of material properties (microstructure, density, fracture strength, and fracture toughness) on both test specimens and bars sectioned from components and the results of failure analyses of rig/engine tested components. The ceramic component fabrication subsection describes the ongoing ceramic component process development activities at the selected ceramic suppliers for the Allison effort, including AlliedSignal Ceramic Components, Corning Inc, Kyocera Industrial Ceramics Corporation, Norton Advanced Ceramics, Ceramics Process Systems, and Schuller International Inc.

Allison's approach to ceramic component technology development continues to be one of subcontracting process development to the domestic ceramic manufacturing community and working in an iterative development loop with those suppliers in areas of component design, fabrication, characterization, and rig/engine data feedback. While basic ceramic materials development is not part of this program, the program integrates material developments from DoE/ORNL programs, supplier in-house activities, and other sources as they become available for component fabrication efforts.

## 3.1 MATERIALS AND COMPONENT CHARACTERIZATION

### 3.1.1 Material Properties and Microstructure

#### 3.1.1.1 Objective/Approach

The materials and component characterization efforts have focused on the testing and evaluation of candidate ceramic materials and components being developed for use in advanced gas turbine engines. The primary objective of this task is to establish a data base of appropriate material characteristics to support the design, analysis, development, and testing of hot section ceramic components. A secondary objective is to evaluate new candidate ceramic materials and suppliers and to assess which, if any, should be used in subsequent component development. The materials characterization activities have focused on microstructure, density, flexural strength, and fracture toughness evaluations of various ceramic materials. Fracture surface analysis is also used to determine the nature and location of strength-controlling flaws. In addition, tensile strength and time dependent strength characteristics are evaluated for select materials.

#### 3.1.1.2 Accomplishments/Results

The ceramic materials and components evaluated during this reporting period include:

- Norton Advanced Ceramics' NT230 siliconized SiC
- Ceramics Process Systems' SRS201 sialon
- Ceramics Process Systems' SRS201 sialon gasifier turbine rotors

#### 3.1.1.3 Discussion

**Norton Advanced Ceramics NT230 SiC.** Characterization of Norton Advanced Ceramics' NT230 SiC was conducted during this reporting period. The NT230 material was a reaction sintered SiC with approximately 5 to 15% free silicon. The test specimens (MIL-STD 1942) were sectioned from billets fabricated by pressure slip casting using the Dorst automated pressure slip casting equipment. The billets were cast using porous plastic molds at a pressure of approximately 2070 KPa (300 psi), compared to 520 KPa (75 psi) used for conventional pressure slip casting. The average density of this material measured 3.045 g/cc (0.111 $lb/in^3$), slightly lower than the density of 3.121 g/cc (0.113 $lb/in^3$) measured for the standard NT230 SiC material.

Both longitudinally ground and as-processed tensile surface conditions were evaluated. The strength characteristics of both the Dorst high pressure slip cast NT230 SiC material and NT230 SiC produced using conventional plaster molds and low pressure are summarized in Table 3.1.1-I.

*Table 3.1.1-I.*
*Strength characteristics of Norton Advanced Ceramics NT230 siliconized SiC.**

| | Strength - MPa (ksi) | |
|---|---|---|
| Temperature - °C (°F) | Machined surface** | As-processed surface** |
| 25 ( 77) | 405.75 (58.85) m = 8.15<br>[369.21 (53.55)] | 280.55 (40.69) m = 9.24<br>[209.39 (30.37)] |
| 1000 (1832) | 462.70 (67.11)<br>[440.71 (63.92)] | 310.33 (45.01)<br>[290.96 (42.20)] |
| 1150 (2102) | 383.62 (55.64)<br>[427.26 (61.97)] | 209.67 (30.41)<br>[305.78 (44.35)] |
| 1250 (2282) | 438.02 (63.53)<br>[422.44 (61.27)] | 167.61 (24.31)<br>[332.88 (48.28)] |
| 1370 (2500) | 327.43 (47.49)<br>[468.49 (67.95)] | 291.58 (42.29)<br>[404.72 (58.70)] |

* The material was fabricated using high pressure slip casting on the Dorst machine with plastic molds.
** Shown in brackets ([ ]) are the strengths of conventionally plaster slip cast NT230 SiC.

The typical strength-controlling defects observed in the Dorst cast material were internal pores (Figure 3.1.1-1). The typical fracture origins observed in the as-processed specimens were surface and internal pores, often associated with surface depressions (Figure 3.1.1-2).

**Ceramics Process Systems SRS201 Sialon.** Characterization of Ceramics Process Systems' (CPS) SRS201 sialon material was conducted during this reporting period. The material was produced by Quickset injection molding using process parameters developed for gasifier rotor fabrication. The test specimens were sectioned from billets and had an average density of 3.232 g/cc (99.1% theoretical density).

The test specimens complied with MIL-STD 1942. Both machined and as-processed surface conditions were evaluated. The material


TE95-1654

*Figure 3.1.1-1. Strength controlling defect observed in NT230 siliconized SiC tested at room temperature with a machined surface condition.*

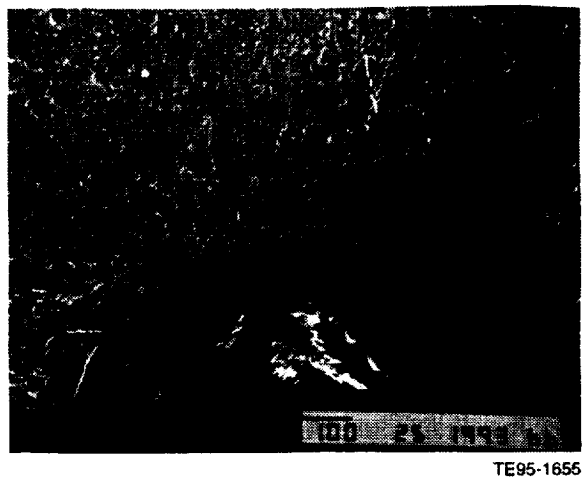
TE95-1655

*Figure 3.1.1-2. Typical failure origin (surface depression/pore) observed in Norton NT230 SiC tested with an as-processed surface.*

strength characteristics are summarized in Table 3.1.1-II The typical fracture origins of the machined specimens tested at room temperature were internal pores (Figure 3.1.1-3). Machined bars tested at 1370°C (2500°F) were observed to have failed from surface flaws (Figure 3.1.1-4), with evidence of heavy oxidation. Specimens with an as-processed surface condition tested at room temperature had shallow surface depressions as the primary fracture origins (Figure 3.1.1-5). These depressions were often associated with surface pores. The as-processed specimens tested at high temperature failed from oxidized surface flaws, similar to the machined samples.

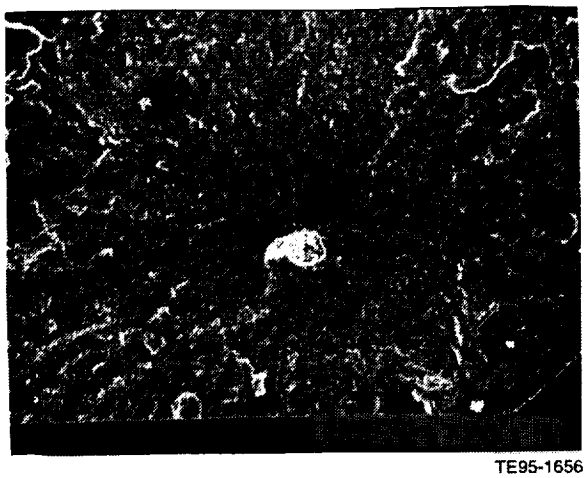

TE95-1656

*Figure 3.1.1-3. Primary strength controlling defect (internal pore) observed in CPS Quickset molded SRS201 sialon material tested with a machined surface at room temperature.*

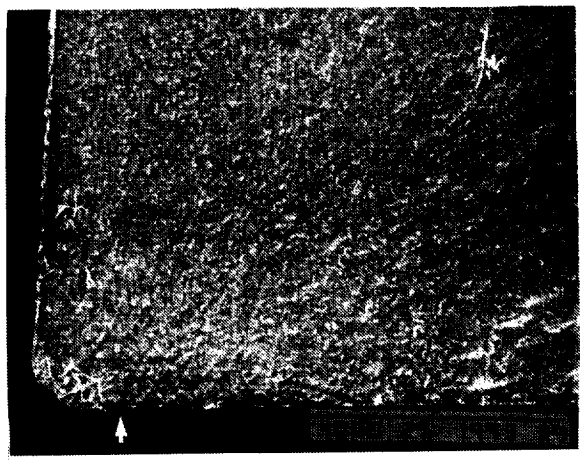

TE95-1657

*Figure 3.1.1-4. Typical fracture origin (surface flaw on heavily oxidized surface) found in CPS SRS201 sialon machined bars tested at 1370°C (2500°F).*

*Table 3.1.1-II.*
*Strength characteristics of CPS SRS201 sialon billets.**

| | Strength - MPa (ksi) | |
|---|---|---|
| Temperature - °C (°F) | Machined surface | As-processed surface |
| 25 (77) | 753.45 (109.28) (m=8.0) | 386.72 (56.09) (m=14.1) |
| 850 (1562) | 535.03 (77.60) | 450.15 (65.29) |
| 1000 (1832) | 630.73 (91.48) | 418.03 (60.63) |
| 1150 (2102) | 674.51 (97.83) | 406.51 (58.96) |
| 1250 (2282) | 553.16 (80.23) | 388.17 (56.30) |
| 1370 (2500) | 380.66 (55.21) | 289.44 (41.98) |

* Samples were manufactured using the Quickset injection molding process and were taken from billets.

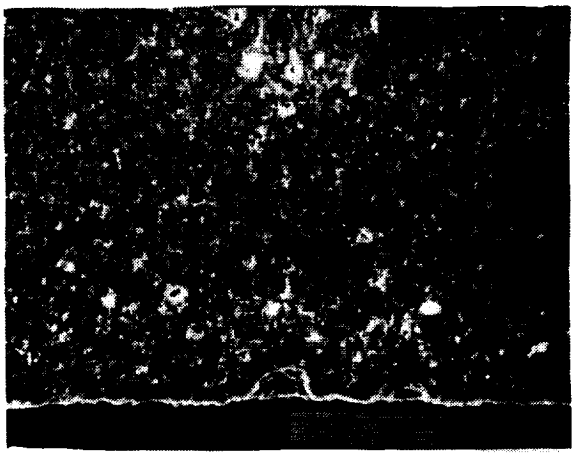

TE95-1658

*Figure 3.1.1-5. Primary fracture origin (shallow surface depression/pore) observed in CPS SRS201 sialon tested with an as-processed surface condition.*

Characterization of CPS SRS201 sialon rotors was also conducted. The 26-blade configuration rotors were fabricated by Quickset injection molding followed by pressureless sintering. Test specimens complying with MIL-STD 1942 were sectioned from the rotors and the mechanical properties evaluated. The rotors had an average density of 3.229 g/cc (99.0% theoretical density).

The material strength characteristics are summarized in Table 3.1.1-III. All specimens were evaluated with a machined surface condition. Shown for comparative purposes are the strengths obtained for the SRS201 sialon material sectioned from billets. The strengths of the rotor test bars were comparable with the strengths of specimens sectioned from billets, with a significant increase in Weibull modulus for the rotor test bars (from 8.0 to 17.8). The typical fracture origins of the rotor specimens tested at room temperature were internal inclusions and pores (Figure 3.1.1-6). The inclusions were composed primarily of iron silicide. A majority of the specimens evaluated at elevated temperature were observed to have failed from surface inclusions and flaws (Figure 3.1.1-7).

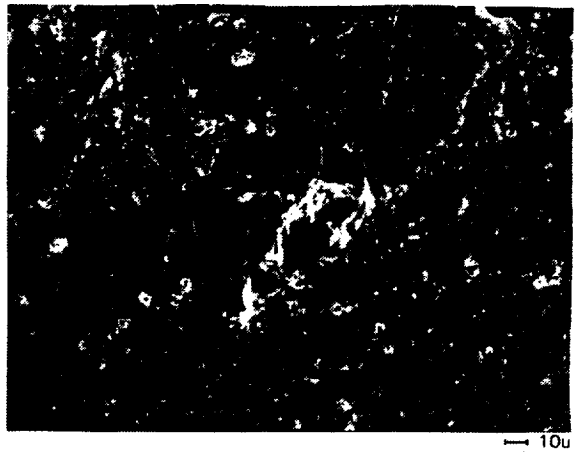

10u

TE95-1659

*Figure 3.1.1-6. Typical strength controlling defect (internal inclusion) observed in machined CPS SRS201 sialon specimens sectioned from an AGT-5 gasifier turbine rotor. The inclusion was composed primarily of iron silicide.*

*Table 3.1.1-III.*
*Strength characteristics of CPS SRS201 sialon rotor bars.**

| | Strength - MPa (ksi) | |
|---|---|---|
| Temperature - °C (°F) | Rotor bars** | Billet bars** |
| 25 (77) | 695.88 (100.93) (m=17.8) | 753.45 (109.28) (m=8.0) |
| 850 (1562) | 599.22 (86.91) | 535.03 (77.60) |
| 1000 (1832) | 585.57 (84.93) | 630.73 (91.48) |
| 1150 (2102) | 602.32 (87.36) | 674.51 (97.83) |
| 1250 (2282) | 501.11 (72.68) | 553.16 (80.23) |
| 1370 (2500) | 391.34 (56.76) | 380.66 (55.21) |

* The test specimens were fabricated by Quickset injection molding followed by pressureless sintering.
** The samples were sectioned from the rotors. All specimens were tested with a machined surface condition.

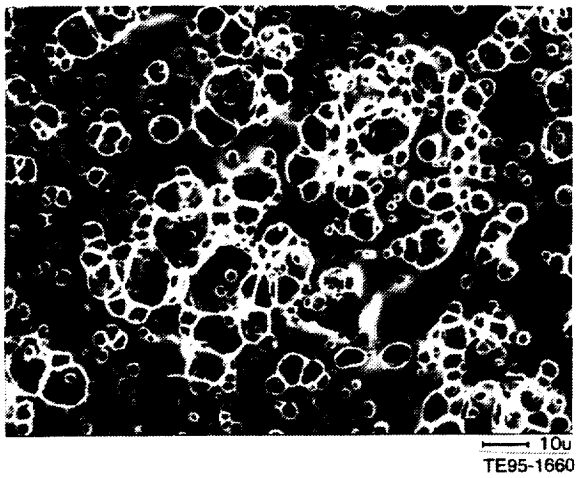


*Figure 3.1.1-7. Fracture origin (surface flaw in heavily oxidized surface layer) observed in CPS SRS201 sialon rotor bars tested at 1370°C (2500°F).*

Bars tested at a temperature of 1370°C (2500°F) failed from surface flaws with evidence of heavy oxidation.

## 3.1.3 Failure Analysis

### 3.1.3.1 Objective/Approach

Failure analysis details the results of fractographic analyses of ceramic and metallic components that experienced unscheduled damage during rig/engine testing and evaluation. Fractographic analysis is one of the most powerful tools used in the failure analysis of engine or rig-tested components. A careful study of the general and detailed features of the topography of a fracture by visual assessment and scanning electron microscopic (SEM) examination with elemental X-ray analysis provides a wealth of information concerning the failure origin and the failure mode(s). Analysis of hardware failures allows the separation of design features from material deficiencies, defects, or nonoptimum fabrication procedures and can suggest appropriate corrective measures.

### 3.1.3.2 Accomplishments/Results

- Failure analysis of gasifier module C5, containing a Kyocera SN252 15-blade gasifier rotor and a Norton Advanced Ceramics NT230 advanced concept scroll, was conducted. The assembly was tested in hot rig S/N 14, buildup (BU) 27. Failure of the gasifier assembly was caused by heavy rub between the rotor blade tips and the shroud.
- Failure analysis of gasifier assembly C6, containing a Norton NT164 20-blade gasifier rotor and a Norton NT230 advanced concept scroll, was conducted. The assembly was tested in the 300-hour durability test in hot rig S/N 14, BU 35. The shroud fractured due to rotor blade tip rub.
- Failure analysis of another C6 assembly subjected to the 300-hour durability test in hot rig S/N 14, BU 38 was conducted. This C6 assembly consisted of a Norton NT230 advanced concept scroll and a Norton NT154 20-blade gasifier rotor. The assembly failed due to foreign object damage (FOD). The origin of the iron based material was not identified.
- Failure analysis of the Kyocera all-ceramic gasifier assembly from the 300-hour durability test was conducted. The assembly consisted of an SN252 20-blade rotor and an SN252 initial design scroll. The test was conducted in hot rig S/N 12, BU 45. The rotor was released from the shaft due to seal rub.
- Failure analysis of the poppet valve combustor was conducted. The unit contained a Norton NT230 valve seat and a Norton NT154 valve, and was tested in hot rig S/N 15, BU 3. The combustor failed due to overheating.

### 3.1.3.3 Discussion

**Hot Rig S/N 14, BU 27.** The gasifier assembly C5, composed of a Kyocera SN252 silicon nitride 15-blade rotor and a Norton NT230 siliconized SiC advanced concept scroll was tested. The assembly failed at 55,000 rpm and 1227°C (2240°F) during a slow acceleration from 70% gasifier speed (N1). The rig had been up to 95-96% N1 twice and the highest turbine inlet temperature (T4) observed was 1337°C (2440°F). Total time of the assembly was 1.15 hours, but the rotor had accumulated 12.63 hours of run time.

Inspection showed the rotor lost only some blades but the scroll was shattered. Figures 3.1.3-1 and 3.1.3-2 show the aft and forward views of the rotor. The remaining blade tips exhibited rub marks (Figure 3.1.3-3), and rub


*Figure 3.1.3-1. The aft view of the gasifier rotor. The part failed in hot rig S/N 14, BU 27*

marks were also recorded on the broken shroud. Figure 3.1.3-4 shows the larger recovered pieces from the broken shroud with different rub marks or no mark at all. The heaviest rub marks appeared as a yellow glaze, indicative of oxidation at high temperature. Apparently, localized heavy rub between the rotor tip and the shroud fractured the shroud. Fractured shroud pieces then shocked the rotor and the rotor rubbed into the heat shield as evidenced by the forward side of the rotor hub in Figure 3.1.3-2. The jolt also scored the rotor shaft and the impeller shroud.

**Hot Rig S/N 14, BU 35.** A C6 gasifier assembly containing a Norton NT230 siliconized silicon carbide advanced concept scroll was tested in hot rig S/N 14, BU 35 with a Norton NT164 silicon nitride 20-blade rotor. The rig ran for a total of 50.1 hours and was shut down when the gasifier failed to accelerate.


*Figure 3.1.3-2. The condition of the forward hub face of rotor 5K9.*

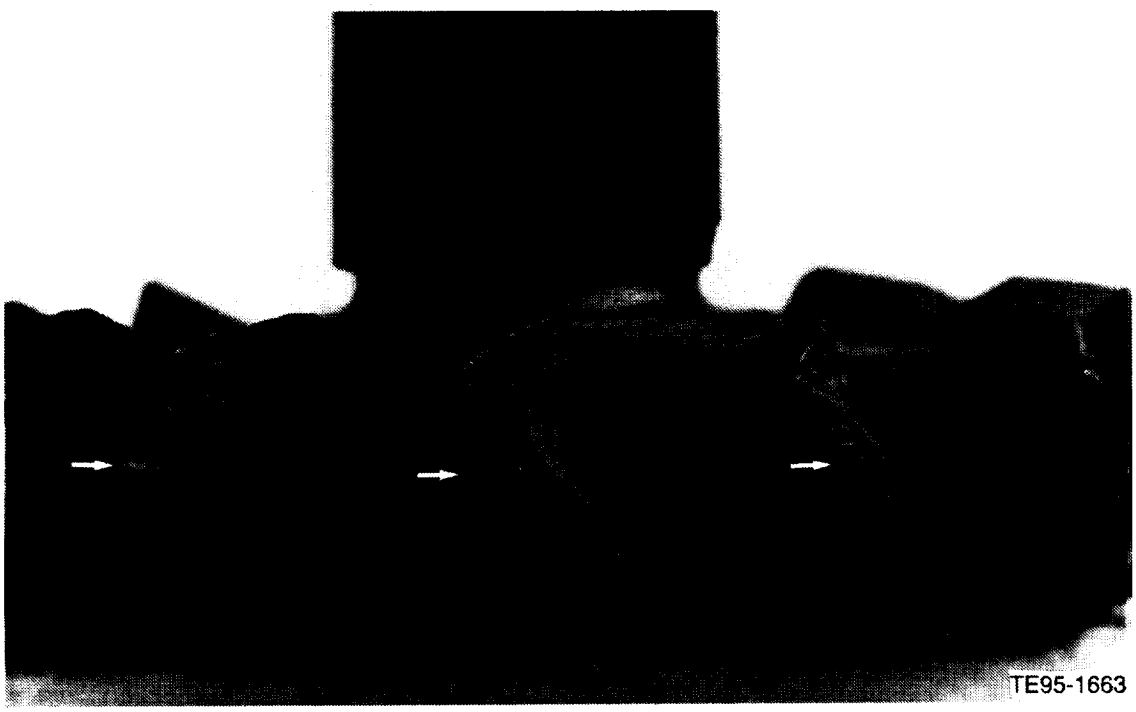


*Figure 3.1.3-3. Condition of the rotor blade tip rub (indicated by arrows).*

Inspection revealed the shroud broke off cleanly from the scroll and was stuck to the nozzle (Figure 3.1.3-5). The shroud broke radially into more pieces, but the pieces were held together by the undamaged silicon nitride piston rings. One of the key slots was chipped at the base. There were two heavy rotor blade tip rub marks by the rotor blade tips at the 1 o'clock location and light rub marks at the 7 o'clock location in the aft view. Fracture of the shroud was initiated at the edge of the larger heavy rub marks. The fracture surface of the primary origin is shown in Figure 3.1.3-6. The origin was probably damaged by impact with the blade tip. The rotor blades also suffered some minor damage (Figure 3.1.3-7). One blade lost the corner of the trailing edge tip, and the leading edges of several other blades were chipped. Failure of the scroll originated at the blade tip rub mark on the shroud.

**Hot Rig S/N 14, BU 38.** Another C6 gasifier assembly containing a Norton NT230 advanced concept scroll and a Norton NT154 20-blade rotor failed after 26.35 hours into the 300-hour durability test.

After borescope inspection at 26.1 hours, the gasifier assembly C6 failed during the first acceleration to 90% speed. The scroll broke into pieces and the rotor lost all blades. Total part time was 26.35 hours for the scroll and 35.45 hours for the rotor. No heavy rub marks were found on the remaining pieces of the shroud. The cause of fracture of the scroll was probably a secondary failure.

Most rotor blades experienced multiple fractures, but none exhibited the fracture origin that could cause the rotor failure. On the forward hub face, there was an eccentric rub mark extending more than 180 degrees (Figure 3.1.3-8). The apparent cause was a foreign object falling into the hub area while the rotor was running. X-ray energy dispersive analysis of the rub trace found small oxidized iron material smeared on the hub face (Figure 3.1.3-9). The cause of the rig failure was probably from FOD.

**Hot Rig S/N 12, BU 45.** The Kyocera all-ceramic gasifier, an SN252 20-blade rotor and an SN252 initial design scroll, failed during an attempt at a 300-hour durability test.

Rotor 5K23 had a new rotor shaft installed and the whole assembly was proof tested in an all-metallic assembly for 3.1 hours. Early in the durability run, the rotor came off the shaft at 59,000 rpm and at T4 of 1120°C (2048°F). Total durability test time was 0.3 hour. The shroud was

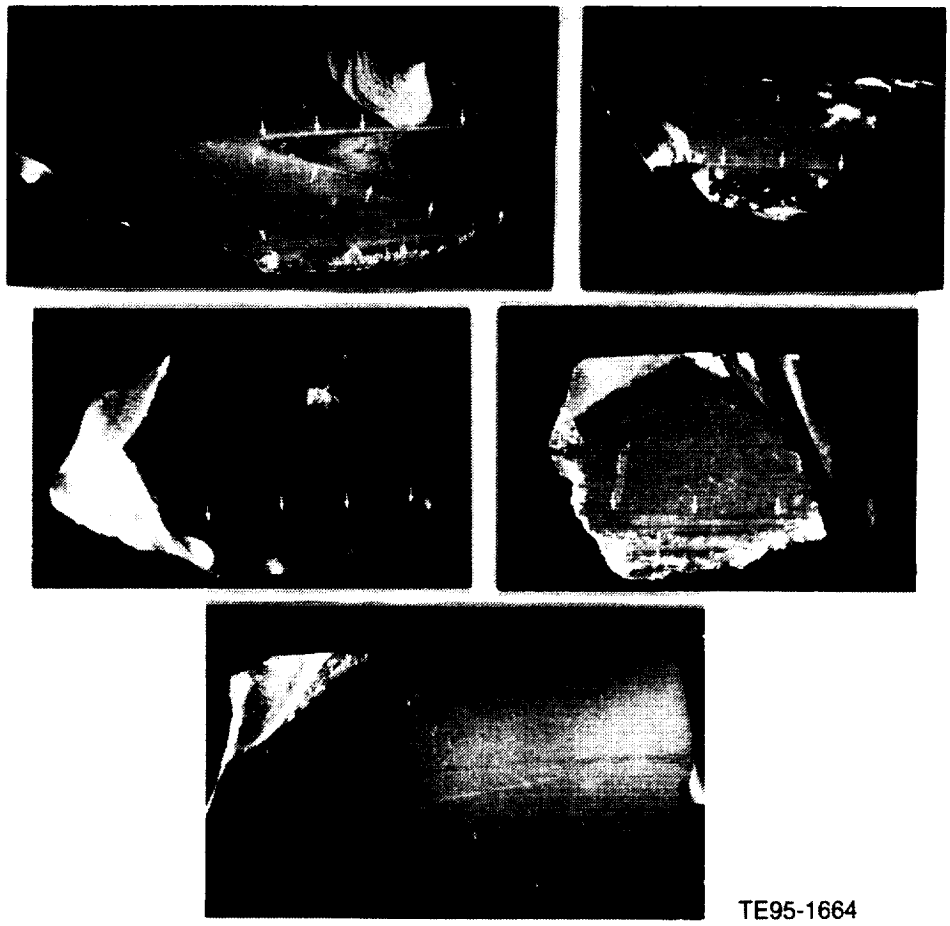


*Figure 3.1.3-4. Pieces of the shroud exhibiting heavy rub by the blade trailing edge tips (top), moderate tip rub (middle), and no rub (bottom). Fine arrows outline the rub marks.*

slightly damaged at the aft and was repaired for possible future use.

The rotor lost all blades (Figure 3.1.3-10). Blades fractured at the root and received damage from multiple impacts. The stub shaft of the rotor was clean except for two spiral chatter marks. Based on the color of these marks, the wider yellowish mark was caused by the end of the metal shaft rubbing on the inside diameter and the thinner mark by the heat shield base. The inside diameter of the metal shaft was clean except for one spot at the end where the filler material was gone (Figure 3.1.3-11). The outside surface of the metal shaft exhibited a polished dark band at the corresponding location of the seal (Figure 3.1.3-12). SEM examination of the band showed a smeared surface (Figure 3.1.3-13). X-ray energy dispersive analysis indicated the smeared surface was the shaft material rubbing in the presence of oxygen. The abnormal rubbing between the shaft and the seal was hot enough to oxidize the metal shaft surface. Apparently, rubbing also caused the metal shaft to expand and release the rotor.

**Hot Rig S/N 15, BU 3.** The first poppet valve combustor with a Norton NT230 siliconized silicon carbide valve seat and a Norton NT154 silicon nitride valve failed after a total of 15 starts during the hot rig test. Testing was terminated after the engine surged. Total testing time was approximately three hours.

Post test inspection revealed the metallic inner and outer liners melted, probably caused by a fuel fire. Figure 3.1.3-14 shows the as-torndown condition of the inner liner. Half of the forward section was burned out by the fuel fire. The fire also burned a hole in the outer liner (Figure 3.1.3-15). The outer housing casting was found at the bottom of the forward end of the inner

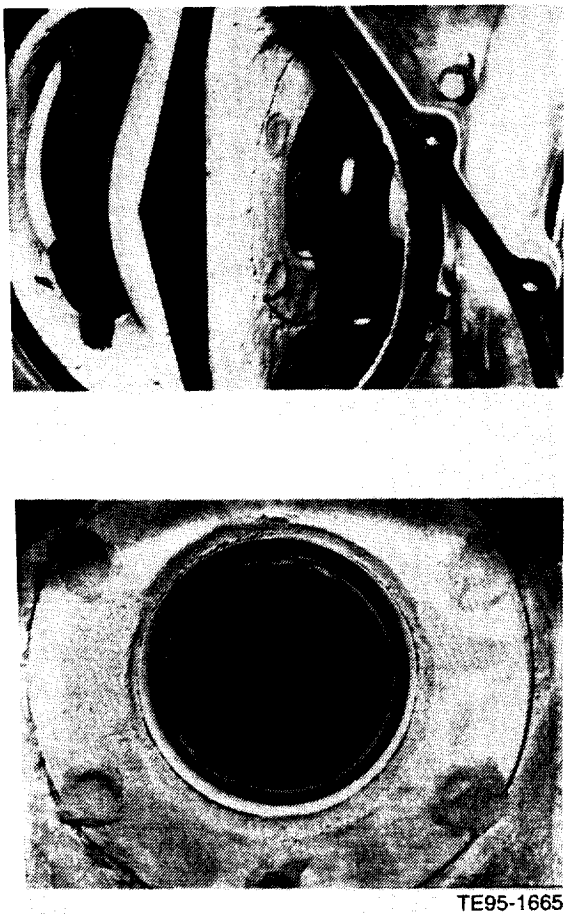

TE95-1665

*Figure 3.1.3-5. As-torndown condition of the gasifier assembly C6 tested in hot rig S/N 14, BU 35. The assembly was pulled back slightly to reveal the broken scroll (top). The separated shroud was held in place in front of the dummy power turbine nozzle (bottom).*

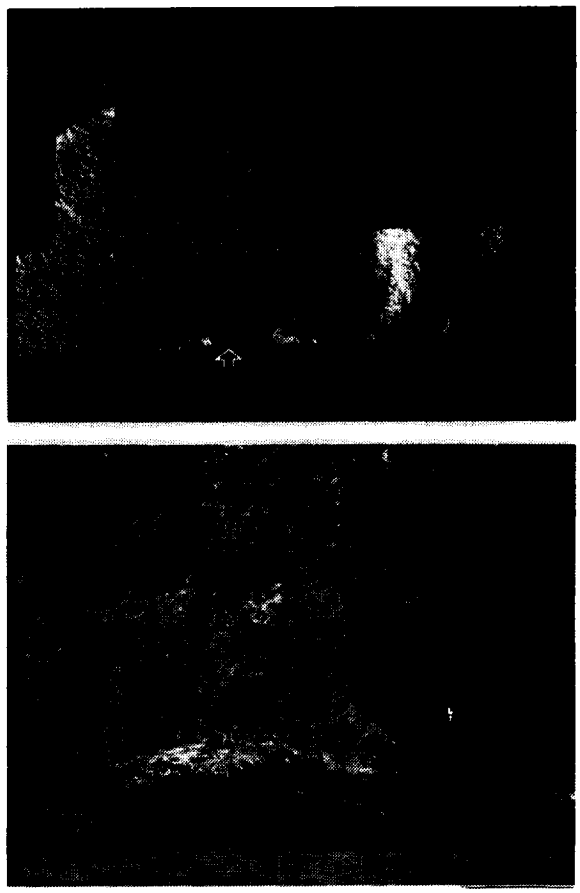

TE95-1668

*Figure 3.1.3-6. Fractographs of the shroud. The hollow arrow points to the origin, which is shown in the lower photo.*

and outer liners. The cavity of the outer housing casting had accumulated molten metal from the liners (Figure 3.1.3-16), and large chunks of carbon deposits were also found in the other half of the casting cavity. Two broken pieces of the inlet end of the siliconized silicon carbide valve seat were retained in the casting by the molten metal.

Figures 3.1.3-17 and 3.1.3-18 show the reconstructed valve seat. The primary failure origin was at the outlet outside diameter. The main crack propagated along the dome and ended at the outlet outside diameter approximately 225 degrees from the origin (Figure 3.1.3-19). Around the origin area, the surface of the valve seat displayed brownish and glassy oxides, indicative of high temperature operation. The valve seat fractured by thermal stress. Figure

Trailing Edge View

TE95-1669

*Figure 3.1.3-7. As-torndown condition of the gasifier rotor. One blade's trailing edge tip was chipped (arrow).*

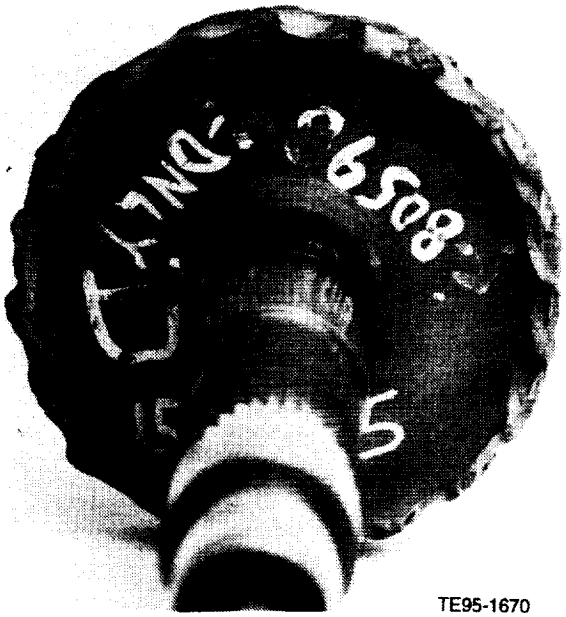


*Figure 3.1.3-8. As-torndown condition of gasifier rotor. Small arrows outline the rub marks on the forward hub face.*



*Figure 3.1.3-9. Scanning electron microscope micrographs of the hub face rub mark. Small arrows indicate the rub mark (top), and iron material (bottom) found in the rub mark.*

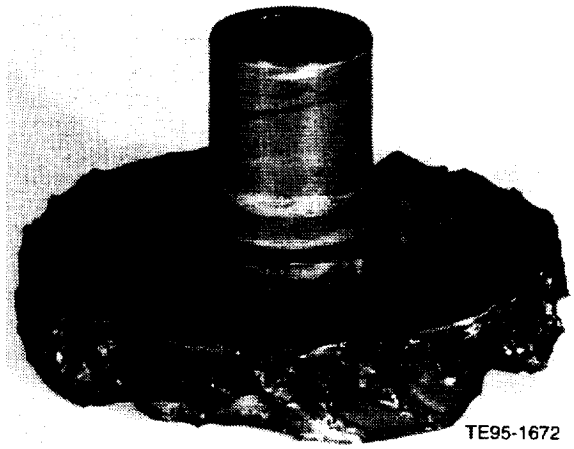


*Figure 3.1.3-10. As-torndown condition of the gasifier rotor, P/N 5-67200, S/N 5K23.*

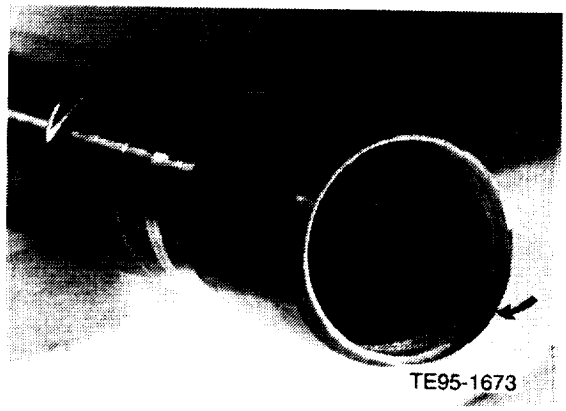


*Figure 3.1.3-11. As-torndown condition of the rotor shaft. The arrow points to the spot on the inner diameter where the filler material was rubbed off by the rotor stub shaft.*

3.1.3-20 shows the fractograph of the origin area. Heavy oxidization of the fracture surface obscured the original feature.

The as-torndown condition of the valve is shown in Figure 3.1.3-21. Carbon was deposited on the front face of the valve, and pits were found on the back face and on the outside diameter as shown in Figure 3.1.3-22. Metallic deposits (Figure 3.1.3-23) were on the center or the edges of the pits. The pits were formed by reaction of the metallic deposits and silicon nitride at high temperature.

The cavity between the valve seat and inner liner apparently had a fuel fire that caused overtemperature operation. Melt-down occurred at the inner liner and outer liner. The valve seat failed by thermal stress at the seat outlet outside


*Figure 3.1.3-12. As-torndown condition of the rotor shaft. Arrows outline the dark rub mark on the outer diameter of the shaft.*

diameter, and the valve back side was pitted due to the reaction between the molten metal and silicon nitride.

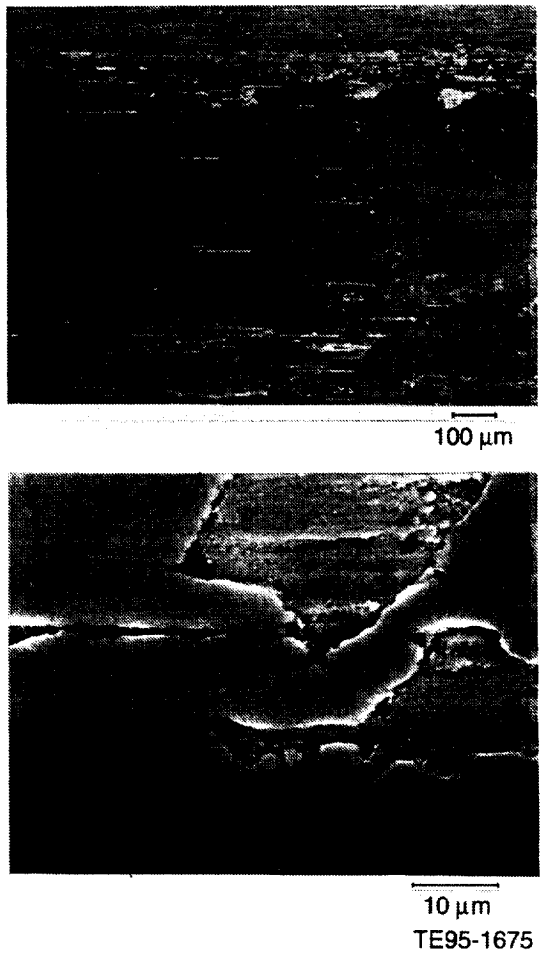


*Figure 3.1.3-13. Scanning electron microscope micrographs of the dark rub mark indicated on the rotor shaft outer diameter.*

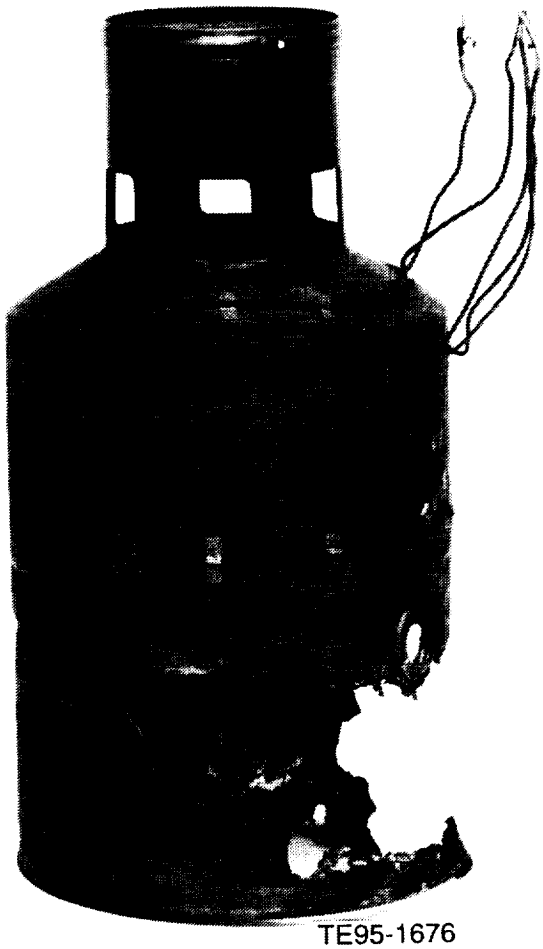


*Figure 3.1.3-14. As-torndown condition of the inner liner of the poppet valve combustor.*


*Figure 3.1.3-15. As-torndown condition of the outer liner of the poppet valve combustor.*

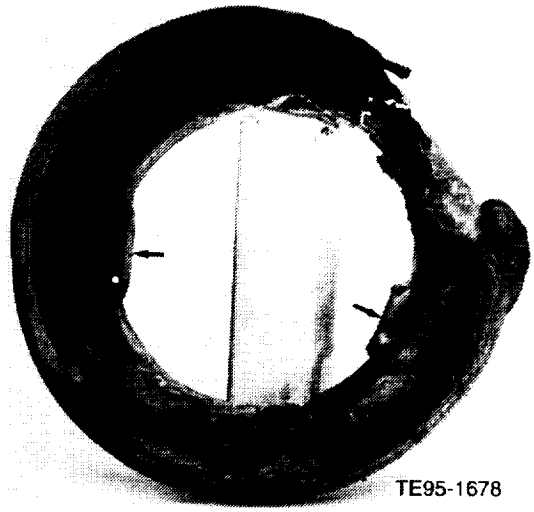


*Figure 3.1.3-16. As-torndown condition of the outer housing casting. Molten metal (at lower right) and carbon (upper left) were built up in the casting. Broken pieces of the valve seat (arrows) were held in position by the molten metal.*


*Figure 3.1.3-17. Reconstructed valve seat. The heavy arrow points to the fracture origin and the slender arrows indicated the main crack propagation direction.*


*Figure 3.1.3-18. Opposite view of the reconstructed valve seat showing the main crack ended at the outlet outside diameter, approximately 225 degrees from the origin.*

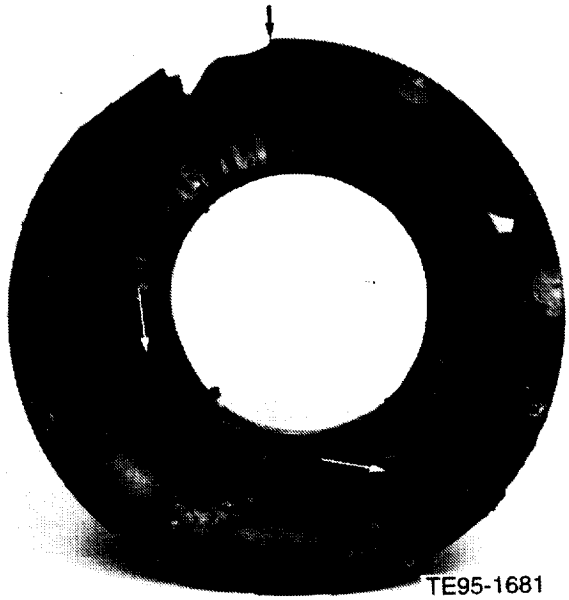


*Figure 3.1.3-19. Aft view of the valve seat. The arrow points to the origin. Slender arrows indicate the main crack propagation direction.*


*Figure 3.1.3-20. Optical fractograph of the valve seat origin area (hollow arrow) at the outside diameter.*

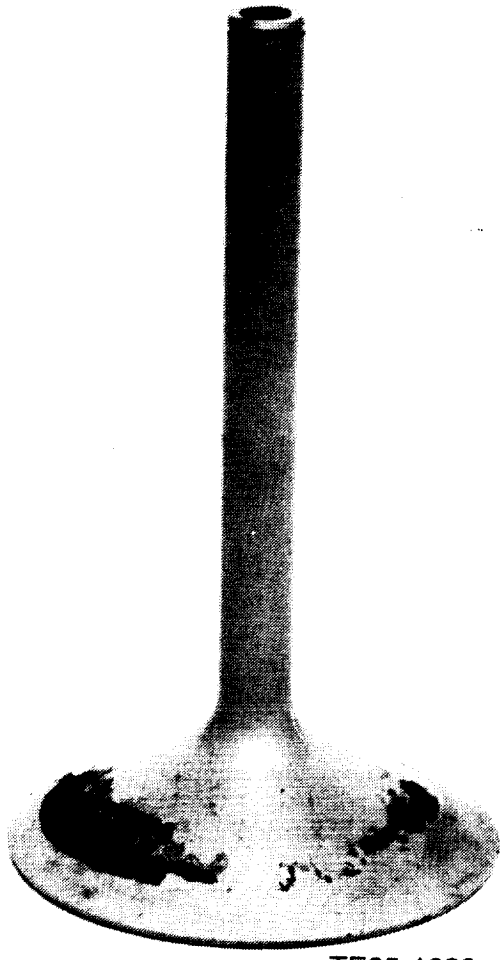


*Figure 3.1.3-21. As-torndown condition of the valve. The black material is deposited carbon.*

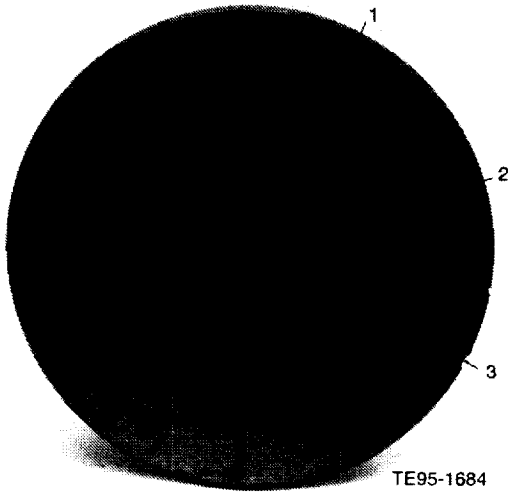


*Figure 3.1.3-22. Aft view of the valve. Pits were found at the back and outside diameter of the valve.*

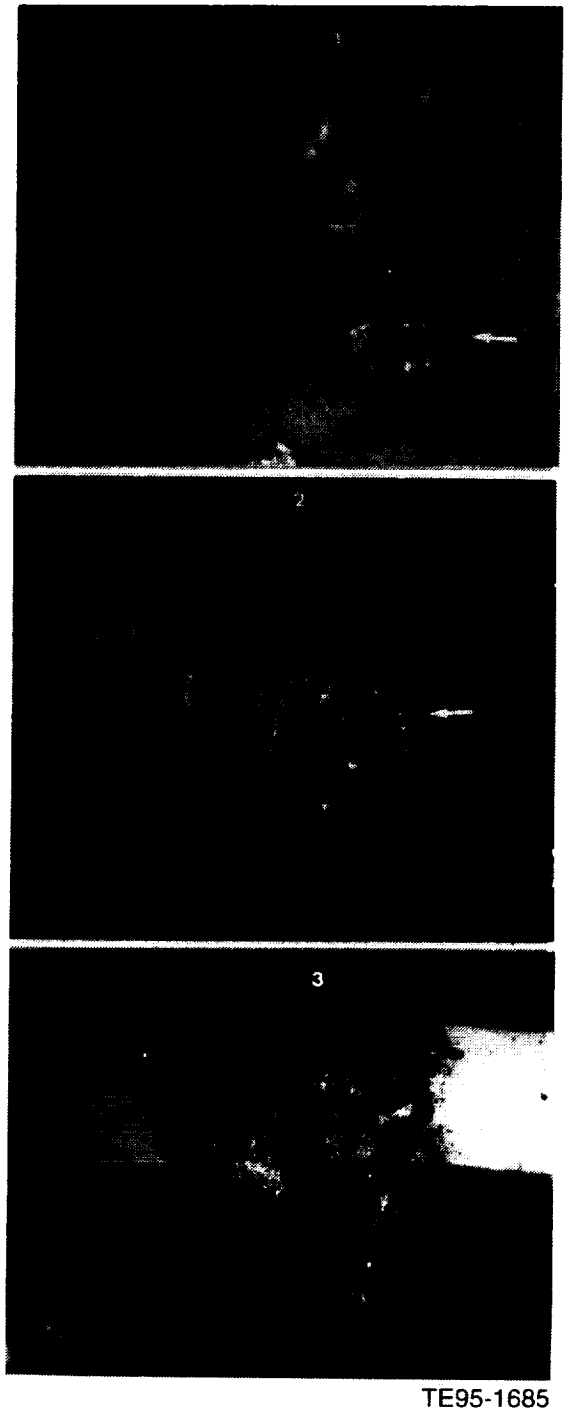


*Figure 3.1.3-23. Pits found at the back side of the valve (1 and 2 in the top photos) and at the outside diameter (3 in the bottom photo). Arrows point to the metallic deposits.*

## 3.2 CERAMIC COMPONENT PROCESS DEVELOPMENT AND FABRICATION

### 3.2.2 Schuller International

#### 3.2.2.1 Objective/Approach

Efforts at Schuller International have been directed toward the development of an injection moldable insulation system addressing low cost, high volume production for automotive gas turbines. The primary approach has been modifying the insulation material system for improved injection molding properties while developing the molding process for both simple and complex engine components. Additional developmental items being addressed include evaluation and improvements to insulation/metal bondability, cyclic durability, and erosion resistance.

#### 3.2.2.2 Accomplishments/Results

- A modified molding system was developed that resulted in improved mold filling and surface finish.
- Mold modifications were conducted to utilize the improved molding system for engine hardware.
- The cyclic durability burner rig was modified to accommodate both insulated gasifier housings and molded flat samples.
- The temperature capability of the burner rig was increased to 1315°C (2400°F).
- Injection molded insulation demonstrated improved metallic substrate bondability.

#### 3.2.2.3 Discussion

Summaries of all activities of Schuller International in support of the program during 1993 and 1994 are given in the annual reports provided by Schuller. The reports are included in Appendices A and B of this document.

### 3.2.4 Corning, Incorporated

#### 3.2.4.1 Objective/Approach

The objective of the regenerator activity with Corning, Inc., is the development of the materials and processing technology required for the fabrication of a reliable, low cost, high performance, one-piece extruded ceramic regenerator disk capable of operating for 3500 hours in an automotive gas turbine environment at temperatures up to 1150°C (2102°F) at the regenerator inlet.

Two ceramic material systems are being developed for this effort, lithium-aluminosilicate (LAS) and magnesium-aluminosilicate (MAS). In addition, commercially available sodium-zirconium phosphate compositions are being characterized for thermal and mechanical properties but are not subject to development activities. The extrusion die development approach has focused on the development of large diameter dies with a cell count of approximately 1100 rectangular cells/in.$^2$.

#### 3.2.4.2 Accomplishments/Results

- LAS compositions were developed that exhibited improved salt and sulfur corrosion resistance with reduced shrinkage.
- MAS compositional development resulted in increased retained strength after thermal exposure with decreased thermal expansion.
- NZP materials from LoTEC and VPI were procured and evaluated.
- A large diameter extrusion die was designed and fabricated with 1100 cells/in.$^2$.
- MAS regenerator disks were successfully extruded and fired.

#### 3.2.4.3 Discussion

Summaries of all activities of Corning, Inc., in support of the program during 1993 and 1994 are given in the annual reports provided by Corning. The reports are included in Appendices C and D of this document.

### 3.2.5 AlliedSignal Ceramic Components

#### 3.2.5.1 Objective/Approach

A ceramic component development effort was initiated with AlliedSignal Ceramic Components (ASCC) in October 1994. The objective of the ASCC HVTE-TS activity is the demonstration of gelcasting as a viable production process for the manufacturing of ceramic components. The gasifier turbine rotor is the primary focus of the component development efforts. The material

being used is AS800 $Si_3N_4$, a high temperature in-situ reinforced silicon nitride. The first year technical effort is focused on the two tasks of the fabrication of AS800 test specimens for Allison material characterization and the development and demonstration of process parameters for fabrication of gelcast axial rotors using reusable hard tooling.

### 3.2.5.2 Accomplishments/Results

- 100 slip cast AS800 $Si_3N_4$ test specimens (50 machined and 50 as-processed) were delivered to Allison for evaluation.
- Initial gelcasting trials of an existing axial turbine wheel were conducted.
- Hard tooling for an AGT-5 turbine rotor was designed and is being fabricated.

### 3.2.5.3 Discussion

Summaries of all activities of ASCC in support of the program during 1994 are given in the annual report provided by AlliedSignal. The report is included as Appendix E of this document.

## 3.2.6 Ceramics Process Systems

### 3.2.6.1 Objective/Approach

A development program with Ceramics Process Systems was conducted addressing fabrication of gasifier turbine rotors utilizing pressureless sintered SRS-201 duophase sialon material. Quickset low pressure injection molding was selected as the fabrication process. The program was directed toward fabrication of 20-blade rotors. The two major development areas were improvement of the rotor material (SRS-201 sialon) to improve the as-processed and machined surface strengths and Weibull modulus and the development and implementation of process parameters required to fabricate Quickset injection molded rotors that would meet all dimensional and structural requirements, including a proof spin test to 125,000 rpm.

### 3.2.6.2 Accomplishments/Results

- Improvements in the SRS-201 sialon material resulted in an average room temperature strength of 821 MPa (119 ksi) with a Weibull modulus of 13.1 for MIL-STD 1942 A-bars.
- Material (A-bars) sectioned from SRS-201 sialon rotors had an average room temperature strength of 953 MPa (138 ksi) with a Weibull modulus of 22.3 and a 1370°C (2500°F) strength of 516 MPa (75 ksi) with m=18.7.
- The as-processed strength of the SRS-201 was increased to 552 MPa (80 ksi) at room temperature and 477 MPa (69 ksi) at 1370°C (2500°F).
- 20-blade rotors were fabricated with excellent surface finish and dimensional tolerances. Proof spin testing resulted in 4 of 5 rotors passing the 125,000 rpm spin speed.

### 3.2.6.3 Discussion

Summaries of all activities of CPS in support of the program during 1993 are given in the annual report provided by CPS. The report is included as Appendix F of this document.

## 3.2.9 Norton Advanced Ceramics

### 3.2.9.1 Objective/Approach

The ceramic component development efforts being conducted with Norton Advanced Ceramics were directed towards two AGT-5 components, the gasifier turbine rotor and the turbine scroll. The turbine rotor activity was focused on fabrication of 20- and 26-blade configuration parts. Pressure slip casting was utilized for component production of both NT154 and NT164 silicon nitrides. Development of process parameters for the use of high pressure automated pressure slip casting was also addressed. The turbine scroll efforts have been focused on pressure slip casting of reaction sintered NT230 SiC. Extensive development and optimization of the automated high pressure casting process, including slip optimization, plastic mold formulation, and casting trials were conducted. In late 1994, a decision was made to transition the scroll development and fabrication activities to use NT164 $Si_3N_4$.

### 3.2.9.2 Accomplishments/Results

- The 20- and 26-blade configuration rotors of NT154 and NT164 $Si_3N_4$ were fabri-

cated, proof spin tested, and delivered for rig/engine evaluation.

- Process parameters and porous plastic mold materials were developed for automated high pressure slip casting of $Si_3N_4$ rotors.
- The cast strength of NT230 SiC slip was increased for pressure drain casting of AGT-5 scrolls.
- NT230 SiC slip and the porous plastic mold formulation were optimized for automated high pressure slip casting.
- Four NT230 SiC scrolls delivered to Allison for rig/engine test activities.
- NT154 and NT164 $Si_3N_4$ scrolls were successfully cast and densified.

### 3.2.9.3 Discussion

Summaries of all activities of Norton Advanced Ceramics in support of the program during 1993 and 1994 are given in the annual reports provided by Norton. The reports are included in Appendices G and H of this document.

# IV. COMPONENT RIG DEVELOPMENT AND TEST

## 4.1 COMPONENT RIG DEVELOPMENT

### 4.1.1 Combustor Rig Development

Test rig capability for automotive gas turbine low emissions combustor development is being provided. A natural gas-fired air topping heater was purchased to increase current laboratory air heating capability to achieve the elevated combustor inlet temperatures of regenerative engine cycles. Capacity will be 1.5 lb/sec of air at 982°C (1800°F), sufficient for all operating conditions.

The combustor rig (Figure 4.1.1-1) will accept interchangeable spool pieces for testing various combustor configurations. Orientation of the combustor within the rig will be identical to that in the engine. A turbine scroll will be incorporated to enable measurement of the TIT profile by thermocouple rakes located immediately downstream of the scroll. Emissions samples can be withdrawn through probes located at either of two axial planes downstream of the scroll.

The HVTE-TS poppet valve combustor and its variable geometry actuating mechanism installed in the combustor rigs are shown in Figure 4.1.1-2. Also shown in this view is a periscope with video capability for viewing the flame from the control room. Metal turbine scrolls will be cast for the periscope option; however, when measuring the TIT profile, a scroll without the periscope mount will be installed to avoid disruption of the normal flow in the scroll.

A plan view of the rig installed in the Combustion Research Facility at Allison is shown in Figure 4.1.1-3. The air topping heater will be located immediately outside the laboratory wall, closely coupled to the rig inlet to minimize heat losses at the extremely high combustor inlet temperatures required.

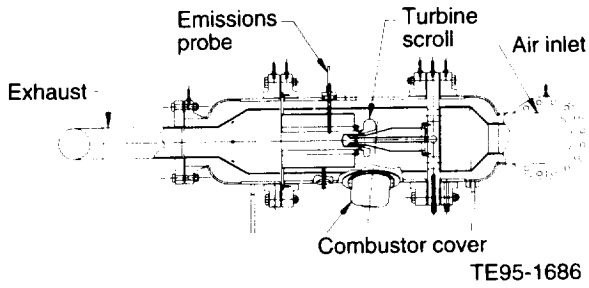


*Figure 4.1.1-1. Automotive gas turbine combustor test rig.*

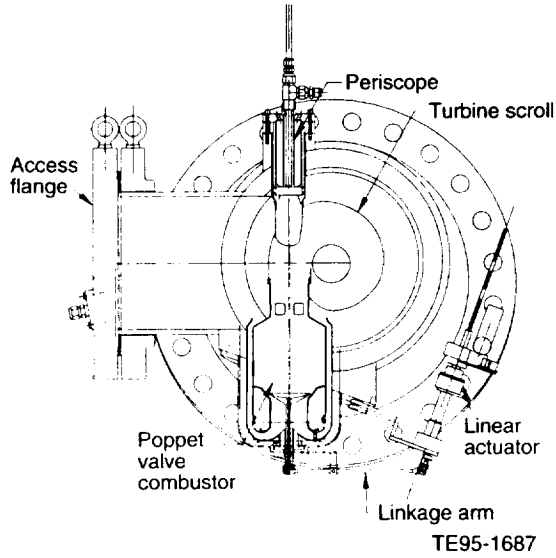


*Figure 4.1.1-2. Poppet valve low emissions combustor installed in combustor test rig.*

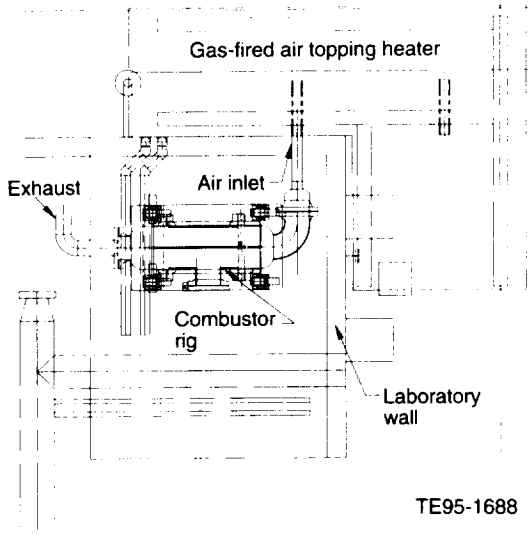


*Figure 4.1.1-3. Plan view of combustor test rig and air topping heater installed in research laboratory.*

Design of the combustor rig was in progress at the end of 1994.

## 4.1.2 Hot Gasifier Rig Development

### 4.1.2.1 Objective/Approach

The hot gasifier rig is under constant development to enhance the rig's capability to test ceramic gasifier components under full reference power train design (RPD) conditions. A secondary objective was to transfer all activities from the GM Technical Center to Allison Engine Company. These activities included rig and engine testing, metal hardware design and fabrication, and drafting.

### 4.1.2.2 Accomplishments/Results

- Completed the design and fabrication of squeeze film dampers for both the compressor and turbine bearings.
- Verified the damped bearing system in a fully instrumented gasifier housing with a ceramic scroll and rotor.
- Transitioned all design and test activities from the GM Technical Center to Allison Engine Company
- Inventoried, packaged, and shipped hardware and test rig components to Allison.
- Initiated the selection and design of a new test facility located at Allison.
- Completed the construction of engineering and shop facilities.
- Completed the installation and set up of a Unigraphics CAD system.

### 4.1.2.3 Discussion

*Rotor dynamics.* In 1992, rotor dynamic analysis predicted rotor instabilities in the operating range of the engine. Also in 1992, testing with full shaft dynamic instrumentation confirmed the presence of predicted rotor instabilities (for more details see the 1992 ATTAP annual report). To stabilize the gasifier rotor, both the compressor and turbine bearings needed squeeze film dampers. Sealed dampers were incorporated into the bearing carriers to ensure proper damping and to limit oil flow requirements. Figure 4.1.2-1 shows the cross section of the compressor bearing and damper configuration. The turbine damper is of a similar design.

The damped bearing system was tested in the gasifier hot rig with three proximity probes and two accelerometers. The gasifier used a full ceramic turbine assembly because the dampers were designed for the lighter turbine. A listing of the ceramic parts and test history is described in subsection 4.2.3.3 (Hot Gasifier Testing S/N 14 Build 32). Figure 4.1.2-2 shows the measured peak-to-peak shaft deflections for the gasifier rotor over the operating speed range. The design goal of limiting deflections to less than 0.001 in. was achieved. The rotor also behaved as predicted, with decreasing deflections with increasing speed. The deflections are reduced with speed because the dampers become more effective at their design speed. Upon disassembly and inspection, the dampers showed no signs of wear. All subsequent builds used this damper system.

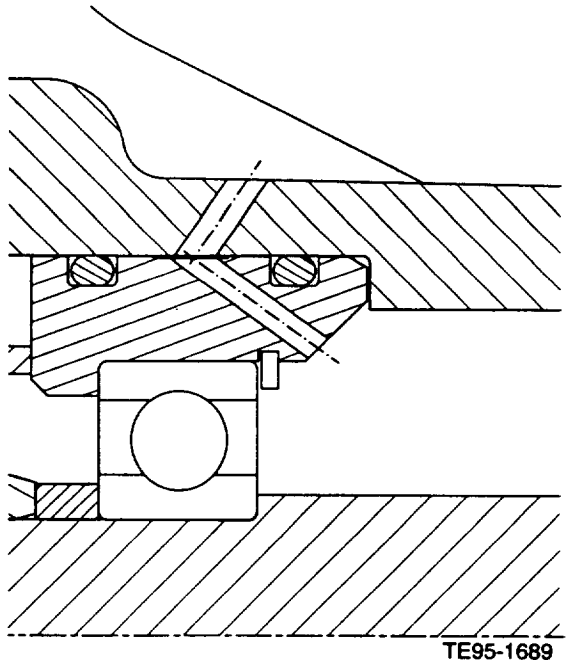


*Figure 4.1.2-1. Damped bearing cross section.*

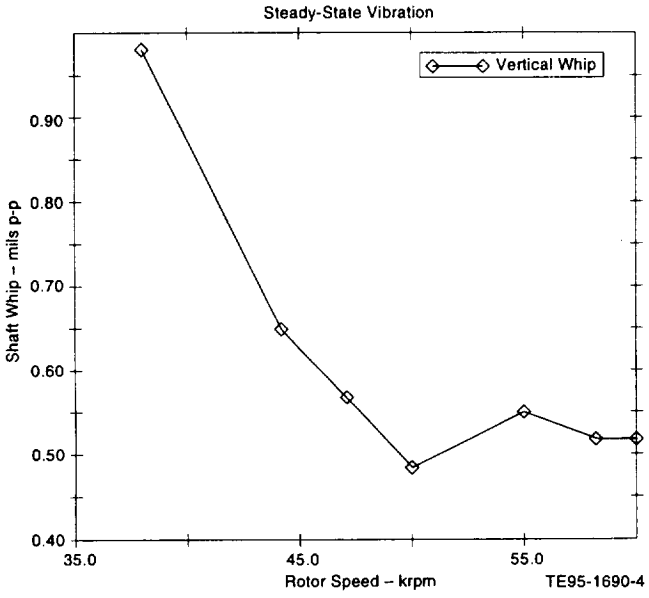


*Figure 4.1.2-2. AGT-5 S/N 14 BU 32 steady-state vibration.*

*Relocation.* In order to continue the testing program initiated in the GM Tech Center, engineering and test facilities were established in Indianapolis, Indiana at the Allison Engine Company facility. Test rigs located at the GM Tech Center were disassembled and shipped to Allison.

A complete inventory of hardware and tooling was completed while the hardware was boxed and cataloged for shipment to Allison. The project completely transitioned to Allison by late 1993. Test equipment included the gasifier hot rigs, engines, dynamometer, and supporting hardware.

Engineering personnel were relocated in October 1994 with the assembly, machine shop, and garage areas completed in December 1994.

The engineering staff was equipped with Unigraphics CAD systems with such features as three-dimensional solid modeling, parametric modeling capabilities, interface to rapid prototyping systems, improved surface capabilities, and commonality with subcontractor/vendor CAD systems.

## 4.1.4 Regenerator Rig Development

### 4.1.4.1 Control System

The regenerator test rig was delivered from the GM Tech Center to Allison. While the test stand was mechanically operational, the control system software was unfinished. The software was originally developed for AGT-5 applications including 1) the AGT-5 regenerator rig, 2) the AGT-5 engine test rig, and 3) the Chevrolet Caprice.

Significant modifications had been started in adapting the control system software development package to incorporate the controls necessary to operate the regenerator rig test stand. Software development remained before the control system could safely operate the existing regenerator rig test stand.

Modifications to the control system were begun in October 1994 by Allison HVTE-TS controls personnel. Reorganization of the control source code was accomplished to facilitate easier understanding of the completeness of the code.

Significant effort was put into the understanding of the basic organization of the control system design theory. It was determined that a steady-state speed control was the short term rig operation target. The durability cycle software for the rig test stand required the most development.

Early in December, it was recommended the existing control system be replaced with a newly developed system. The durability cycle software required substantial development, the supplier for the controller hardware was no longer in business, spare parts were not available.

Several trials were undertaken to get the software to operate the regenerator rig safely in a controlled, steady-state manner.

### 4.1.4.2 Design Of Cold Flow L-Seal Test Rig

Allison has established a target 3% leakage goal for the entire regenerator system. This is a very

aggressive target. In order to reach this goal all parts of the regenerator seal system must be functioning in an optimum manner. A key part of the seal system is the secondary L-seals, and in order to support their development a special test fixture has been designed.

The fixture, shown in Figure 4.1.4-1, is designed to test one D-shaped seal section. Six Ds comprise one engine set of secondary seals. The fixture will accommodate the two L-seal segments, that comprise the D, and the helper springs. The clear plexiglass cover plate allows the L-seals and springs to be observed during the test. Shims allow for axial extension of the L-seal, which simulate seal platform wear or different regenerator build clearances. The cover plate has a large opening in the center allowing the leakage air to vent. It also allows Pitot probes to be inserted and swept around the interior of the D to locate sources of leakage. The L-seals and springs fit into a groove machined into a removable plate that in turn fits into the base plate of the flow fixture. By making the plate removable, it is possible to use the same fixture for a variety of springs and L-seal configurations.

### 4.1.4.3 Design of Single Disk Hot Flow Performance Rig

The single disk hot flow performance rig is planned to be used for regenerator system development testing beginning in the third quarter of 1995. This rig accepts a single disk and the seals from either side of the engine. The rig is shown in plan view in Figure 4.1.4-2. The rig operates at steady-state engine conditions, with electrically heated inlet air and gas side inlet air heated by a gas-fired burner.

The rig air plumbing consists of heavy wall 300 series stainless external pipe, to carry pressure loading, with a durable internal liner of Hastelloy X sheet to withstand high temperature operation and thermal cycling. To reduce heat loss, the space between the pipe and liner is injected with insulation supplied by the program's insulation subcontractor.

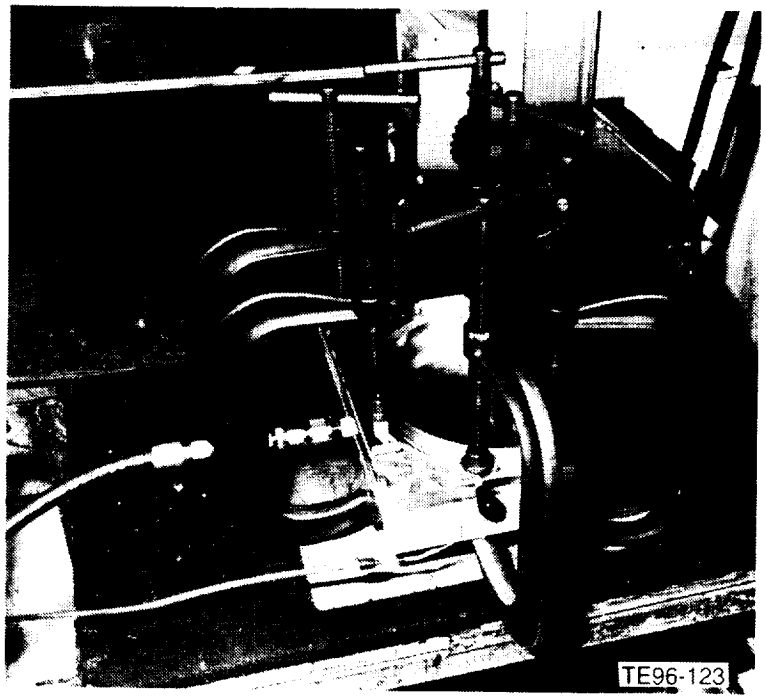


*Figure 4.1.4-1. Cold flow test fixture for measuring secondary seal leakage.*

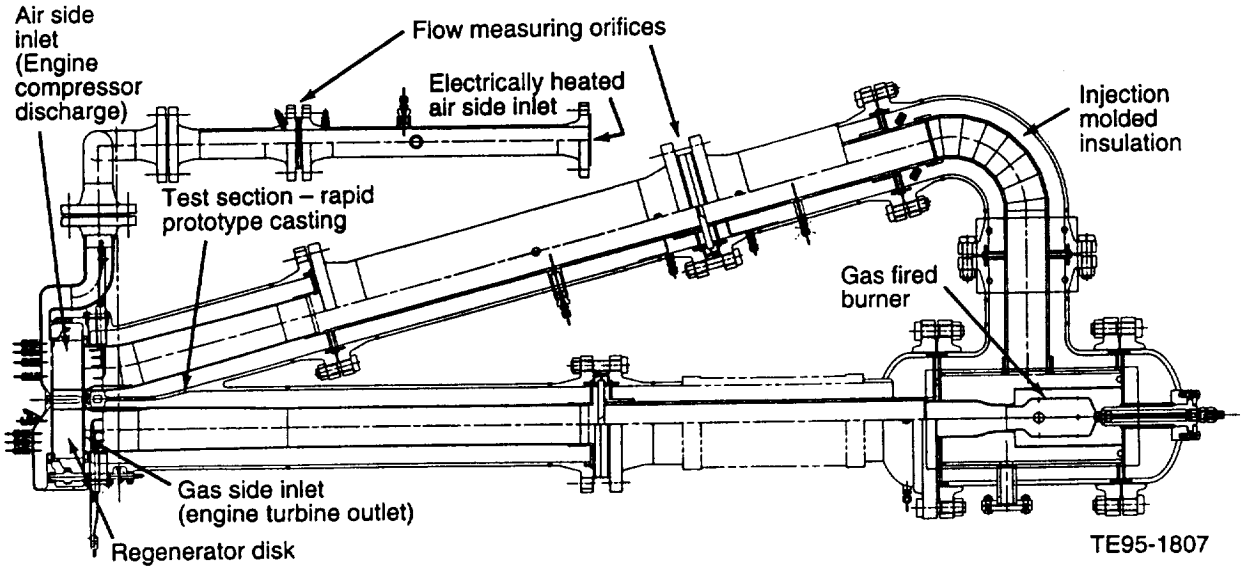


*Figure 4.1.4-2. Plan view of single disk hot flow regenerator rig.*

Orifices upstream and downstream of the high pressure half of the disk measure airflow. The difference between these flows is regenerator system leakage, the measurement of which is the primary purpose of this rig. Extensive pressure and temperature instrumentation at the inlet and exit of both the air and gas halves of the disk provide data to calculate pressure drop and disk thermal effectiveness and to assess flow distribution. A torque meter in the drive system measures disk drive torque, useful in evaluating seal wearface materials and clamping forces. In addition, to measure disk and seal performance parameters under controlled, high temperature conditions, the rig can evaluate mechanical design integrity with short-term durability tests.

Thousands of development hours have been accumulated on similar rigs designed to test both the 25 in. diameter disk regenerator system of the IGT404 engine and the 18 in. system of the AGT-100. The HVTE-TS rig builds upon this experience and improves on it in two important areas. First, the test section of the HVTE-TS rig eliminates many test section hot joints that must be sealed, monitored, and resealed over time to maintain accurate leakage measurements. Secondly, the HVTE-TS rig operation, data gathering, and data reduction functions are all computer controlled by a PC dedicated to the rig. This provides consistent operation, shorter data analysis periods between tests, reduced operating manpower requirements, and enhanced data storage and retrieval.

### 4.1.4.4 Regenerator Transient Gasifier Rig

A regenerator transient rig has been designed and modified consisting of an engine without the power turbine. It uses twin regenerator disks.

The rig fulfills two purposes:

1. exposes regenerator disks to thermal cyclic transients similar to those expected in the developmental engines
2. exposes regenerator disks to NaCl salt typical of seashore and winter drilling environments to check chemical stability

A test stand and the gasifier were assembled at Allison. Figure 4.1.4-3 shows the rig installed on the test stand. The rig is currently ready to continue control system development testing and to begin cycle development testing.

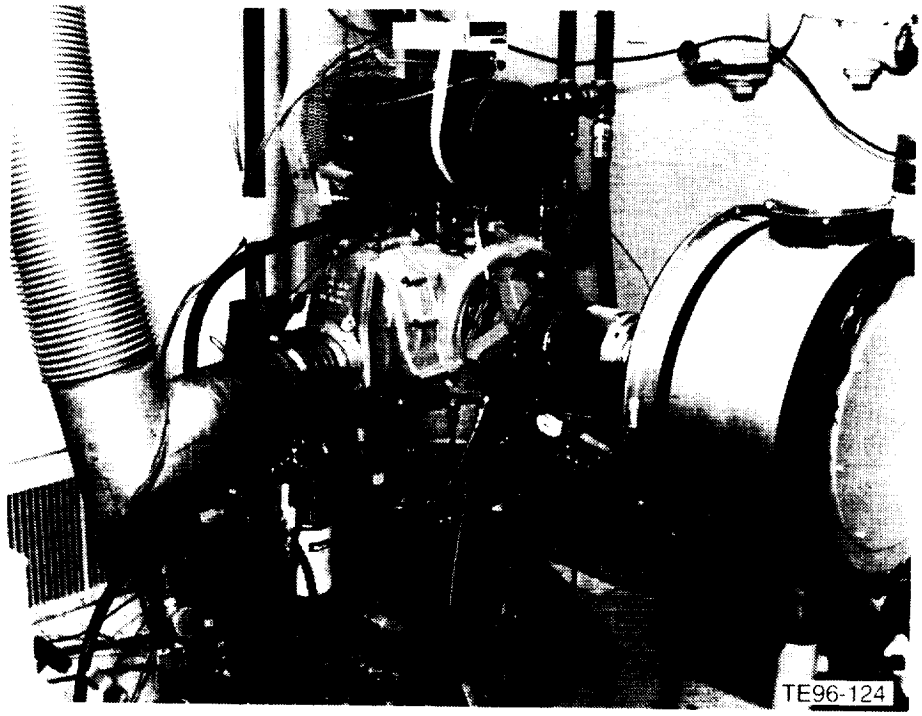


*Figure 4.1.4-3. Regenerator transient gasifier rig installed in an Allison test cell.*

### 4.1.4.5 Thermal Cyclic Sample Rig

A gas-fired thermal cyclic sample rig has been used for many years by Allison to expose 1.5 x 2.5 x 3 in. samples of regenerator disk material to simulated engine acceleration temperatures to determine loss in strength. The rig was modified to more closely follow engine cycle acceleration temperature spikes.

A 10,000 cycle test was run on an extruded AS sample with no identifiable loss in hot face strength. No explanation for this unusual result was found. The cycle was devised to simulate AGT-5 accelerations with 2090°F momentary peak temperature. Next, a 10,000 cycle test on EX22 MAS was repeated, simulating AGT-5 acceleration with 2090°F peak temperature. For the repeated test, all rig improvements were in place to ensure accurate temperature. The MAS retained 31% of original strength based on the assumption that the third through fifth slices represent original strength. This 31% retained strength compares to the 22% measured in 1990 before rig improvements.

Strength measurements were run on unexposed samples of MAS with, and without, an extruded outer skin. The average MOR strength of 18 bars from the sample with skin was 342 psi and the sample without skin was 384 psi. These measurements were well within normal sample variation. Nevertheless, it was agreed that samples should be supplied without skin to eliminate potential problems.

Predictions of the development engine regenerator inlet temperature transients were obtained for accelerations and starts. Much less severe than on previous engines, accelerations involved only an 80°F step increase in temperature to 1800°F. Starts were much more severe, with a rapid step from ambient to 1900°F, held for three seconds, and followed by a one second decrease to 1250°F. A rough simulation of starts was undertaken. Ten percent was added to the 1900°F peak to account for burner pattern. The fastest possible steps were made from 1350°F to 2090°F for three seconds and back to 1350°F for 13 seconds. Since the cyclic rig depends on valving excess air, ambient low temperatures cannot be simulated.

## 4.2 COMPONENT RIG TESTING

### 4.2.3.3 Hot Gasifier Testing

**4.2.3.3.1 Objective/Approach.** Hot gasifier rig testing is used to screen/proof test and evaluate structural ceramic components (combustors, gasifier turbine components, and regenerators) prior to introduction into the AGT-5 test-bed engine(s). The rig is a complete gasifier from the AGT-5 engine, where the ceramic turbine drives the compressor supplying air to the turbine. This type of rig duplicates real engine conditions to prove ceramic durability while saving the cost of full engine test.

**4.2.3.3.2 Accomplishments/Results.**

- tested five all-ceramic gasifier turbine assemblies with an accumulated 82.9 hours, including durability schedule testing peak conditions of 1327°C (2420°F) at 97% speed
- five of five ceramic turbine rotors passed proof testing with metal turbine scrolls
- tested new bearing and damper system for the gasifier turbine shaft in the hot gasifier rig

**4.2.3.3.3 Discussion.** Hot gasifier rigs were used in 1993 to test six ceramic rotors and five ceramic scrolls. Five all-ceramic gasifier assemblies were proof tested with two assemblies run on the durability schedule for a total of 82.9 hours. The durability cycle was modified to simulate the 1992 RPD update on the Combined Federal Driving Cycle (CFDC). The cycle was modified to better simulate real world vehicle use and to avoid premature failure of supporting metal hardware and insulation damage. The new cycle is one hour long, while the CFDC is about 55 minutes. There are two starts per hour with one 10-minute soakback. The maximum rotor speed during the new cycle is 90%, corresponding to an RIT of 1150°C (2100°F). All durability testing in 1993 was done on the new cycle, which is also being used for the 300-hour durability test attempts.

All-ceramic rotors were proof tested on a modified durability cycle for 10 hours with peak conditions of 95% speed at 1150°C (2100°F) before installation into an all-ceramic gasifier assemblies. The proof testing was done in the gasifier hot rig with a metal scroll and vane assembly. In 1993 five of five ceramic rotors were proof tested with no failures.

*S/N 14 Build 27 (1.1 hours).* An all-ceramic gasifier assembly consisting of a Norton advanced concept scroll and Kyocera 15-bladed rotor was tested to 97% gasifier speed and 1327°C (2420°F). Table 4.2.3-I lists the major ceramic parts tested in this build. The housing was instrumented with three proximity probes to monitor shaft dynamics. The leads to the probes were burned off by an air leak early in the test and did not yield useful information. The gasifier assembly ran for 1.1 hours before all the ceramic hardware was destroyed during a slow acceleration from idle. After reviewing the video tape of the turbine, eight rubs were observed in various locations. The complete failure analysis is described in subsection 3.1.3.

*S/N 14 Build 32 (4.3 hours).* An all-ceramic gasifier assembly consisting of a Norton advanced concept scroll and a Norton 20-bladed rotor was tested to 95% gasifier speed and 1150°C (2102°F). Table 4.2.3-I lists all of the ceramic parts tested in this build. To reduce vibratory shaft deflections and subsequent tip rubs, squeeze film dampers were installed over both the turbine and compressor bearings. Complete shaft dynamic instrumentation was installed with three proximity probes and two accelerometers. The new bearings and dampers ran successfully, limiting shaft deflections to 0.001 in. peak to peak. The new damper parts showed no signs of wear.

When assembled to the turbine housing, the piston ring flange of the scroll was damaged. The scroll breakage was blended out and reinstalled into the housing. At 4.3 hours of running, another piston ring flange crack was observed during a planned shutdown. The breakage was too severe to continue testing. After a thorough inspection of all the parts, it was found that piston rings were bottomed out on the

*Table 4.2.3-I.*
*Ceramic parts on test.*

| Component | Serial number | Supplier | Material |
|---|---|---|---|
| S/N 14 BU 27 | | | |
| Scroll | KX61200 | Norton | NT230, SiC |
| Tab mount ring | | Norton | NT154, $Si_3N_4$ |
| Seal ring | | Norton | NT154, $Si_3N_4$ |
| Rotor (15Nb) | 5K9 | Kyocera | SN252, $Si_3N_4$ |
| S/N 14 BU 32 | | | |
| Scroll | KX61314 | Norton | NT230, SiC |
| Tab mount ring | | Norton | NT154, $Si_3N_4$ |
| Seal ring | | Norton | NT154, $Si_3N_4$ |
| Rotor (20Nb) | 122X-1 | Norton | NT164, $Si_3N_4$ |
| S/N 14 BU 35 | | | |
| Scroll | KX61227 | Norton | NT230, SiC |
| Tab mount ring | | Norton | NT154, $Si_3N_4$ |
| Seal ring | | Norton | NT154, $Si_3N_4$ |
| S/N 14 BU 38 | | | |
| Scroll | KX244-18 | Norton | NT230, SiC |
| Tab mount ring | | Norton | NT154, $Si_3N_4$ |
| Seal ring | | Norton | NT154, $Si_3N_4$ |
| Rotor (20Nb) | 1538-75 | Norton | NT154, $Si_3N_4$ |
| S/N 12 BU 45 | | | |
| Scroll | KX61234 | Kyocera | NT230, SiC |
| Rotor (20Nb) | 5K23 | Kyocera | NT154, $Si_3N_4$ |

scroll. The interference was the result of oversized piston rings and oxidation of the power turbine nozzle.

*S/N 14 Build 35 (50.8 hours).* An all-ceramic gasifier assembly, consisting of a Norton advanced concept scroll and a Norton 20-bladed rotor, was tested to 95% gasifier speed and 1150°C (2102°F). Table 4.2.3-I lists the major ceramic parts tested in this build. During initial running, the shaft deflections were relatively large at 3 mils peak to peak. The turbine rotor was replaced in an attempt to reduce vibrations but there was no significant change in vibrations. The original rotor was rebalanced using a more rigorous method, but the shaft deflections were not reduced. No turbine tip rubs or excessive bearing wear was observed, so the rig started durability test.

After 25 hours of running, the turbine assembly was removed from the rig for a scheduled inspection. All the parts looked good with no measurable change in turbine tip clearance. The turbine was installed into the hot rig for further testing. One hour later a regenerator ring gear

attachment failed. A 1/8 inch chip in one of the turbine blades was observed after the regenerator failure. Another regenerator was installed and testing was resumed. The rig ran without incident until hour 50 when the rotor failed to pull through a start after a 10-minute soakback. The scroll shroud was fractured and several rotor blades were chipped. The complete failure analysis is described in subsection 3.1.3.

*S/N 14 Build 38 (26.4 hours).* An all-ceramic gasifier assembly consisting of a Norton advanced concept scroll and a Norton 20-bladed rotor was tested to 95% gasifier speed and 1150°C (2102°F). Table 4.2.3-I lists the major ceramic parts tested in this build. The scroll mount hardware was modified so the metal cross key tabs were positioned by metal-to-metal contact instead of relying on clamp load friction to maintain centering. The modifications were done to prevent turbine rotor tip rubs caused by the scroll moving off center.

Initial proof testing of the all-ceramic turbine went without incident, so the rig was placed on the durability schedule. After 26.3 hours of running, the turbine assembly was removed from the rig for a scheduled inspection. All the turbine parts looked good, so the rig was reassembled for further durability testing. On the first acceleration following the inspection, the rotor and scroll broke. There were no signs of tip rub observed in the video tape of the test. The ceramic scroll and rotor were broken into many small pieces. The complete failure analysis is described in subsection 3.1.3.

*S/N 12 Build 45 (0.3 hours).* An all-ceramic gasifier assembly consisting of a Kyocera scroll and a Kyocera 20-bladed rotor was tested to 95% gasifier speed and 1150°C (2102°F). Table 4.2.3-I lists the major ceramic parts tested in this build. The hot rig housing, S/N 14 , was replaced by S/N 12 because the insulation had deteriorated to the point that replacement was justified. A metal turbine assembly was installed in the hot rig to verify its installation before the ceramic hardware was installed. During proof testing, the ceramic rotor was released from the metal shaft. The rotor was debladed, while the scroll shroud suffered some trailing edge chips and one crack. On disassembly, it was found that an outdated seal carrier was used, greatly reducing the amount of cooling air circulating to the metal/ceramic joint. The complete failure analysis is described in subsection 3.1.3.

All testing to date on ceramic scrolls and rotors is summarized in Table 4.2.3-II.

*Table 4.2.3-II.*
*Ceramic component data base.*

| Supplier | Number of blades | Material | Hours on test 1993 total | Hours on test Cumulative total | Peak speed-% | Peak temperature-°C (°F) |
|---|---|---|---|---|---|---|
| Norton | 20 | NT154 | 35.5 | 35.5 | 90 | 1150 (2102) |
| Norton | 20 | NT154 | 12.3 | 12.3 | 95 | 1150 (2102) |
| Norton | 20 | NT164 | 62.6 | 62.6 | 95 | 1150 (2102) |
| Norton | 20 | NT164 | 15.9 | 15.9 | 95 | 1200 (2192) |
| Norton | 20 | NT154 | 0.0 | 224.7 | 100 | 1350 (2460) |
| Norton | 20 | NT154 | 0.0 | 12.0 | 100 | 1180 (2155) |
| Kyocera | 15 | SN252 | 12.6 | 12.6 | 97 | 1327 (2421) |
| Kyocera | 15 | SN252 | 0.0 | 229.0 | 101 | 1385 (2552) |
| Kyocera | 15 | SN252 | 0.0 | 22.4 | 100 | 1380 (2515) |
| Kyocera | 20 | SN252 | 0.0 | 279.8 | 100 | 1380 (2515) |
| Kyocera | 20 | SN252 | 0.3 | 13.1 | 100 | 1150 (2100) |
| Kyocera | 20 | SN252 | 0.0 | 0.5 | 100 | 1115 (2040) |
| Kyocera | 20 | SN252 | 0.0 | 22.7 | 100 | 1408 (2566) |
| Kyocera | 15 | SN252 | 0.0 | 0.8 | 90 | 1277 (2331) |
| Kyocera | 15 | μSiC | 0.0 | 0.0 | 40 | N/A |
| Kyocera | 20 | SN252 | 0.0 | 1000.7 | 98 | 1395 (2543) |
| Kyocera | 20 | SN252 | 0.0 | 3.9 | 90 | 1160 (2120) |
| Kyocera | 20 | SN252 | 0.0 | 7.9 | 101 | 1150 (2102) |
| Kyocera | 15 | SN251 | 0.0 | 365.0 | 100 | 1150 (2102) |
| Total | | | 139.2 | 2322.1 | | |

| Supplier | Type | Material | 1993 total | Cumulative total | Peak speed-% | Peak temperature-°C (°F) |
|---|---|---|---|---|---|---|
| Kyocera | Standard | SN252 | 0.3 | 0.3 | 90 | 1150 (2102) |
| Norton | Advanced | NT230 | 26.4 | 26.4 | 90 | 1150 (2102) |
| Norton | Advanced | NT230 | 50.8 | 50.8 | 95 | 1150 (2102) |
| Norto | Advanced | NT230 | 4.3 | 4.3 | 95 | 1150 (2102) |
| Norton | Advanced | NT230 | 1.1 | 1.1 | 97 | 1327 (2420) |
| Kyocera | Advanced | SN252 | 0.0 | 267.7 | 100 | 1380 (2515) |
| Norton | Standard | NT230 | 0.0 | 1.5 | 100 | 1050 (1920) |
| Kyocera | Standard | SN252 | 0.0 | 13.5 | 100 | 1380 (2515) |
| Kyocera | Standard | SN252 | 0.0 | 196.5 | 100 | 1385 (2525) |
| Norton | Standard | NT230 | 0.0 | 8.9 | 100 | 1350 (2460) |
| Kyocera | Advanced | SN252 | 0.0 | 1.1 | 82 | 930 (1706) |
| Kyocera | Advanced | SN252 | 0.0 | 5.2 | 100 | 1406 (2563) |
| Kyocera | Advanced | SN252 | 0.0 | 7.2 | 99 | 1406 (2554) |
| Total | | | 82.9 | 584.5 | | |

# V. PERFORMANCE AND DURABILITY TESTING

## 5.1 COMBUSTION TESTING

Design of the AGT-5 poppet valve premixing combustor shown in Figure 5-1 was described in the 1992 Allison Annual Report. The combustor contains two ceramic parts by Norton Advanced Ceramics, an NT154 silicon nitride valve and an NT230 silicon carbide valve seat. Initial engine testing of this combustor was performed from July through October of 1993 on an engine dynamometer stand at the GM Tech Center. Steady-state emissions measurements were taken over a range of engine speeds spanning the bulk of the automotive emissions driving cycle (Figure 5-2). Poppet valve position was also varied during testing. Valve position control and fuel transfer from start to main nozzle are described in subsection 1.4.4.

Some test results were extremely encouraging. Poppet valve positions were found at which all three regulated pollutants met California ULEV standards; that is, under steady-state conditions, the combustor met program goals. In fact, assuming 42 miles per gallon (mpg) for the RPD vehicle, emissions were about one half of their regulated levels as predicted (Figure 5-2). The lean stability of the combustor was also better than expected; however, the combustor was susceptible to flashback and could not be lit reliably with a spark ignitor.

The five engine builds during which the poppet valve combustor was tested are summarized below.

### 5.1.1 Build 3

Testing included several ignition attempts at various valve positions. Initially, ignition could be achieved, but the engine would not accelerate to idle speed. Further attempts were required to find a valve position at which the engine could be started and successfully accelerated to idle speed.

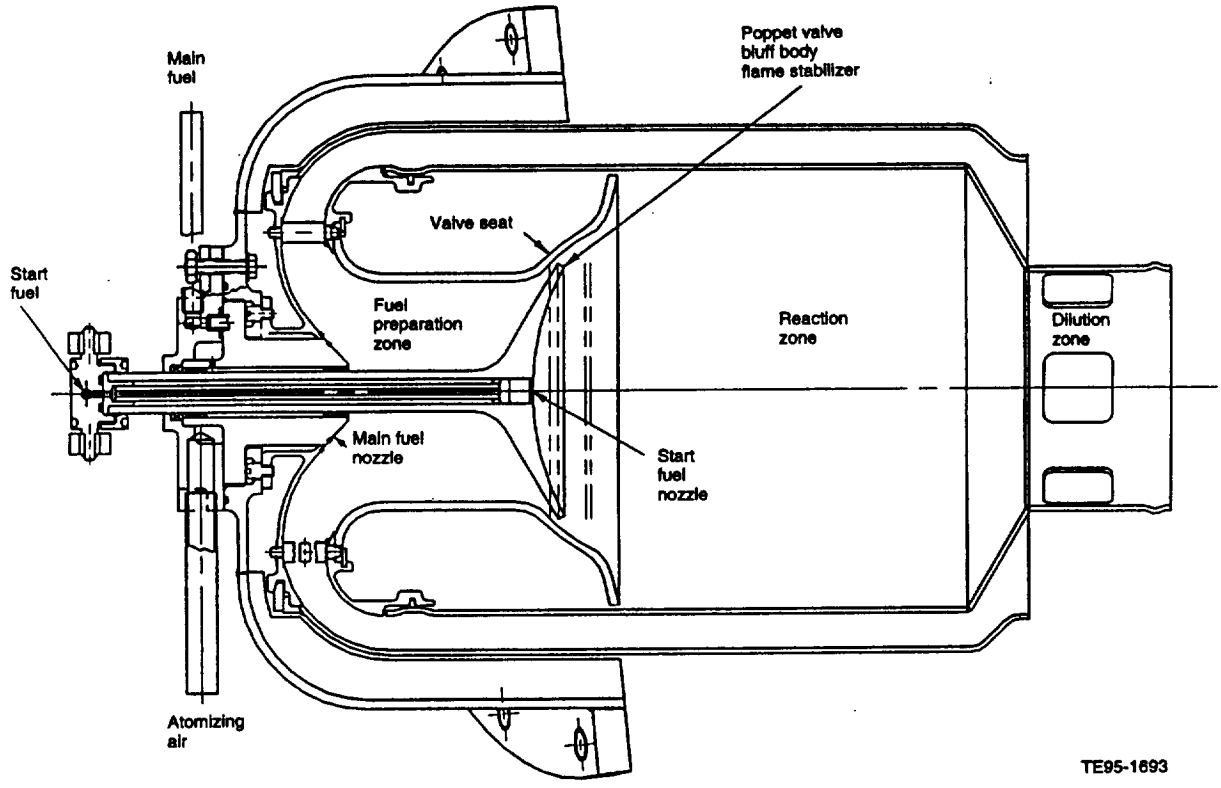


*Figure 5-1. Poppet valve premixing combustor.*

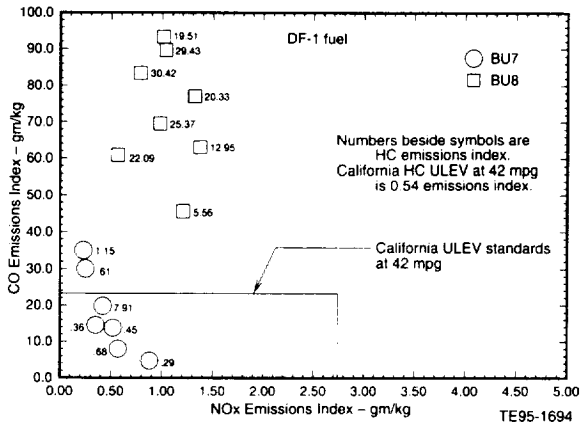


*Figure 5-2. Poppet valve combustor steady-state emissions test results.*

Fuel transfer from start to main nozzle was attempted following a brief warm-up period. Solenoid valves were used to open the fuel line to the main nozzle and, after a one-second delay, close the fuel line to the start nozzle. Fuel transfer was successful as the engine continued to run smoothly.

Three hardware failures occurred during Build 3. A start fuel nozzle was damaged due to insufficient cooling air. Following a fuel transfer, air is used to blow out the start nozzle. Air then continues to flow for cooling. The overheating problem was remedied by increasing the differential pressure on the purge/cooling air.

Two viton seals were damaged during soakback following shutdown. The seals are located in the flange through which main fuel and atomizing air enter the combustor. This flange was later determined to run at 204°C (400°F) when the combustor is operating, but reaches 427°C (800°F) following shutdown. One seal was replaced by graphite and the other by ceramic rope and no further problems were encountered.

The third hardware failure was caused by a pool of fuel that formed in the combustor following initial unsuccessful start attempts. This fuel ignited, possibly on the first successful start, causing damage to the valve seat and metal combustor parts. Means for draining fuel following a false start were designed into most areas of the combustor; however, a low spot in the casting that supports the valve seat and inner liner did not have a drain hole. Fuel pooled and ignited at this location, causing the damage. A drain hole was added for subsequent builds and no further problems with fuel pooling were encountered. Further details of the failure analysis are included in subsection 3.1.3.

The combustor never did behave as it had when operating in the premixing mode. Both stability and emissions were insensitive to valve position. Damage to the inner liner allowed air to bypass the fuel preparation zone and directly enter the reaction zone causing a diffusion flame mode of operation. $NO_x$ emissions were on the order of half of their levels with the standard AGT-5 diffusion flame combustor, but were much higher than expected if the poppet valve combustor had been operating as intended.

### 5.1.2 Build 4

Modifications for Build 4 included a drain hole added to the inner casting to prevent the fuel pooling problem encountered in Build 3. Also, a zirconia thermal barrier coating was added to the inside surface of the inner liner to reduce metal temperatures. Finally, a manually adjustable blocker ring was installed over the dilution holes to allow diversion of more air through the fuel preparation and reaction zones.

This test extended over a period of several days, during which all attempts to light the poppet valve combustor were unsuccessful. Different igniters were tried as well as variations in igniter position, igniter immersion depth, poppet valve position, start fuel flow, and dilution hole blocker ring position. All igniters were checked outside the engine to ensure they were firing properly. The combustor could not be lighted by spark ignition.

### 5.1.3 Build 5

For Build 5, a methane/oxygen torch igniter was installed in place of the spark ignitor. The combustor lit successfully; however, fuel was observed leaking out around the torch ignitor mounting adapter and the engine was shut down. Because the torch did not fit tightly in the ignitor hole in the inner liner, fuel was able to leak between the torch and the inner liner. The combustor was removed to inspect for damage, but none was found.

### 5.1.4 Build 7

In preparation for Build 7, a patch designed to fit tightly around the torch ignitor was attached to the inner liner. Build 7 was the most successful in the poppet valve combustor test series.

The engine was started and accelerated to idle and the torch ignitor was shut off. A small amount of fuel was still leaking from the torch ignitor mounting bracket so the engine was shut down. The dilution hole blocker ring was moved to the half open position to increase combustor pressure drop and the engine was restarted. Fuel was no longer leaking from the ignitor mounting bracket and the blocker ring was maintained in the half open position for the remainder of the test.

The engine was restarted and fuel transferred from start to main nozzle. Several steady-state data points were taken at various gasifier speeds at various valve positions. Emissions measured at these points are plotted as the round symbols in Figure 5-2. Valve positions were found where all three regulated emissions $NO_x$, CO, and UHC met California ULEV standards assuming 42 mpg for an RPD vehicle.

Occasionally, the combustor would flashback during steady-state operation. At times, a noise could be heard from the control panel indicating that combustion instability or that compressor surge had caused the flashback. At other times, there was no audible warning. When flashback occurred, all inner liner metal temperatures increased, as did $NO_x$ emissions. More sophisticated means of detection were not necessary. No damage was observed due to flashback. All temperatures along the length of the inner liner increased when the flame flashed back into the fuel preparation zone. During flashback, as well as during operation on the start nozzle, $NO_x$ emissions were about 50% higher than with the standard AGT-5 diffusion flame combustor. After flashback, normal premixing operation could be restored by transferring fuel to the start nozzle and then transferring back to the main nozzle.

Several attempts were made to accelerate the engine from 60% to 70% gasifier speed to continue testing, but the engine would not respond. Fuel nozzle carboning was suspected as the cause of the problem. Even with both start and main nozzle solenoids open, the engine would not accelerate to 70% speed. The test was stopped and the nozzles removed for flow checking. Subsequently, a test cell control problem was found to be responsible for the inability to accelerate. Flow check confirmed the nozzles were not obstructed.

### 5.1.5 Build 8

During testing of Build 8, the combustor was more susceptible to flashback and the compressor more susceptible to surge than in the previous build. Several data points were taken at various gasifier speeds, but when speed was increased to 70%, flashback problems increased. The dilution hole blocker ring could be moved to a more open position to alleviate surge and to a more closed position to alleviate flashback. However, a reliable window of operation with neither surge nor flashback could not be found, so testing was stopped.

Measured emissions are plotted as the square symbols in Figure 5-2. The low emissions of Build 7 could not be duplicated in Build 8. $NO_x$, CO, and UHC were all higher in Build 8. ULEV standards were not met at any of the steady-state test points. Further investigation and understanding of poppet valve combustor performance will be deferred until the AGT-5 engine test stand is operational at Allison.

## 5.2 TEST SUMMARY

Initial testing of the ATTAP poppet valve premixing combustor was performed in an AGT-5 gas turbine engine on an engine dynamometer stand at the General Motors Technical Center. Emissions measurements were taken at steady-state conditions at various gasifier speeds. This range comprises the bulk of the current automotive emissions driving cycle. Valve position was also varied.

Some results were extremely encouraging. In Build 7, valve positions were found at which all three regulated pollutants met California ULEV standards, i.e. under steady-state conditions the combustor met program goals. In fact, assuming 42 mpg for an RPD vehicle, emissions were

about one half of their regulated levels as predicted.

The excellent emissions measured in Build 7 could not be duplicated in Build 8. The cause was not determined and further investigation will be performed on the AGT-5 engine stand at Allison.

The combustor was susceptible to flashback. The difficulty associated with performing combustor development testing in an engine rather than a rig was evident since in most cases it was difficult to determine whether flashback was caused by combustor or compressor instability. In cases of more severe compressor surge, the cause was obvious. Other times, without audible clues, the cause was not obvious. In the future, instrumentation capable of detecting disruptions in flow through the engine will be installed.

Other conclusions and recommendations from this test series are as follows:

- The ignitor opening through the inner liner needs to be well sealed to avoid fuel leakage. If possible, the ignitor should preferentially be located on the top of the combustor.
- Additional development is required to light the combustor with a spark ignitor rather than having to resort to a torch ignitor.
- The start fuel nozzle material should be upgraded or additional cooling air supplied. The start nozzle should be designed to survive with cooling air pressure set equal to the main nozzle atomizing air pressure of 7 psid.
- The flow number of the start fuel nozzle should be reduced to improve atomization at start fuel flows and the ability to ignite. The spray angle should also be increased to get more fuel in the vicinity of the ignitor.
- Seals in the fuel nozzle mounting flange must be able to withstand 427°C (800°F) during soakback.
- Flashback occurred both during compressor surge and during apparently normal operation.
- $NO_x$ emissions and all inner liner wall temperatures increase after flashback.
- The silicon nitride valve and silicon carbide valve seat were not damaged by flashback; however, flashback still must be eliminated to meet $NO_x$ goals.
- Following flashback the fuel preparation zone could be cleared of flame by transferring fuel from main nozzle to start nozzle and back again.
- As would be expected, flashback tendency decreased as dilution hole area was reduced and surge tendency decreased as dilution hole area was increased.
- For the purpose of these tests, the method of flashback detection ($NO_x$ and wall temperatures) was sufficient; however, it remains to be determined whether some more rapidly responding means of flashback detection will be required to reliably meet $NO_x$ goals over the transient driving cycle.
- The lean stability of the poppet valve combustor was much better than expected. Correlations of bluff body flame stability and chemical kinetic stirred reactor modeling had both predicted blowoff at certain low speed operating conditions. This did not occur.

# APPENDIX A

Schuller International
1993

NOTE: INFORMATION SUBMITTED THAT IS DEEMED TO BE
PROPRIETARY IN NATURE
HAS BEEN DELETED.

# ADVANCED TURBINE TECHNOLOGY APPLICATIONS PROJECT (ATTAP)
# NASA CONTRACT DEN3-336

## ANNUAL PROGRESS REPORT 1993

## INSULATION FOR GAS TURBINE ENGINE

## ALLISON PO# H321549


SUBCONTRACTOR:

MOUNTAIN TECHNICAL CENTER
SCHULLER INTERNATIONAL
BOX 625005
LITTLETON, COLORADO 80162-5005

PREPARED BY:

PHILLIP C. MARTIN


FEBRUARY 1994

PREPARED FOR ALLISON ENGINE COMPANY

### 3.2.2 SCHULLER

#### Objective/Approach

Efforts at Schuller are aimed at developing an injection moldable insulation capable of low-cost high-volume production for automotive gas turbines. The approach is to modify the insulation material system for improved injection molding properties while developing the injection molding process for both simple and complex engine components. In addition to the development of the molding process, several other developmental items are being addressed including: insulation to metal hardware bond ability, cyclic durability and erosion resistance.

#### Accomplishments/Results

##### Cyclic Durability/Erosion Resistance Testing

- Designed cyclic durability test including a burner system and insulation sample holder.
- Installed cyclic durability/erosion burner system.
- Sound control enclosure installed to reduce the environmental impact of the burner.
- Elevated temperatures in sound enclosure reduced by installing additional ventilation.
- Burner firing cycle adjusted to longer time at >1800°F during flame on portion of cycle and for lower temperature during flame off portion of cycle.
- Cyclic durability test of hand-molded insulation terminated at 10,500 cycles showing only minor surface cracking and no obvious erosion of the insulation surface.
- Cyclic durability test of injection molding insulation terminated at 10,500 cycles showing no surface cracking and no obvious erosion of the insulation surface.
- Injection molded insulation for cyclic durability test appeared to have better bond to sample holder than the hand molded insulation.
- Modified cyclic durability sample holder to observe impact of reduced coolant flow on durability performance of insulation.

##### Pilot-line Molding of Simple Pieces

- Completed design of pilot-line molding with Aeroquip Corporation and issued purchase order for trial molding.
- Aeroquip fabricated the pilot-line gasifier housing molding equipment.
- Initial molding trial identified required modifications to mold, vents, and release liners.
- Replaced fractured polycarbonate gasifier housing mold with aluminum mold.
- Replaced undersized hydraulic piston on injection ram with larger capacity piston.
- Successfully molded four (4) gasifier housings on the pilot molding equipment at Aeroquip. Sent pilot line molded gasifier housings to Schuller for evaluation.

##### Materials Characterization

- Measured thermal conductivity of insulation at different densities.

## Discussion

### Cyclic Durability/Erosion Resistance Testing

The burner system designed to expose the insulation to conditions expected in the operating engine has been installed. The burner exposes the insulation to about 1800°F with an impingement velocity of about 250 feet per second for 15 seconds every 60 seconds. The cyclic exposure is to last for 10,000 cycles or failure, whichever occurs first. The test system design includes a high velocity natural gas burner, an air/fuel ratio control valve, air operated control solenoids, timers and counters, safety shut-offs, and an insulation mounting fixture. Temperatures are monitored during the exposure at the hot and cold surfaces of the insulation and in the fixture. Observations of the exposed surface of the insulation will indicate the possible need for erosion resistant surface treatments. If needed these surface treatments can be applied and tested with this system.

Initial test firings of the burner system showed that sound levels at the burner are high enough to require control measures. Sound level measurements in the vicinity of the burner showed substantial noise levels generated at low frequencies. A sound control enclosure has been constructed to reduce the environmental noise impact of the burner. The sound levels appear to be reduced sufficiently to eliminate the problem. The temperature in the sound enclosure was elevated, requiring additional ventilation inside the enclosure. A higher capacity power ventilator has been installed.

The first insulation sample was hand molded on to the sample holder and test firings to 10,500 cycles were conducted. During this first test, the time-temperature cycle was adjusted to subject the insulation to the most severe conditions anticipated in an operating turbine engine. The burner firing cycle was adjusted to achieve temperatures in excess of 1800°F for a longer time. Plots of typical cycle temperatures follow.

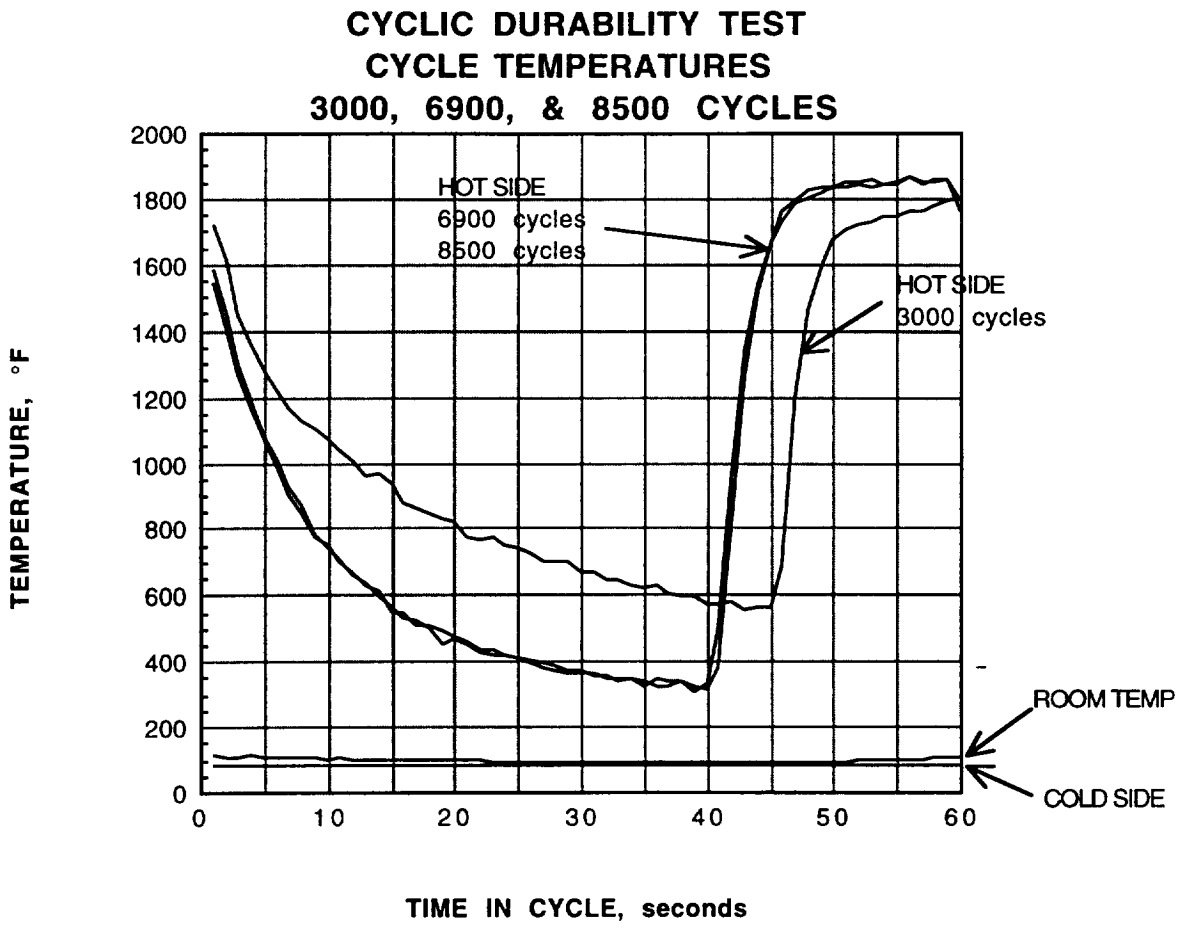
CYCLIC DURABILITY TEST
CYCLE TEMPERATURES
3000, 6900, & 8500 CYCLES
TEMPERATURE, °F
2000
1800
1600
1400
1200
1000
800
600
400
200
0
0
10
20
30
40
50
60
HOT SIDE
6900 cycles
8500 cycles
HOT SIDE
3000 cycles
ROOM TEMP
COLD SIDE
TIME IN CYCLE, seconds

## CYCLIC DURABILITY
## CYCLE TEMPERATURE
## 9000 CYCLES

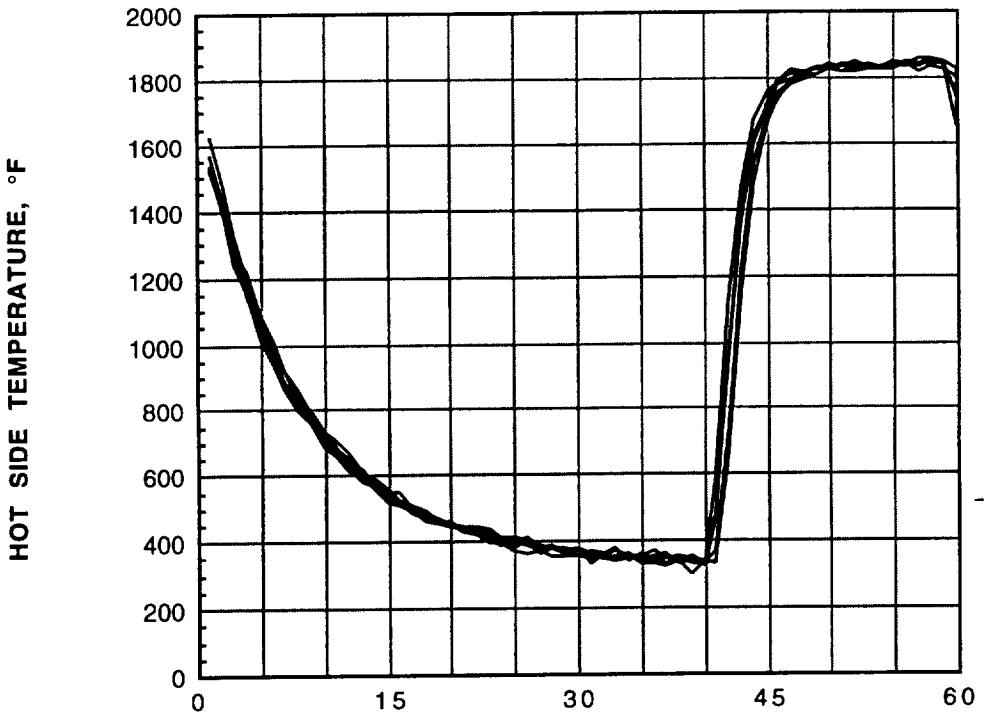

## CYCLIC DURABILITY
## TEMPERATURE CYCLE
## 9000 CYCLES

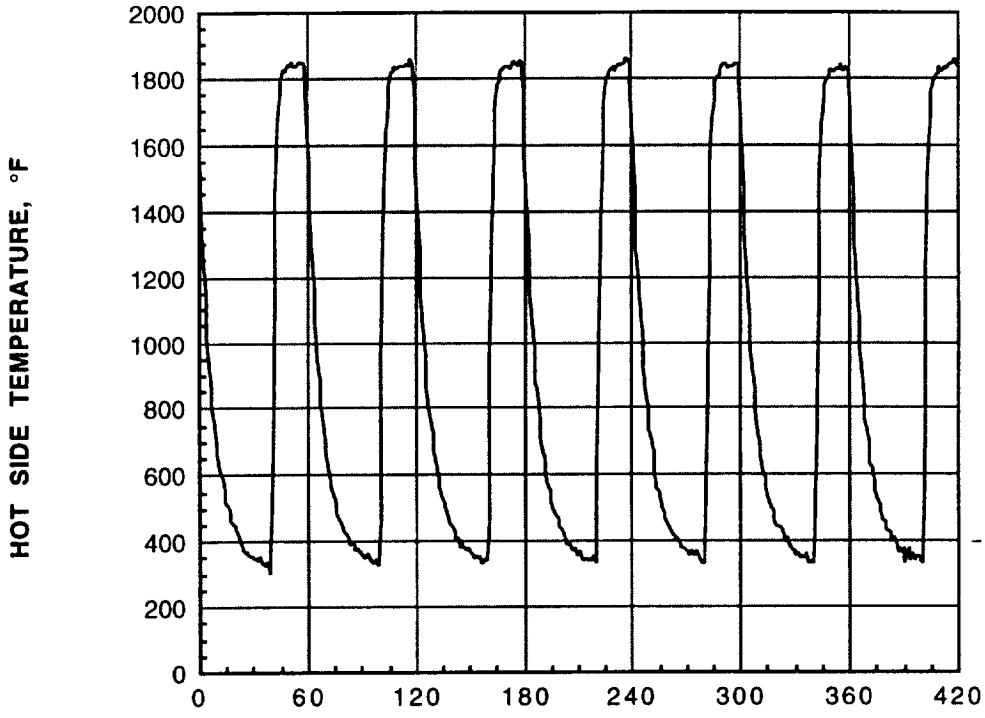

The first insulation sample was exposed to 10,500 cycles. The insulation sample showed no obvious sign of distress from the impact of the 1800°F, 250 ft/s flame. The only damage to the insulation appeared to be from the movement of the hot side thermocouple on the surface of the insulation.

The second test sample was the injection molding insulation with the burner flame normal to the insulation surface. A total of 10,500 cycles was completed with no obvious distress of the insulation. The center portion of the flame contact location on the insulation, a spot about three inches in diameter, appeared to be darkened slightly from the initial blue-green. The insulation remained firmly attached to the sample holder, whereas the first sample of hand molded insulation debonded very early in the test. The insulation surface appeared tough, almost a rubbery feel when pressed by hand.

Modifications of the sample holder have been made to obtain additional temperature measurements. The second sample, referred to above, has been used to evaluate the performance of the insulation with reduced cooling of the insulation on the cold side. The cold side temperature ranged from less than 80°F to 201°F.

## Pilot-line Molding of Simple Pieces

Aeroquip Corporation was issued a purchase order to complete the design, fabrication, and operation of a pilot-line molding operation for molding gasifier housings. Initial trials at Aeroquip to "shake-down" the molding equipment identified several areas of concern that required equipment modifications. These included mold modifications, mold venting, gasifier housing/mold mismatches, and mold release liner flaws. The gasifier housing mold mismatches were eliminated. The mold release liner flaw elimination was addressed by GM.

A confirmation trial injection of the gasifier housing piece and mold resulted in the fracture failure of the polycarbonate mold. The aluminum mold used for single injection molding trials at Schuller was sent to Aeroquip. A purchase order was issued to Aeroquip to modify the equipment to accommodate the mold cavity. After the mold modifications were completed, the molding equipment was tested again. The hydraulic piston on the injection ram appeared to be undersized. A larger capacity piston was specified and ordered. Another purchase order was issued to Aeroquip to modify the molding equipment to accommodate the larger piston.

The trial pilot molding of gasifier housings was conducted at Aeroquip. The first molding attempts resulted in incomplete part coverage at the nose of the gasifier housing. Further attempts resulted in the wet insulation completely filling out the mold and covering the part after clamping the base of the gasifier housing to the bottom flange of the mold cavity. This resulted in complete venting of the mold through the nose. The insulation was then forced to fill out the mold and vent area. Four (4) gasifier housings were successfully injection molded to simulate a production molding operation. The molded parts were transported to the GM Technical Center and dried over-night at 225°F. The finished parts were shipped to Schuller for evaluation.

## Materials Characterization

Thermal conductivity testing of 18 pcf and 22 pcf hand molded insulation in the high temperature calorimeter showed that the conductivity was the same at lower mean temperatures. At higher mean temperatures the higher density insulation showed a lower conductivity. The normal temperatures in an operating engine are not expected to expose the insulation to a mean temperature in excess of 1000°F. Therefor no significant difference in thermal performance is expected as a result of variations in insulation density. A plot of thermal conductivity for these two samples and previously tested insulation at 23 pcf is shown in the following figure.

## THERMAL CONDUCTIVITY
## HAND MOLDED

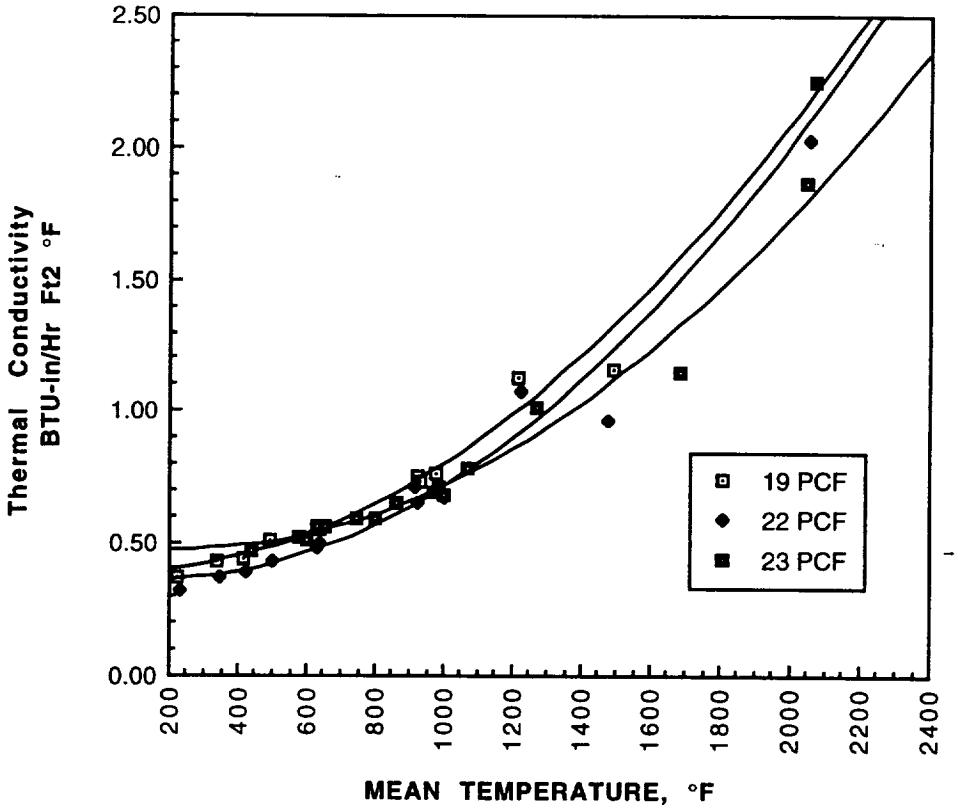

# APPENDIX B

Schuller International
1994

NOTE: INFORMATION SUBMITTED THAT IS DEEMED TO BE
PROPRIETARY IN NATURE
HAS BEEN DELETED.

# ADVANCED TURBINE TECHNOLOGY APPLICATIONS PROJECT (ATTAP)
# NASA CONTRACT DEN3-336

## ANNUAL PROGRESS REPORT
## 1994

## INSULATION FOR GAS TURBINE ENGINE

## ALLISON PO# H321549

## SUBCONTRACTOR:

MOUNTAIN TECHNICAL CENTER
SCHULLER INTERNATIONAL
BOX 625005
LITTLETON, COLORADO 80162-5005

## PREPARED BY:

PHILLIP C. MARTIN

JANUARY 1995

## PREPARED FOR ALLISON ENGINE COMPANY

## 3.2.2 SCHULLER

### Objective/Approach

Efforts at Schuller are aimed at developing an injection moldable insulation capable of low-cost high-volume production for automotive gas turbines. The approach is to modify the insulation material system for improved injection molding properties while developing the injection molding process for both simple and complex engine components. In addition to the development of the molding process, several other developmental items are being addressed including: insulation to metal hardware bond ability, cyclic durability and erosion resistance.

### Accomplishments/Results

#### Molding System Development

- o Modification of the molding system developed.
- o Modified molding system results in improved mold fill-out and improved surface finish with no "popcorning" as seen in prior injection moldings.
- o Started mold modifications for AGT-5 gasifier housing to accommodate the improved molding system.
- o Molded test samples for cyclic durability using the improved molding system.

#### Cyclic Durability/Erosion Resistance Testing

- o Cyclic durability test equipment has been modified to accommodate both insulated gasifier housings and molded flat samples of insulation.
- o Initial testing of an insulated gasifier housing showed some cracking of the insulation at the nose of the gasifier housing.
- o Reinsulated gasifier housing exposed to >5000 cycles with very minor cracking at the edges of the flame impingement area.
- o Modified the erosion/cyclic durability test sample holder to allow improved injection molding.
- o Cyclic durability testing of improved injection molded material started at ~1800°F and increased temperature ~100°F after every 1000 cycles.
- o Cyclic durability testing reached temperatures >2400°F for 1000 cycles with evidence of small cracks in the flame impingement area but no signs of failure of the insulation.
- o Injection molded insulation for cyclic durability test appeared to have better bond to sample holder than the hand molded insulation.
- o Single application injection molded insulation appears to remain intact better than insulation applied in more than one shot of the injection cylinder.

### Materials Characterization

- Measured thermal conductivity of insulation molded using the improved molding system.
- Measured thermal conductivity of alternate insulation materials, including more thermally efficient microporous insulations, molded using the improved molding system.

## Discussion

### Molding System Development

Attempts to mold alternate insulation materials for internal Schuller projects have resulted in development of modifications to the injection molding system for the turbine engine insulation. The modifications result in much improved mold fill-out and surface finish. The improved surface finish eliminates the "popcorning" of the previous injection molding system. The new technique requires some mold modifications. The molding system modifications will permit rapid evaluation of the molding capabilities of alternate materials. Samples for cyclic durability/erosion resistance testing have been molded using this improved technique and have been tested on the cyclic durability test burner. The AGT-5 gasifier housing mold is being retooled to allow molding using the improved molding technique.

### Cyclic Durability/Erosion Resistance Testing

The burner system designed to expose the insulation to conditions expected in the operating engine installed last year has been used to test the insulation for cyclic durability and erosion resistance. The burner was designed to expose the insulation to about 1800°F with an impingement velocity of about 250 feet per second for 15 seconds every 60 seconds. The cyclic exposure is to last for 10,000 cycles or failure, whichever occurs first. The test system design includes a high velocity natural gas burner, an air/fuel ratio control valve, air operated control solenoids, timers and counters, safety shut-offs, and an insulation mounting fixture. Temperatures are monitored during the exposure at the hot and cold surfaces of the insulation and in the fixture. Observations of the exposed surface of the insulation will indicate the possible need for erosion resistant surface treatments. If needed these surface treatments can be applied and tested with this system.

The first insulation samples (both hand molded and injection molded) tested, in 1993, for 10,500 cycles showed no obvious signs of distress from the impact of the 1800°F, 250 ft/s flame. An erosion/cyclic durability test sample, marked "6449-75-5" in the following figure, has been subjected to 1000 cycles on the cyclic test burner holder at >1800 °F and > 250ft/sec (15 seconds "on" - 45 seconds "off") and at ~2000°F for 1000 cycles. There was no evidence of erosion or cracking of the insulation at these two conditions. The burner flame was adjusted to ~2140°F and the sample was subjected to 1000 cycles. There was no evidence of erosion but several small cracks appeared in the flame impingement area. These cracks were very small and could be seen when the insulation was at room temperature. At high fire of the burner, the cracks were not seen. The sample was subjected to ~2220-2240°F for 1000 cycles and to ~2320-2340°F with no further evidence of distress to the insulation. The sample was subjected to ~2400-2420°F. The sample was tested to 1000 cycles with no further evidence of distress to the insulation.

A piece of insulation (~1/2" by 1" by 2-4 mm thick) flaked off from the lower right corner of the sample near the molding injection port, suggesting that this flake may be from a thin layer applied during the second stroke of the injection molding ram. This second layer may not have bonded well to the first layer and separated from the base layer. This observation may provide insight into the cracking and debonding of hand applied insulation seen in test rigs over the testing history of ATTAP.

**EROSION/CYCLIC DURABILITY TEST SAMPLE**
**6449 - 75 - 5**

(BEST PHOTO AVAILABLE)

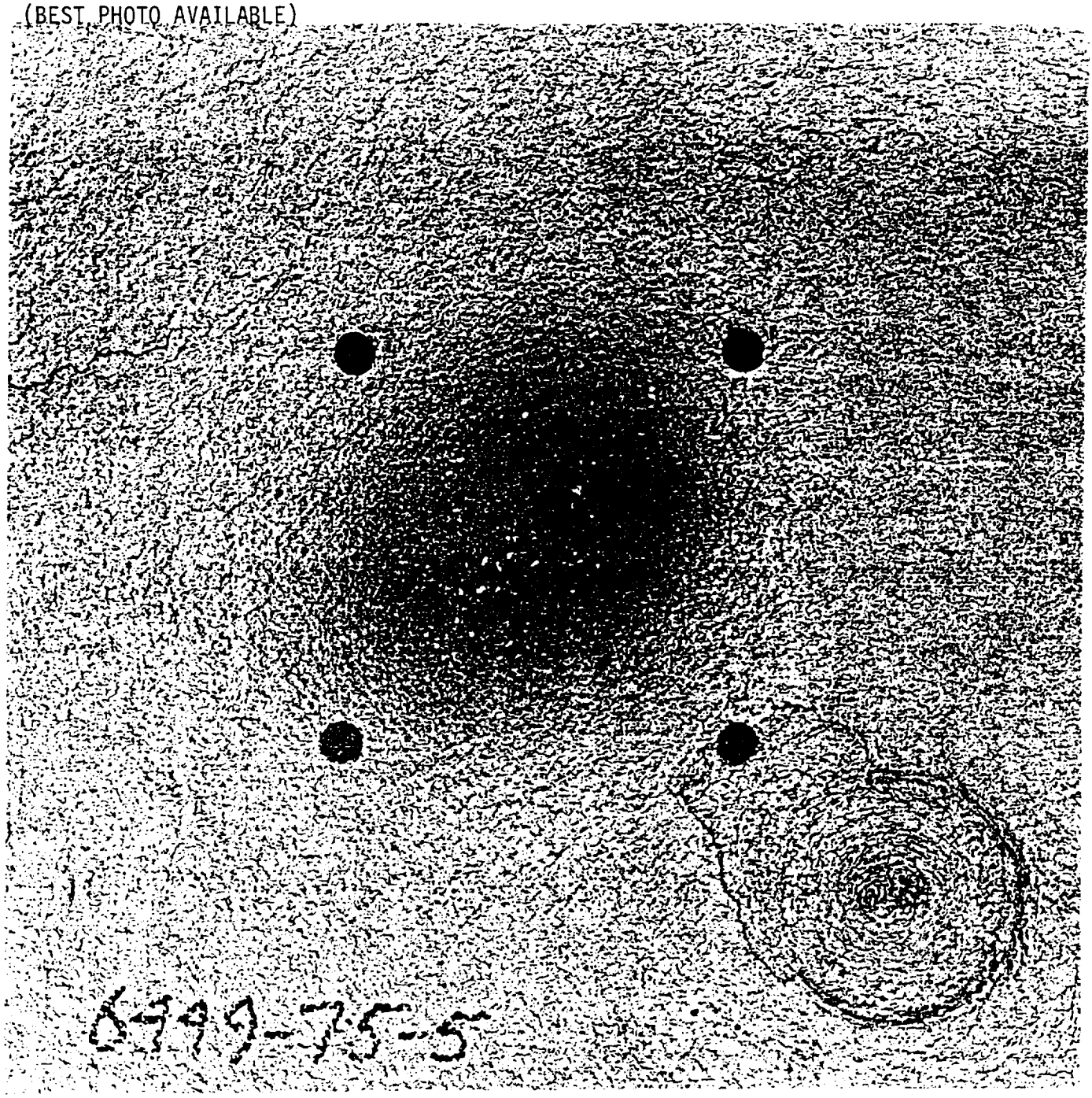

## Materials Characterization

Samples of material molded using the improved molding technique were evaluated for thermal conductivity. The thermal conductivity of the base turbine insulation, molded at 26 pcf, was essentially the same as that for 22 pcf hand-molded material previously tested. The results are shown in the following plot of thermal conductivity.

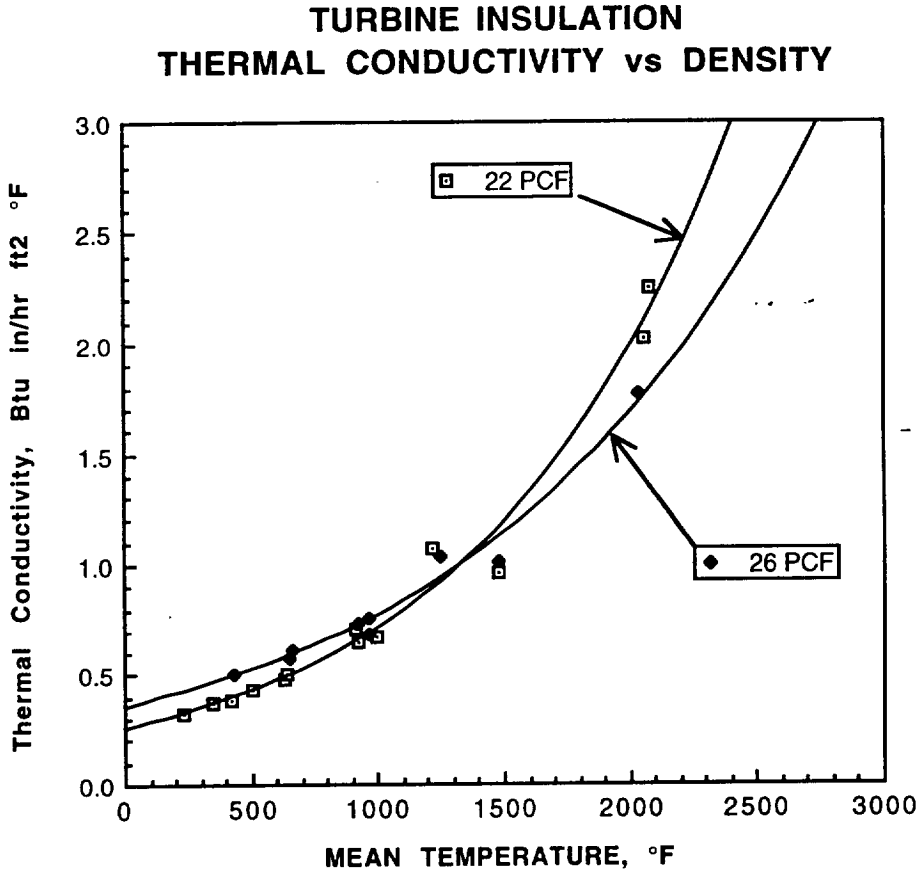


An injection molded sample of a 50:50 by volume homogeneous mixture of turbine and moldable microporous insulation, developed internally by Schuller, was tested for thermal conductivity. The thermal conductivity of this mixture was slightly lower than both of the previously tested turbine insulation samples. The results are included in the attached plot of thermal conductivity. This mixture showed significant shrinkage at higher temperatures, thus limiting its potential usefulness.

An injection molded sample of a 50:50 by volume two-layer composite of turbine and the above referenced moldable microporous insulation was tested for thermal conductivity. The turbine insulation layer was the hot side of this composite, while the more thermally efficient microporous layer was the cold side. The thermal conductivity results are shown in the attached plot along with previously reported results for the injection molded turbine insulation and the 50:50 homogeneous mix of turbine insulation and microporous insulation. The two layer composite and the 50:50 mix were more efficient thermally at the lower mean temperatures than the turbine insulation. However, the microporous layer of the two layer composite evidenced significant shrinkage at the very high mean temperatures. Additional samples will be molded to determine if a workable composite or mixture that is thermally efficient is viable.

## THERMAL CONDUCTIVITY
## TURBINE AND MICROPOROUS

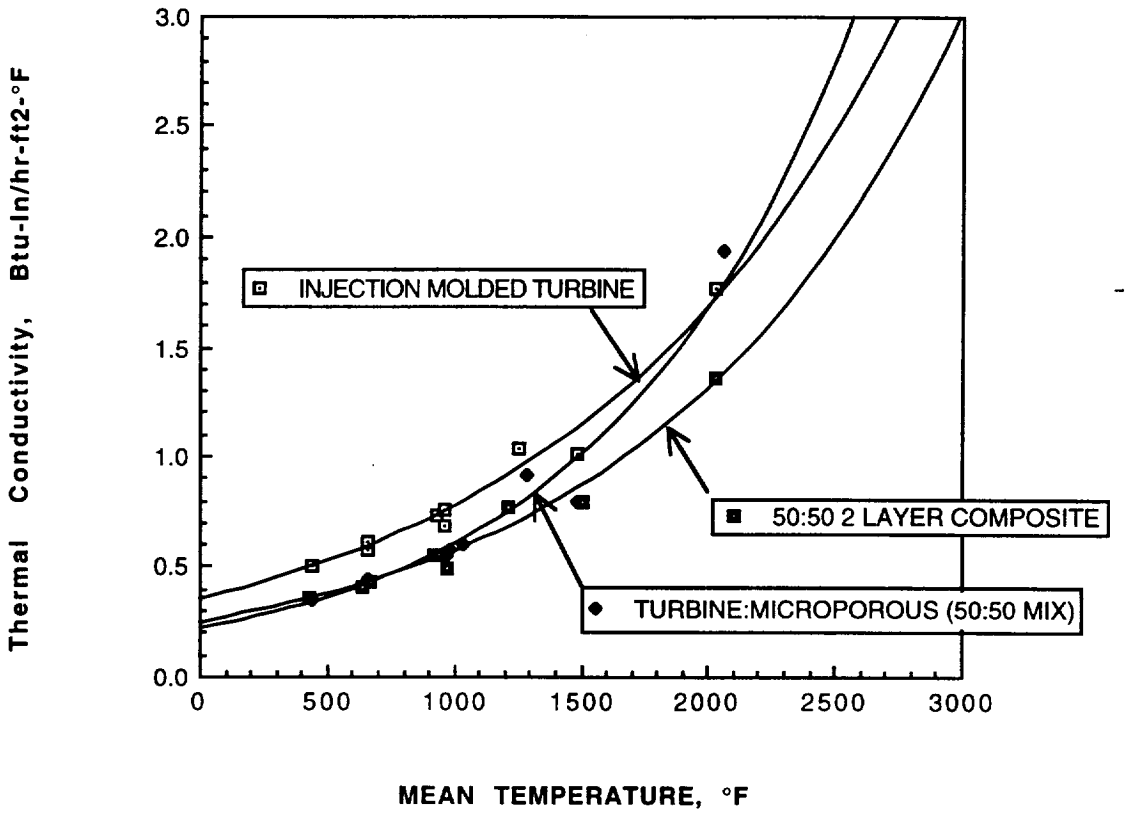

## Plans for Future Work

### Molding System Development

Continued development of the improved molding system should allow the insulation to be applied to many of the insulated parts of the AGT-5 turbine engine including the engine housing. This will involve the fabrication of molds for the simple pieces, mold inserts for the complex piece, and mold lining systems for both. The insulated parts will be available for evaluation both in engines and in test rigs.

### Cyclic Durability/Erosion Resistance Testing

The cyclic durability test burner provides the capability to evaluate the expected physical performance of the insulation at high temperatures. These performance characteristics include thermal shock resistance and erosion resistance to high temperature, high velocity gas flow. As changes are made to the insulation formulations or to the molding process, the performance of the insulation will be evaluated.

# APPENDIX C

Corning, Incorporated
1993

NOTE: INFORMATION SUBMITTED THAT IS DEEMED TO BE
PROPRIETARY IN NATURE
HAS BEEN DELETED.

# ATTAP Advanced Ceramic Regenerator

## 1993 Annual Report

Prepared by J. Paul Day

Corning Incorportaed

OVERVIEW

At the beginning of 1994, as a result of the first full year of work at Corning on the ATTAP Ceramic Gas Turbine Heat Exchanger program, two basic courses were set, one for the materials and one for the die.

The number of materials of prime interest was modified, first by adding LAS materials back into the list and then by eliminating MAT from initial consideration. Thus, LAS and MAS materials were of most interest because of cost, with AS and NZP materials being carried along as fall-back positions.

A most likely die concept was identified for the making of a die which would enable the extrusion of a cellular ceramic substrate having a cell density of about 1100 cells per square inch.

This document is a report of the progress made on the project at Corning during 1993 with respect to the tasks indentified in the proposed statement of work for the year.

PRELIMINARY ACTIVITIES

DETERMINE THE INSTANTANEOUS THERMAL EXPANSION REQUIREMENT FOR MAS - The thermal expansion behavior of the EX-22 MAS material is shown in Figure 1. MAS materials such as EX-22 tend to loose considerable strength as a result of the 10,000 thermal cycle exposure of the standard Allison thermal cycling test. This is thought to be the result of the development of microcracks because of the relatively high thermal stresses developed at high temperatures. This in turn is thought to be because of the elevated high temperature slope shown in the thermal expansion curve.

The task was to determine the highest thermal expansion slope which would allow the material to survive the rotary heat exchanger application. This was to be determined using the thermal cycling test in place at Allison.

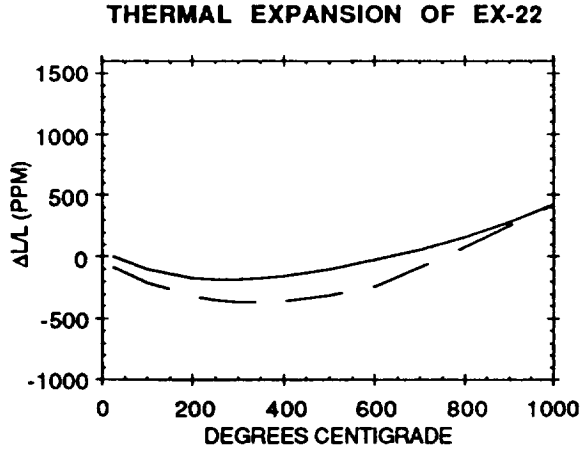


Figure 1: The Thermal Expansion Behavior of Candidate Cordierite (MAS) Material - EX-22.

The thermal cycling test has been in operation at Allison for several years; the purpose being to screen materials for cycling stability by measuring the amount of strength retained after the cycling exposure.

During analysis of samples exposed to the thermal cycling test it was discovered that the test top temperature was several hundred degrees higher than programmed. As a consequence, the equipment was adjusted to more nearly approximate the expected thermal conditions during the most severe acceleration cycle of the turbine engine.

This adjustment has resulted in the retained strength for the most likely MAS candidate (EX-22) to rise by about 50%, from 23% to about 35% of the original strength after the 10,000 cycle exposure.

Unfortunately, the cycle had not been verified by the end of the year so that we don't yet know if this is the final number or if the equipment needs additional adjustment. The target for the retained strength is 50%. As a consequence, we do not know that the present MAS composition is not acceptable under the present criterion. It has also not yet been demonstrated that the retained strength from this test correlates with product performance.

ESTABLISH A THERMAL CYCLING TEST AT CORNING - In order for us to more readily screen materials for this application, it was proposed that a thermal cycling test be installed in the Product Development area in the Corning R&D center. The equipment purchased during the 1992 contract was installed and brought to the point of operation.

No additional work on the Corning thermal cycling test was performed during 1993.

CERAMIC MATERIALS TECHNOLOGY

Five materials have been identified for study for the regenerator application. These are:

Lithium-aluminosilicate (LAS)
Aluminosilicate (AS)
Magnesium-aluminosilicate (MAS)
Mullite-aluminum titanate (MAT) and
Sodium-Zirconium Phosphate (NZP)

In the first round of evaluation it was decided that no work would be performed on MAT materials and that no NZP composition work would be performed within Corning. DOE funded programs elsewhere have developed processes for making and characterizing NZP powders (18-22). For this program powders would be purchased from these outside sources and property data generated for comparison to the more established materials such as MAS and LAS. Work would, however, also be carried out on LAS, AS, and MAS materials within Corning.

The following is a summary of the materials related activities during 1993.

LITHIUM-ALUMINOSILICATE (LAS) - The most attractive features of LAS materials are the very low thermal expansion and the reasonably high temperature capability. Poor corrosion resistance against salt and sodium, high firing shrinkage, and the high cost resulting from a low volume glass melting operation are the primary drawbacks. Each of these was addressed during 1993

activities. Figure 2 shows the low and reversible thermal expansion behavior of LAS, making it a very attractive candidate for the automotive heat exchanger application

With The Present LAS Composition, Develop A Batch Which Will Be Manufacturable. - Past experience with LAS materials has been primarily associated with the wrapping process for forming cellular products. Although powdered glass, the traditional LAS heat exchanger starting material, can be extruded, the process has not been refined and is expensive because not only is the present glass expensive but also because excessive binder is required.

Starting with the raw glass, a procedure was developed to mill and extrude the glass with a reduced amount of binder and extrusion aids.

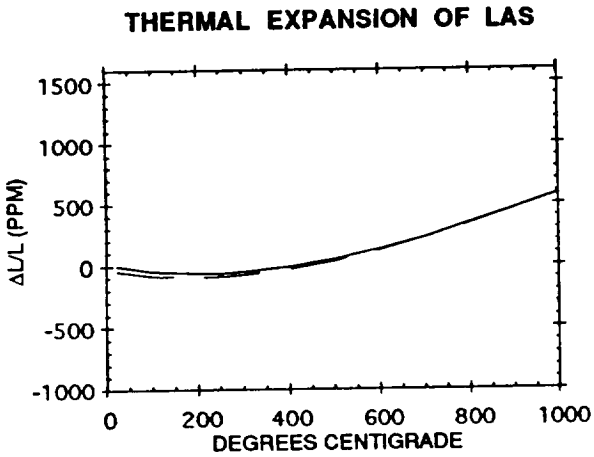


Figure 1:The Thermal Expansion Behavior of a Typical Lithium-Aluminosilicate Material

Eliminate All Sources Of Sodium In The As-Extruded Product - Sodium elimination was identified as an important issue to pursue because the level of sodium in the starting material reduces the amount of sodium which can be absorbed during use before breakage would be expected to occur. A significant level of sodium is introduced into the final product by the organic ingredients during what would be considered normal extrusion operation.

An binder/extrusion aid system for LAS glass has been identified and developed which eliminates sodium from the final batch. Further work on this extrusion system will be carried out during the next year.

Reduce The Firing Shrinkage Of LAS Materials - Shrinkage reduction has been identified as the primary manufacturing issue associated with LAS materials. High shrinkage tends to increase the firing distortion and cracking. It would, however, make the die manufacturing simpler. The present LAS shrinkage is about 18%.

During 1993 two techniques were identified which will reduce the shrinkage below 10%, the preliminary target. Both of these techniques are considered proprietary technology for which patent applications are being prepared.

High shrinkage can result in distortion and/or cracking which increase waste and cost and reduce productivity. As the shrinkage increases, the diameter of the die necessary to form the part increases also. If shrinkage is reduced at the expense of porosity, the strength will most certainly be reduced and also, important for this particular product, the through wall leakage will increase, resulting in lower heat exchange efficiency.

A dual effort to reduce shrinkage involves both modification to the inorganic portion of the batch and reduction in the amount of organic material used to facilitate extrusion. About 20% of the organic component has been eliminated, resulting in a modest shrinkage reduction. However, changes in the inorganic batch have resulted in the shrinkage being reduced from 18% to as little as 4%. The extent to which these techniques can be employed will be determined by the physical property and thermal cycling data which are yet to be completed.

Salt Corrosion -

Personnel at Corning spent considerable time sifting through the information still available.

Based on data from the Ford program Table 1 was generated, comparing the salt contamination level to the projected regenerator life.

Table 1: Projected Regenerator Life With Salt Contamination in the Air or Fuel

| NaCl in Air (ppm) | NaCl in Fuel (ppm) | Projected Life (Hours) |
|---|---|---|
| 1.3 | 76 | 140 |
| 1.0 | 60 | 178 |
| 0.1 | 6 | 1776 |
| 0.042 | 2.5 | 4262 |
| 0.04 | 2.4 | 4440 |
| 0.0007 | 0.4 | 26640 |

A report was issued detailing the analysis of the salt durability data leading to the conclusion that LAS is sufficiently durable against salt for the envisioned automotive application. Another key conclusion from the investiagtion is that Ford considered sodium to be the problem for land-based vehicles; salt was a concern but was not demonstrated to be a problem in practice.

An ion-exchange of sodium from salt for lithium in the glass-ceramic results in an increase in thermal expansion coefficient and eventually to breakage of the part in service.

Modified LAS compositions have been identified which exhibit increased tolerance to salt attack. These compositions are also derived from glasses. During the year data were generated which give the assurance that the physical and thermo-mechanical properties of the resulting glass-ceramic compositions are at least as good as the base LAS composition while at the same time the salt durability has increased by at least a factor of three.

LAS Product Cost - The most significant issue for an automotive application of any technology, after the performance of the the technology itself, is the cost. The key driver in developing the extrusion of large high

cell density regenerators is the very high price of the wrapped ceramic parts, partially due to the present low quantities required but mainly as a result of the expensive process for making the product.

In preparation for the initiation of the ATTAP Extruded Ceramic Regenerator project, Corning funded an internal cost estimate for the part size being considered at the time. This cost estimate was revisited during 1993.

Taking into account the current product size, a complete review of the previous cost estimate indicates that both LAS and MAS products are in the range of the target.

Both the organic and the inorganic components of the LAS extrusion batch contribute significantly to the overall cost. Any reduction in the organic level is a direct cost savings. Two approaches to the reduction of the cost of the inorganic component of the extrusion batch have been shown to be feasible. Further work is necessary in order to demonstrate that these approaches can be scaled, and that the final product properties are acceptable.

Make Large High Cell Density LAS Parts When The Die Is Available - Parallel paths were being pursued to develop the hardware and at the same time the ability to process the material. This objective was established assuming that the die and the materials would both be available for extrusion during 1993.

Sufficient LAS glass was milled for a large extrusion and the batch preparation was developed as indicated above. However, the die was not available until later in the year than initially anticipated and LAS was not the first material to be extruded. The combination of these two issues prevented us from extruding and further processing LAS materials during 1993.

ALUMINOSILICATE (AS) - The AS material is derived from LAS glass-ceramic by a hydrogen for lithium ion-exchange in sulfuric acid, which forms HAS, followed by a firing step to drive off the water. This procedure yields a material which is very resistant to chemical attack but which has a 250°C lower temperature capability. This material is more expensive than LAS because it has all of the LAS expenses plus the ion-exchange and refire steps, in addition to the disposal of lithium sulfate laden liquid sulfuric acid.

Demonstrate the Proprietary Ion-Exchange Process - During 1993 a process was demonstrated which eliminates the liquid sulfuric acid ion-exchange process and also the disposal of the sulfuric acid after use. Preliminary evaluation of the experimental results indicates that this new ion-exchange process does work on 3 inch diameter pieces. Scale-up of this process to full sized pieces is yet to be demonstrated.

MAGNESIUM-ALUMINOSILICATE (MAS) - MAS materials of the type which were developed for the automotive catalyst support application are of particular interest because of the relatively low average thermal expansion and low manufacturing cost. The challenge is to simultaneously maintain the thermal shock resistance and reduce the through-wall porosity to an acceptably low level. Another concern is the high thermal expansion at high temperature.

Porosity Reduction - As is shown in Table 2, we have been successful in reducing the porosity, first from about 35% to about 25% with one set of raw materials and then to 12% with another set. The 25% porous material gives acceptable leakage values. Unfortunately, the very low porosity has been achieved at the expense of a very high shrinkage of 25%, which is unacceptable for a product of the type and size considered here.

Table 2: MAS Materials and Properties

| | EX-20 | EX-22 | EX-?? |
|---|---|---|---|
| Thermal Expansion Coefficient ($10^{-7}$ cm/cm/K) | 5 | 3 | 4 |
| Porosity (%) | 35 | 25 | 12 |
| Strength (MPa) | 21 | 42 | 60 |
| Shrinkage (%) | 2 | 8 | 25 |

Make Large High Cell Density EX-22 MAS Parts When The Die Is Available - Four Extrusions of EX-22 material were made during 1993. The first two were performed in our production facility and proved less than completely successful due in part to the batch handling which the experimental composition necessitated.

As a result of these two experiments, new front-end hardware was designed and built for the R&D extruder. This allowed us to make another two very successful extrusions at much lower cost and with much higher quality. This hardware was funded from Corning capital.

Pieces from these extrusions were successfully fired and a single one-piece extruded part was finished and supplied to Allison during 1993.

High Temperature Thermal Expansion Reduction - All attempts to reduce the high temperature thermal expansion of cordierite have proven futile. Unlike the lower temperature range, the high temperature portion of the expansion appears to be directly related to fundamental properties of the cordierite crystal and has been beyond our ability to reduce.

From the experiments which we have conducted during 1993, we conclude that the EX-22 material has the best combination of properties of any cordierite for this application. Modifications to the composition may produce minor improvements but we do not anticipate major changes in properties.

SODIUM-ZIRCONIUM PHOSPHATE (NZP) - NZP powders were acquired from Virginia Polytechnic Institute and LoTEC, Incorporated for evaluation in a series of tests in comparison to the LAS and MAS materials. Firing shrinkage, porosity, strength, thermal expansion, and chemical durability were evaluated and are reported in the following sections.

LoTEC Material - Two compositions were acquired from LoTEC, Inc. These were barium silicon zirconium

phosphate (Ba/Zr/P/Si) and calcium strontium zirconium phosphate (Ca/Sr/Zr/P).

VPI Material - Both of the VPI materials are compositions of calcium magnesium zirconium phosphate (Ca/Mg/Zr/P), each formed into a powder using a different method.

Firing Shrinkage - This processing parameter is, as indicated earlier, important for processing without high firing cracking and material losses. Table 3 shows the shrinkage data for the 4 compositions evaluated. The target for the project is a shrinkage of less than 10%, as low a value as possible obviously being preferred. The second VPI composition is the only one which does not meet this goal.

Porosity - The porosity data for these four processed powders are also shown in Table 3. One would expect to find the porosity of the fired piece to be high if the firing shrinkage is low, and visa versa. This is the case for the VPI materials but not for the LoTEC materials. Based on leakage data, an initial target of less than 25% porosity has been established for the porosity. One of the LoTEC compositions and one of the VPI compositions each has a porosity within the desired range. However, when both the firing shrinkage and the fired porosity are considered, the LoTEC calcium/strontium composition is the only one which meets these requirements.

Table 3: NZP Processing Data

| | | | Firing Shrinkage (%) | Fired Porosity (%) |
|---|---|---|---|---|
| LoTEC - | Ba/Zr/P/Si | | 5.7 | 29.7 |
| | Ca/Sr/Zr/P | | 5.0 | 15.6 |
| VPI - | Ca/Mg/Zr/P | I | 9.7 | 42.5 |
| | | II | 29.7 | 16.2 |

Strength - Four point bending modulus of rupture data from extruded circular rods were used to determine the strength of the NZP compositions. Table 4 contains the MOR data for the four compositions being evaluated. The target strength of the regenerator composition is 30 MPa. Only one of the four compositions is even close to this target, again the calcium/strontium composition from LoTEC. In spite of the very high shrinkage and the relatively low porosity of the second VPI composition, the strength is still less than 50% of the goal.

Thermal Expansion - There are at least four issues to be taken into account when considering thermal expansion: the first being the average value of the coefficient over some reasonable range of temperature such as room temperature to 800 or 1000°C; the second is the expansion coefficient over a high temperature range such as 400 to 800°C; the third is the presence or absence of irregularities in the thermal expansion curve which would suggest reordering of the structure, for example from a phase transformation; and the fourth is the presence or absence of hysteresis, which could indicate the presence of microcracks or another mechanism which would emerge during thermal or mechanical cycling.

Table 4: NZP Strength

| | | | Modulus of Rupture (MPa) |
|---|---|---|---|
| LoTEC - | Ba/Zr/P/Si | | 17.1 |
| | Ca/Sr/Zr/P | | 29.0 |
| VPI - | Ca/Mg/Zr/P | I | 2.4 |
| | | II | 11.5 |

The data in Table 5 present the average and high temperature thermal expansion coefficients for the four NZP compositions being considered. The target average coefficient is less than $8x10^{-7}$/K while there is no target yet set for the high temperature coefficient. The LoTEC calcium/strontium shows an acceptable average value while the high temperature coefficient is less than double. The second VPI composition has very low average value and also a quite low high temperature coefficient. The other compositions are unacceptably high.

Table 5: NZP Coefficients of Thermal Expansion

| | | | CTE ($10^{-7}$ cm/cm/K) | |
|---|---|---|---|---|
| | | | Average | HT Slope |
| LoTEC- | Ba/Zr/P/Si | | 16.3 | 17.2 |
| | Ca/Sr/Zr/P | | 4.8 | 8.6 |
| VPI - | Ca/Mg/Zr/P | I | 11.6 | 22.8 |
| | | II | 0.8 | 10.2 |

Figure 3 contains the thermal expansion curve of the LoTEC barium/silicon NZP composition, showing a very low hysteresis but a flattening of the curve above about 700°C, indicating some sort of reversible transition within the structure.

The LoTEC calcium/strontium NZP thermal expansion curve is displayed in Figure 4. In this case there is an absence of evidence for phase transitions but there is considerable hysteresis. Subsequent experiments indicated that the hysteresis was recoverable with time at room temperature, indicating the presence of microcracking.

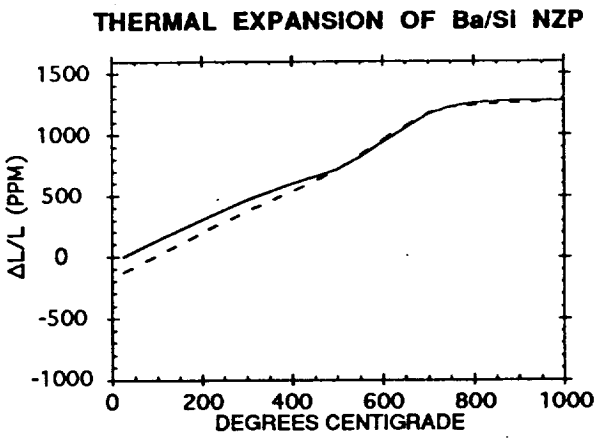


Figure 3: The Thermal Expansion Behavior of One of the Barium/Silicon NZP Materials Supplied by LoTEC, Inc.

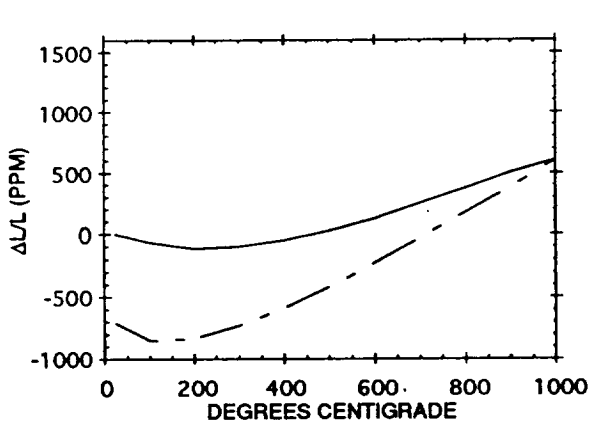


Figure 4: The Thermal Expansion Behaviour of One of the Calcium/Strontium NZP Materials Supplied by LoTEC, Inc.

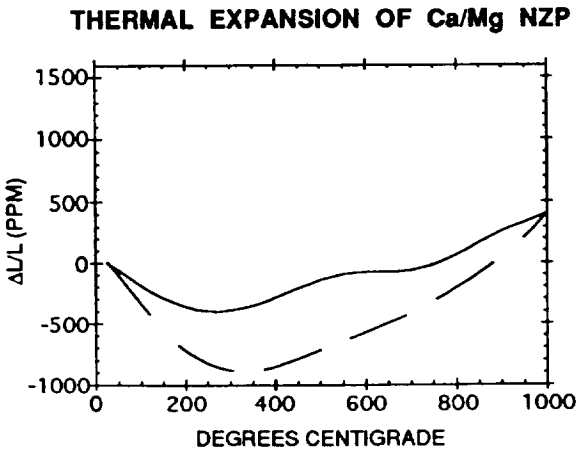


Figure 5: The Thermal Expansion Behaviour of the Sol-Gel Derived Calcium/Magnesium NZP Material Supplied by Virginia Polytechnic Institute.

The curve in Figure 5 is the thermal expansion of the second VPI material, showing the low thermal expansion but significant hysteresis and also features which could be evidence of a phase transition of some sort. In this case it is also suspected that the hysteresis is due to the presence of microcracks, which, under the proper circumstances, is not an unacceptable situation.

Salt Durability - Salt durability is important for automotive applications because of the presence of salt on the roads, in the air, or in the fuel. Durability is measured by heating a sample, which has been immersed in a salt solution, to 850°C for one hour. Two measurements are monitored to determine durability: the change in the average thermal expansion coefficient; and the change in length. A target for length change of less than 300 ppm has been set.

Both sets of salt durability data are to be found in Table 6. None of the compositions possesses a length change value less than the target while three of the four are within 200% of that value. However, the LAS composition being considered also fails to meet this stringent salt durability criterion. The large thermal expansion change associated with the LoTEC calcium/strontium composition is also of concern but there is as yet no goal for this property after salt treatment.

Table 6: NZP Salt Durability

| | | | CTE ($10^{-7}$ cm/cm/K) Before | CTE ($10^{-7}$ cm/cm/K) After | Growth dL/L (ppm) |
|---|---|---|---|---|---|
| LoTEC- | Ba/Zr/P/Si | | 16.3 | 16.9 | 445 |
| | Ca/Sr/Zr/P | | 4.8 | 12.8 | -526 |
| VPI - | Ca/Mg/Zr/P | I | 11.6 | 7.3 | 1036 |
| | | II | 0.8 | 11.0 | 538 |

Sulfur Durability - Sulfur from the fuel reacts at high temperatures with water vapor from the exhaust to form a sulfuric acid vapor which can attack components of the exhaust stream. A liquid sulfuric acid durability test, therefore, gives a quick first look at the sulfur durability of a material. Care should be taken, however, to view this as a preliminary indication of durability because the actual reaction is between the material and a vapor rather than a liquid.

As shown in Table 7, all of the calcium containing compositions were severely reacted with the acid. Only the LoTEC barium containing composition survived, and with very little reaction.

Table 7: NZP Sulfuric Acid Durability

| | | | Weight Loss (%) |
|---|---|---|---|
| LoTEC- | Ba/Zr/P/Si | | 0.004 |
| | Ca/Sr/Zr/P | | Dissolved |
| VPI - | Ca/Mg/Zr/P | I – | Dissolved |
| | | II | Too Friable |

SAMPLES

Supply Assemblies As Needed - Four wrapped regenerators were supplied to Allison during 1993. These were for use with existing engines in testing of other pieces of hardware or for testing of the regenerator components themselves.

Extruded Product Samples - Extrusions using the large high cell density die and the EX-22 material were very successful.

Dispite defects in the extruded samples associated with the process we were required to use for these particular experiments, parts were made which demonstrate that this die and this material can be combined to produce essentially the size and quality targeted for this product. A large extruded high cell density MAS blank was produced and supplied for display at the annual Contractors' Coordination Meeting in Dearborn.

One large extruded high cell density EX-22 part was finished and supplied to Allison for testing during 1993.

Cycling Test Samples - In support of the Allison cycling test rig and the investigation involving the cycling thermal stability of the candidate materials, numerous small high cell density samples of both LAS and MAS materials were supplied to Allison.

DIE DEVELOPMENT

The approach taken to develop an extrusion die capable of making an unfired part 1100 rectangular cells per square inch was to couple the experience which had been developed for forming thin slots with the extant capability to produce large diameter dies.

The initial experiments were performed on 1-3 inch diameter dies to determine the parameters for drilling the holes and cutting the slots for such a high cell density configuration. These experiments were so successful and the large die making capability so advanced by the time this die was to be manufactured, that an intermediate die, having 800 rectangular cells per square inch with an extruded piece diameter of 6 inches, was abandoned in favour of the final product.

The final design has feed holes each of 0.039 inch diameter. The slots which form the cellular structure are a total of over 0.1 miles long and the target slot width is 0.005 inches. Finite element analysis was employed to arrive at a design which would be mechanically robust. As a result of considerable experience making large dies for the manufacture of other cellular products, a special stainless steel was identified for this part. There are also proprietary elements of the design which were employed to prevent permanent deformation of the die during the extrusion process itself.

Complete The Construction Of The Large High Cell Density Die - The construction of the die proceeded as planned with some time delay due to measurements during the construction to insure that the construction was correct. The die was successfully completed during the third quarter of 1993. The result of this effort was the successful manufacture of a die which has the capability of producing products of the size and having the cell density and wall thickness required for this product.

Using this die we were, as indicated above, able to successfully extrude the EX-22 batch at both the manufacturing and the R&D facilities. Virtually all of the flaws which were seen in the first two extrusions using this die were due to batch handling problems. The third and fourth extrusions, in the R&D extrusion facility, demonstrated that the die was of very high quality.

As a result of the nature of the slitting process, the extruded wall thickness of MAS is approximately 6 mils whereas the wall thickness target is 5 mils. Now that the die has been shown to perform with the thicker wall, die coating work will begin to identify the process which will eventually be used to plate the die so that the wall thickness will be reduced to the required dimension.

SUMMARY OF 1993 ACTIVITIES

It has not yet been possible to determine the instantaneous thermal expansion requirement for MAS. This is due both to the lack of complete data from the thermal cycling test and also the result of lack of correlation of this test with turbine operation for the contemplated engine and application.

Although some equipment was installed at Corning toward a thermal cycling test, the work was stopped.

Modified LAS compositions have been identified which exhibit increased tolerance to salt attack.

A process has been established to taking LAS glass through milling, extrusion, and firing, and utilizing a reduced level of binder.

A binder/extrusion aid system containing no sodium has been demonstrated for extrusion LAS glass.

LAS materials have been developed with lower shrinkage. This provides a process improvement in terms of lower material losses due to reduced firing cracking and piece distortion.

Salt corrosion has been demonstrated not to be the reason for failure of the Ford program in the mid '70s.

A decision was made to first test the new large high cell density die using MAS materials. Consequently, as a result of limited time with the die, no large LAS were extruded.

A more cost effective process has been demonstrated whereby LAS glass-ceramic is ion-exchanged to form HAS and, after refiring, AS material. One of the benefits of this new process is the dramatically reduced requirement for disposal of sulfuric acid laden materials.

Attempts to reduce the porosity and the thermal expansion coefficient of MAS materials while maintaining the other properties at acceptable levels have been successful.

A large high cell density extruded MAS part was supplied to Allison during 1993.

All attempts to reduce the high temperature thermal expansion of MAS materials have resulted in failure.

Baseline experiments have been performed on four NZP materials to establish general properties.

A die capable of extruding high cell density pieces has been built and demonstrated.

Samples of MAS composition EX-22 were extruded and fired successfully. Regenerator cores of this material with approximately 1150 cells per square inch will be finished and supplied to Allison for rig testing.

REPORTS

"Salt Corrosion of LAS Materials" by J. Paul Day, issued to Allison January 21, 1993.

PUBLICATIONS

"Regenerator Core Development at Corning" by David H. Hickman , in Proceedings of the Annual Automotive Technology Development Contractors' Coordination Meeting 1992, SAE publication # P-265, p 347-352.

"A Rotary Heat Exchanger for Automotive and Other Ground Based Gas Turbine Applications" by J. Paul Day, ASME Paper 94-GT-124, 1994.

PRESENTATIONS

"ATTAP Extruded Ceramic Regenerator Material/Process Development", by J. Paul Day, David H. Hickman, and G. Daniel Lipp, at the Annual Automotive Technology Development Contractors' Coordination Meeting, October 18-21, 1993 in Detroit, MI.

# APPENDIX D

Corning, Incorporated
1994

NOTE: INFORMATION SUBMITTED THAT IS DEEMED TO BE
PROPRIETARY IN NATURE
HAS BEEN DELETED.

# Extruded Rotary Gas Turbine Heat Exchanger

1994
Annual Report

January 16, 1995

to-
Allison

from-
J.P. Day
Corning Incorporated

# Extruded Rotary Gas Turbine Heat Exchanger

## 1994 Annual Report

Corning Incorporated

by J.P. Day

As in past years, development during 1994 of an extruded rotary heat exchanger for the automotive gas turbine was a combination of materials and hardware. The element of ultimate product cost played a large role in focusing the program.

## LAS Materials Technology

Although there were several aspects to the LAS work during 1994, the primary focus was cost reduction of the overall process, including the process for making the glass. Thus, firing shrinkage reduction is especially important for the improvement it will bring to firing selects (% good pieces out of firing) as well as control of dimensions, etc. Likewise, extrusion batch modifications, which will reduce firing shrinkage, will also reduce the cost of incoming raw materials. Significant progress was made during the year in identifying the LAS process concepts which will not contribute to reduced cost or improved material; however, there is still considerable work required to demonstrate conclusively that the remaining concepts will contribute.

### Shrinkage Reduction

Two basic approaches were taken in an attempt to reduce the firing shrinkage of the LAS composition. The results of the first approach, one consisting of changing the nature of the materials in the batch while maintaining the original glass oxide composition, are presented in Table 1.

**Table 1**

LAS Sample Set #1 - Shrinkage Reduction Experiment

| Comp. | Strength (MPa) | Shrinkage (%) | Expansion (ppm/K) | Porosity (%) |
|---|---|---|---|---|
| 1 | 64.5 | 19.0 | 0.45 | 0.83 |
| 2 | 45.4 | 11.0 | 0.56 | 25.4 |
| 3 | 32.1 | 8.7 | 0.54 | 29.9 |
| 4 | 25.0 | 7.4 | 0.56 | 32.4 |
| 5 | 30.8 | 6.7 | 0.57 | 32.3 |
| 6 | 22.5 | 5.7 | 0.54 | 34.5 |
| 7 | 14.8 | 4.5 | 0.54 | 35.0 |

The first composition is the original batch. Subsequent compositions represent increasing levels of the modified glass. With this technique, the firing shrinkage can be reduced to below 5%. However, the strength drops to less than 25% of the original mixture and the porosity rises to 35%. For all of these compositions, the expansion differences are insignificant. The material property targets are $\geq$ 30 MPa strength and $\leq$ 25% porosity. With these criteria, only the first and second compositions are acceptable. Samples of the first and second compositions were extruded and fired in high cell density rectangular parts for thermal cycling testing at Allison.

The conclusion from this set of experiments is that the firing shrinkage can indeed be reduced by this batch modification. All of the properties, however, need to be assessed to assure compliance with product requirements. This technique can possibly be combined with other LAS batch modifications to aid in the shrinkage control.

The other technique of shrinkage reduction, modification of the extrusion batch combined with a change in the glass batch, will be considered in conjunction with the experiments on low-cost LAS materials.

### Characterization of Other LAS Compositions

Due to the lack of continuity in funding, effort, and personnel during the year, all of the LAS materials work was performed on standard production LAS compositions.

### Complete Sodium Elimination

Sodium is detrimental to the low thermal expansion characteristics of the LAS composition. While efforts are underway to reduce the composition's susceptibility to sodium incorporation and, while efforts are being made to determine the level of sodium to which the gas turbine regenerator will be exposed over the life of the product, it was recognized that sodium was also being introduced into the composition during processing via additives to the extrusion batch.

We have been successful in identifying a sodium free substitute additive which functions in virtually identical manner to the sodium containing additive. This new extrusion aid will be employed in the final LAS batch formulation if required.

### Low-Cost Materials

Two approaches to the material cost reduction have been identified: using only glass but making the glass from low cost raw materials; and incorporating materials other than glass into the extrusion batch. The first of these would only be of incremental benefit, whereas the second has the potential of yielding the factor-of-ten reduction in cost that the product needs. Therefore, we have concentrated on the second concept during 1994.

The property data from the first raw materials experiment are contained in Table 2. Where gaps appear in the data, the fired samples were too fragile for the measurements indicated.

**Table 2**

LAS Sample Set #2 - Extrusion Batch Raw Material Substitution Experiment

| Composition | Porosity (%) | Expansion (ppm/K) | Strength (MPa) | Shrinkage (%) |
|---|---|---|---|---|
| 1 | 44.6 | -0.44 | 1.8 | 0.0 |
| 2 | | | | |
| 3 | 43.6 | -1.05 | 4.1 | 0.6 |
| 4 | 37.5 | -1.13 | 6.0 | 2.5 |
| 5 | | | | -7.8 |
| 6 | | | | -6.5 |
| 7 | | | | -5.1 |
| 8 | 0.9 | -0.01 | 64.7 | 20.5 |
| 9 | 1.0 | 0.34 | 52.5 | 16.0 |
| 10 | 0.9 | 0.69 | 68.3 | 14.0 |
| 11 | 0.8 | 0.96 | 80.3 | 12.8 |
| 12 | 0.9 | 0.26 | 87.7 | 15.9 |
| 13 | 0.9 | 0.59 | 98.5 | 14.0 |
| 14 | 1.0 | 0.88 | 91.6 | 13.1 |
| 15 | | | | -8.8 |
| 16 | | | | -8.9 |
| 17 | | | | -6.1 |
| 18 | | | | -5.6 |

Note that composition #8 is the LAS glass while the six batches following are extrusion batch modifications which incorporate that glass as one of the constituents. These data provided the confidence we needed to pursue more detailed and more scientific experiments incorporating to types of additives these six compositions contain. The porosity can be held low while the shrinkage is reduced and the strength is increased. Unfortunately, the expansion does increase - this, however, is a consequence of the way the batches were formulated and is corrected in future experiments.

The second raw materials experiment incorporates both substitutions in the melted glass and raw materials in the extrusion batch. The data from this set are shown in Table 3.

**Table 3**

LAS Sample Set #3 - Raw Material Substitutions in the Glass in Combination with Extrusion Batch Raw Materials

| Composition | Shrinkage (%) | Expansion (ppm/K) | Strength (MPa) | Porosity (%) |
|---|---|---|---|---|
| 1 | 3.7 | 0.62 | 30.9 | 38.4 |
| 2 | 5.1 | 0.15 | 35.6 | 33.7 |
| 3 | 9.4 | 0.63 | 47.8 | 27.3 |
| 4 | 7.1 | 0.38 | 43.7 | 31.4 |
| 5 | 7.7 | 0.52 | 45.9 | 30.9 |
| 6 | 6.8 | 0.17 | 39.6 | 31.9 |
| 7 | 7.9 | 0.13 | 46.7 | 29.9 |
| 8 | 10.5 | -0.18 | 41.0 | 30.0 |
| 9 | 8.0 | 0.32 | 50.8 | 23.7 |

In this set the shrinkage is quite low while both the strength and thermal expansion are adequate. The porosity is, however, high and needs to be reduced.

The cost savings of some of the compositions shown here approach 50% of the original glass batch cost, without taking into account cost reduction due to scaling the process to high volume production.

The conclusions we draw from these experiments are: 1) firing shrinkage can be reduced to below 10% without severely increasing the expansion or reducing the strength but the porosity with the present techniques is too high; 2) there is significant materials cost benefit to incorporating less expensive raw materials in the LAS extrusion batch and these compositions have, for the most part, acceptable physical properties.

The glass composition work was begun only during the fourth quarter of 1994 and has progressed quite satisfactorily in a very short period of time. Additional compositions were melted and processed but the data are not yet available for presentation and discussion.

### LAS Processing

With the many changes being made in the LAS extrusion batch, we decided to institute a processing experiment to document the effects these changes have on extrusion properties and the need for expensive organic binders and extrusion aids. Consequently, a factorial experiment was designed to evaluate the effects of 5 batch variables on various extrusion and product quality parameters. The analysis of the data was not completed by the end of the year.

## MAS Materials Technology

### Next Generation MAS

Little MAS work was performed until near the end of 1994 because of the limited funds available. During the year, discussions were held as to ways in which EX-22 could be improved for this application. An effort was begun to implement these ideas. Raw materials were acquired, compositions were written, and samples were prepared. However, no data were available by year-end.

### Strength Loss Mechanism

Few thermal cycling tests were run at Allison.
Consequently, no cycled samples were made available to us for evaluation so that little progress has been made in understanding this phenomenon.

### Core Post-Mortem

No MAS cores were tested at Allison so that none were available to us for post-mortem examination.

## AS Material Technology

Because AS materials are derived from LAS materials, any concern for cost with LAS will be even greater for its derivative AS material. Hence, the most important AS work that can be done at present is the cost reduction effort on LAS materials. It is for this reason that most of the materials effort during 1994 was focused on LAS material cost.

### Scale-up Low Cost Ion-Exchange

Some experiments were performed early in the year to evaluate the scale-up of a more cost effective ion-exchange process than using liquid sulfuric acid. These experiments, although not completely successful, did indicate that the process could be scaled.

### AS From Other LAS Compositions

As indicated under the LAS section, no other LAS compositions were investigated during 1994 so that no ion-exchange evaluations were performed on other LAS compositions during the year, either.

## Extrusion

No large high cell density MAS extrusions were made during 1994 because the inventory of parts from 1993 extrusions was sufficient for the needs of Allison.

The two large high cell density LAS extrusions were disappointing. The first was completely unsuccessful whereas the second yielded only poorly formed pieces. The problem appears to lie with a combination of physical and chemical interactions, exacerbated by the large size and extended time required by the process. At year-end we are still in the process of sorting out these interactions.

## Die Technology

Recent developments in die manufacturing technology being explored by engineers developing dies for the automotive application have been identified as a possible solution to the problem of making a large unsupported single piece die. As the end of the year drew to a close, these new methods were just beginning to be investigated. No data or conclusions are yet available.

## Samples

Several sets of samples were supplied to Allison for thermal cycling testing. Also, two full-sized extruded high cell density MAS parts were delivered during the year.

## Assemblies

### Product Design

Considerable progress has been made in identifying the needs of the product and the restrictions of the process and materials, especially the product cost. The discussion continues.

## Documentation

### Presentations

"Ceramic Gas Turbine Heat Exchanger Development" by J.P. Day at the Low-Expansion Materials Symposium at the 96th Annual Meeting of the American Ceramic Society, Apr. 27, 1994 in Indianapolis, IN.

"A Rotary Heat Exchanger for Automotive and Other Ground Based Gas Turbine Applications" by J.P. Day at the International Gas Turbine and Aeroengine Congress and Exposition, June 15, 1994 in The Hague, Netherlands.

"ATTAP Extruded Ceramic Regenerator Material/Process Development" by J.P. Day at the DOE Contractors' Coordination Meeting, Oct. 25, 1994 in Dearborn, MI.

### Prepared for Publication (copies attached)

"ATTAP Extruded Ceramic Regenerator Material/Process Development" by J.P. Day, 1994 CCM Proceedings.

"Ceramic Gas Turbine Heat Exchanger Development" by J.P. Day and D.H. Hickman, ACS Low Expansion Ceramics Symposium Proceedings.

### Publications (copies attached)

"ATTAP Extruded Ceramic Regenerator Material/Process Development" by J.P. Day, D.H. Hickman, and G.D. Lipp, SAE Publication #P-278, p287-292, May 1994.

"A Rotary Heat Exchanger for Automotive and Other Ground Based Gas Turbine Applications" by J.P. Day, ASME Paper #94-GT-124, June 1994.

# APPENDIX E

AlliedSignal Ceramic Components
1994

NOTE: INFORMATION SUBMITTED THAT IS DEEMED TO BE
PROPRIETARY IN NATURE
HAS BEEN DELETED.

ADVANCED TURBINE TECHNOLOGY APPLICATIONS PROJECT

ANNUAL PROGRESS REPORT
COVERING PERIOD SEPTEMBER 1994 THROUGH DECEMBER 1994

SUBCONTRACT NO. H416285 (PRIME CONTRACT NO. DEN3-336)
"DEVELOPMENT OF A PRODUCTION VIABLE MANUFACTURING PROCESS FOR AS800 SILICON NITRIDE COMPONENTS"

AlliedSignal Ceramic Components
TOR - 1/5 - 1 - 27000
2525 West 190th St.
Torrance, CA 90504

January 11,1995

"PREPARED FOR ALLISON ENGINE COMPANY"

## I. INTRODUCTION

The objective of AlliedSignal Ceramic Components (CC) on the ATTAP Phase II program is to demonstrate gelcasting as a viable production process for manufacturing AGT5/hybrid design gasifier turbine wheels, and possibly other components, using AS800 high temperature in-situ reinforced microstructure silicon nitride. The primary goal of the program is the demonstration of a production process which meets all customer requirements of cost, schedule, quantity, and quality.

CC's first year effort is composed of three tasks. The effort of the first task will focus on providing AS800 test specimens to Allison for property evaluation/validation. Task 2 will develop the gelcasting of AS800 gen.1 design turbine wheels utilizing a reusable mold. Task 3 consists of program management and documentation.

After demonstrating the process in the first year, the gelcasting operation will be refined, automated, and scaled-up to meet the 1998 targets of volume (20,000 wheels/yr.) and cost ($100/wheel). Concurrently with the gelcast AS800 wheel development efforts, CC will evaluate the potential for gelcasting scrolls and combustors by forming simpler-shaped analogs of those components through 1995. Plans for post-1995 efforts will depend on 1994-1995 results.

## II. TECHNICAL PROGRESS SUMMARY

### Task 1 - Fabrication and Delivery of AS800 Test Specimens

The goal of this task is to deliver two sets of AS800 silicon nitride test specimens (3mm x 4mm x 50mm bars, 50 machined test surface, 50 as-processed test surface per set) to Allison Engine Company for property evaluation and validation. While gelcasting of AS800 is being developed (on the NIST ATP Program), slip cast AS800 test specimens were prepared for evaluation at Allison. Equivalent mechanical properties for slip cast and gelcast AS800 are assumed because properties were shown to be equivalent for the two techniques in other grades of silicon nitride (GN-10 and GS-44).

The first milestone of the program (November 30, 1994) is delivery of a set of AS800 test bars fabricated by the slip casting method. The process steps were scheduled for an 11/30/94

delivery date to Allison, but the machining subcontractor notified CC of a slip in schedule with a revised shipment date of 12/2/94. The test bars were heat treated, and visual inspection revealed defects on some of the as-sintered surfaces. The defects did not represent the typical surface resulting from CC's fabrication process and therefore failed inspection. Forty five as-sintered specimens and fifty fully machined bars passed inspection, and were shipped to Allison as partial fulfillment of the 11/30/94 milestone. Additional AS800 is being processed to complete the slip cast test bar order in January 1995.

The next program milestone (January 31, 1995), delivery of gelcast AS800 silicon nitride test specimens, depends on progress made in the NIST Advanced Technology Program (ATP). The NIST ATP has the primary purpose of developing gelcast AS800. Under the NIST ATP, a gelcast AS800 plate was fully densified in October for the first time. The microstructure of fully dense gelcast AS800 was compared with a slip cast specimen (the gelcast and slip cast specimens were processed through drying and densification simultaneously). The gelcast microstructure was found to be equivalent to the slip cast microstructure; this is verification that the gelcast AS800 mechanical properties should be equivalent to that of slip cast AS800. When the mechanical properties have been verified in the NIST ATP Program, fabrication of gelcast AS800 test specimens for the second milestone of Task 1 will begin.

Task 2 - Fabrication of AS800 Silicon Nitride Allison Generation-1 Wheels Using Re-usable Tooling

Gelcasting activities:
The objective of this task is to demonstrate the ability to fabricate gen. 1 AS800 silicon nitride wheels using a re-usable mold. While a mold is being fabricated according to the Allison gen. 1 wheel design, the first experimental castings are being performed with a CC-owned tool that was originally used to injection-mold impulse-type axial wheels of a size analogous to the Allison gen. 1 wheel.

The first wheel was gelcast in October, using the existing axial turbine wheel tool and the spin casting technique. The first wheel had a rough hub and broken blades due to incomplete mold filling. Eight wheels were gelcast in the injection molding tool in November and one in early December by the spin casting technique with improved filling results due to refined sealing, casting, and release techniques. Also, rounding out some sharp edges in the mold contributed to the improved filling and decreased the "starved" areas in the castings. The surface finish of the wheels, including even the thinnest sections of the blades, was excellent. Some blades broke from the wheel hub on these castings; the problem was traced to a defect in the mold which allowed slip to leak during casting. The injection molding tool was sent out to a machinist subcontractor who corrected the defect and modified the mold for vacuum gelcasting experiments. Two castings were performed in the modified generic wheel mold. The first wheel was gelcast by the spin technique, the second wheel was vacuum gelcast. All blades remained attached to the wheels. The goal of the next experiments will be to further refine the slip rheology and the slip filling procedure. The wheels will be fully processed to determine the shrinkage factor of gelcast AS800, which is required for fabricating the gen. 1 wheel mold.

Mold fabrication activities:
CC received a print of the APX10034 wheel and six ASCII files of blade contour datum points during a project meeting at Allison on November 4. The APX10034 was selected at the end of November as the final design for the ATTAP Gen. 1 wheel. Work began on the design/fabrication of a re-usable mold. A surface of the blade, from sections AA through FF, was created from the ASCII data using Mastercam software. Further work will be required to complete the wheel design; sections of the blade must be created to extend the blade below the hub rim. CC is in the process of collecting bids from machining subcontractors to complete the design and to fabricate the mold for the Gen. 1 APX10034 wheel.

# APPENDIX F

Ceramics Process Systems
1993

NOTE: INFORMATION SUBMITTED THAT IS DEEMED TO BE
PROPRIETARY IN NATURE
HAS BEEN DELETED.

# QUICKSET™ NET SHAPE FABRICATION OF SRS-201 RPD 20-BLADE PROTOTYPE GASIFIER TURBINE ROTORS ADVANCED TURBINE TECHNOLOGY APPLICATIONS PROGRAM CONTRACT H-321550

Prepared By:

Ceramics Process Systems Corporation
111 South Worcester Street
Chartley, MA 02712-0338

Submitted to:

Allison Engine Company
2001 South Tibbs Avenue
Indianapolis, IN 46241

Contributors to this report:

M.C. Emmilson, CPS
B.E. Novich, CPS
M.A. Occhionero, CPS
E.S. Tormey, CPS

D. Hengst, CarTech

March 30, 1994

**Table of Contents**

**List of Tables**

**List of Figures**

## 1.0 Introduction

Development of technology which would enable effective fabrication of high performance structural ceramic components is necessary for the success of automotive gas turbine heat-engines. Technology development programs, such as the Advanced Turbine Technology Applications Project (ATTAP) sponsored by the Department of Energy and managed by NASA, have made significant progress towards this objective.

Ceramics Process Systems Corporation (CPS), a subcontractor of Allison Engine Company, has focused on cost effective fabrication processes for ceramic heat engine components. CPS has combined near net-shape component forming with pressureless sintering densification techniques to develop a cost-effective means of fabricating ceramic turbine engine components. This approach avoids the high costs associated with pressure assisted densification methods and final component machining.

CPS is currently under contract to deliver spin-tested SRS-201 SiAlON gasifier rotors to Allison Engine Company in mid 1994. Rotors are to be fabricated by the Quickset™ low pressure injection molding process using SRS-201 SiAlON material which is pressureless sintered.

The Quickset™ process, developed by CPS, is described elsewhere (1,2). This process is capable of producing complex-shaped parts that have uniform and reproducible sintered shrinkages which results in exceptional

dimensional control (3). Precise dimensional control allows components to be fabricated to near net-shape which reduces the requirement for expensive ceramic machining. SRS-201 SiAlON is a duophase ceramic material that was developed by CPS for high temperature applications.

## 2.0 Objectives

The program objectives for the RPD 20-blade prototype rotor component development are:

1) **Rotor Materials:** Improve the mechanical properties of pressureless sintered SRS-201 duophase SiAlON.
   - Produce rotors with average hub (bulk) flexure strengths of 120 Ksi (827 MPa) at 25°C and 70 Ksi (482 MPa) at 1370°C[1].
   - Improve as-processed surface mechanical strength to approach rotor hub mechanical strength.
   - Increase the Weibull Modulus to greater than 15 from 25°C to 1370°C.

2) **Deliver RPD 20-Blade Prototype Rotors That Have Past Cold Spin Test:** Integrate Allison designs and SRS-201 SiAlON materials properties

[1] B-Bar 4-point flexure strength (MIL-SPEC 1942A).

into the RPD 20-blade prototype rotor design to deliver specification compliant rotors.

- Eliminate critical strength limiting surface flaws on all high stress component surfaces.
- Meet all dimensional specifications for the as-processed rotor.
- Integrate design feedback into the development program to ensure materials and fabrication success.
- Pass 125,000 RPM cold spin test for RPD 20-blade prototype rotors.

Strength and reliability of a ceramic component are influenced by processing and the materials strength. For example, processing related defects in a strong material will result in a weak component and a decreased reliability. The goals for the Rotor Materials, Program Objective 1, were addressed from both processing and materials development perspectives.

The goals in Program Objective 2, were addressed in similar fashion as the previous rotor development programs. CPS and Allison Engine Co. worked together to design the tooling that ensured the success of specification compliant SRS-201 SiAlON Quickset™ fabricated rotors. Dimensional tolerances of the as-processed rotors were achieved by control of sintering shrinkage. Component testing, will be the ultimate component design and material test for the RPD

20-blade prototype gasifier rotor. Specification compliant engine quality rotors will be cold spin tested at 125,000 RPM. Five cold spin tested rotors will be shipped to Allison Engine Co. for component evaluation.

## 3.0 Rotor Materials Development

Materials development goal was to improve both bulk properties and as-processed surface properties of the SRS-201 SiAlON. The bulk (hub) average mechanical flexure strength program target at room temperature and 1370°C were 120 Ksi (827 MPa) and 70 Ksi (482 MPa), respectively. Additionally, the Weibull modulus, a measure of the material reliability, was to be increased to $\geq$ 15 from room temperature to 1370°C. The program objective for the as-processed surface flexure strength was to increase the as-processed strength to approach that of the bulk strength.

Bulk material strength development focused upon removal of strength-limiting defects identified by mechanical testing and fractography.

Process development work focused on the elimination of these defects.

As-processed surface mechanical strength improvements focused on eliminating molding imperfections that resulted from mold cleaning and non-uniform mold lubrication. By eliminating component surface imperfections the component

strength could be increased.

Additionally, it was necessary to correlate the four-point strength values between A-sized and B-sized flexure test bars (MIL-STD 1942 (MR)) to evaluate mechanical strength data for the RPD sized rotors. The smaller A-bar test specimens were required to adequately[2] characterize the strength of the smaller diameter RPD rotors. However, in previous rotor development programs all mechanical testing was performed on B-sized bars. A- and B-test bar dimensions are summarized in Table 1. A direct strength correlation between A- and B-bars was necessary since the flexure strength values measured on smaller sized A-bars are greater than that of larger sized B-bars for the same material. The strength values increase with decreasing sample size because there is a lower probability of having a strength-limiting defect within a smaller test volume. To compare past mechanical property data to the current program, it was necessary to correlate strength measurements between A-sized and B-sized test bars for SRS-201 SiAlON material.

---

[2] At most only two B-bars could be machined from the RPD rotor. Ten B-bars were used to characterize material strength for AGT-5 rotors in 1992. Fourteen A-bars can be machined from the RPD rotor.

## 3.1 Bulk Rotor Material Development

SRS-201 SiAlON bulk material strength improvements focused upon removing strength-limiting defects which were identified in material testing. Initially, the primary defects observed were irregularly shaped voids which were in the sintered microstructure.

Table 2 summarizes the room temperature mechanical test data for B-bars machined from billets which were fabricated to qualify process improvements. Modest increases in the average room temperature strength was observed. The most significant processing influence, however, was realized in the increase of the Weibull modulus. The mechanical strength data before and after process improvements are graphically summarized in the Weibull plots given in Figure 2 and 3, respectively.

The implementation of process improvements increased the average strength of SRS-201 SiAlON to 119.1 $\pm$ 10.8 Ksi (821.0 $\pm$ 74.8 MPa) which is statistically equivalent to program objective strength value of 120 Ksi (827 MPa). Additionally, process improvements increased the Weibull modulus to 13.1 which is approaching the program objective of $\geq$ 15.

The results of the process improvements were also observed in the fracture surfaces of mechanical test specimens. Observations of material processed after process improvements revealed fracture origins that were smaller and located near, or on, the test bar tensile surface. The smaller defect size indicated that larger defects had been removed from the total defect population. The location of defects near to the tensile surface indicates higher stress failures of the SRS-201 SiAlON material.

A typical defect found in material processed with process

improvements is shown in Figure 4. In general, these defects appear similar, however much smaller than, the void defects formed by polymer agglomerate burn-out. The source of these voids is under investigation.

### 3.2 A-Bar Versus B-Bar Strength Correlation: Four-Point Flexure

A-bar and B-bars were machined from 5/8 inch cross section billets fabricated from the same batch of SRS-201 SiAlON material for the correlation between flexure strength results. All material was co-processed through firing; fired densities values ranged between 3.245 and 3.251 $g/cm^3$. Phase chemistries were similar as compared by x-ray diffraction peak height analysis. Thirty-six A-bars and 30 B-bars were tested in four point flexure at room temperature. The average flexure strength values were 134.3 $\pm$ 10.6 Ksi (926 $\pm$ 72.9 MPa) and 114.4 $\pm$ 12.6 Ksi (789 $\pm$ 87 MPa) for A- and B-bars, respectively. Fracture data are summarized in a Weibull plot given in Figure 5.

The flexure strength values for the B-bars was ~ 85 % of the measured average strength of A-bars. The increased measured strength for A-bars was expected because of the decreased probability of having a strength-limiting defect within a smaller A-bar test volume.

Additionally, twenty bulk A-Bars, machined from RPD 4-blade pre-

prototype rotors hubs were also tested. These data are summarized in a Weibull plot given in Figure 6. The RPD 4-blade pre-prototype rotor average strength value was 136.7 $\pm$ 11.7 Ksi (942.9 $\pm$ 80.4 MPa) which was similar to the A-bar strength value measured on billets.

A plot of average four-point flexure strength as a function of temperature for A- and B-bars is given in Figure 7. In general, the B-bar values are ~ 85 % of the A-bar values at a given test temperature.

### 3.3 As-Processed Surface Properties

The strength of the as-processed surface was to be improved so that it approached the bulk material flexure strength.

As-processed surface strengths were determined to be influenced by the molding process and the sintering atmosphere[4]. From the molding perspective, as-processed surface strengths are influenced by molding imperfections such as pits.

It was necessary to first eliminate molding related defects to adequately address the sintering atmosphere issues. No mechanical testing was

[4] It is also important to note that processing defects which influence the bulk material strength can also influence the as-processed surface strength.

performed during testing of molding processing techniques; visual inspection using a 40 x optical microscope was used to qualify improvements.

In 1992, the as-processed surface room temperature flexure strength was 55 - 60 Ksi (379 - 413 MPa) measured on

B-bars[5].

The as-processed mechanical strength for the SRS-201 SiAlON processed with the improved crucible environment was 80.1 $\pm$ 7.1 Ksi (552.2 $\pm$ 49.0 MPa) and 69.2 $\pm$ 3.9 Ksi (477.1 $\pm$ 26.9 MPa) at room temperature and 1370°C, respectively. An average fracture toughness value of 4.4 $\pm$ 0.3 MPa·$m^{1/2}$ [6] was measured for the as-processed surfaces. The fracture toughness for the SRS-201 SiAlON bulk material is 5.6 MPa·$m^{1/2}$.

[5] Because of the irregular shape of rotor surfaces, mechanical testing of as-processed surfaces were preformed on B-bars machined from 5/8 inch cross section billets.

[6] Fracture toughness determined by controlled flaw method.

The mechanical strength and toughness differences between the bulk and as-process surface properties are clearly related to phase chemistry differences. Further improvements in the as-processed surface strength can be realized.

The as-processed surface was compliant with surface finish specification; the measured surface finish was 0.69 μm which was in the surface finish specification of better than 1.6 μm.

## 4.0 Rotor Fabrication

### 4.1 RPD 4-Blade Pre-Prototype Tooling

As in previous rotor development programs, pre-prototype tooling was fabricated for the following purposes:

1) Establish appropriate gating and venting techniques.
2) Conduct process development work with respect to the hub section prior to receiving the RPD 20-blade prototype rotor tooling.
3) Develop mold treatment techniques that reduced as-molded surface defects.
4) Fabricate RPD 4-blade pre-prototype rotors to correlate mechanical strength of A-bars machined from pre-prototype rotors to B-bars machined from billets.
5) Fabricate RPD 4-blade pre-prototype rotors for developing component

specific drying and firing procedures prior to receiving RPD 20-blade prototype rotor tooling.

The RPD 4-blade pre-prototype tooling was fabricated with a hub geometry that was identical to the RPD 20-blade prototype geometry. The 4-blades were straight having similar length and thickness dimensions as blades of the 20-blade rotor.

CPS received the 4-blade rotor tool in mid September, 1993. The mold concept functioned as designed with only minor venting modifications required.

## 4.2 RPD 4-Blade Pre-Prototype Rotor Process Development

A picture of fired RPD 4-blade pre-prototype rotors are shown in Figure 8. Over 100 RPD 4-blade pre-prototype rotors were molded during process development. All RPD 4-blade pre-prototype rotors were visually inspected after molding in the green state using a 40 x optical microscope.

Initially the pre-prototype tooling was used to establish injection rate profile for the smaller RPD rotor. It is important that the injection profile be well controlled so as not to introduce injection flow textures internally or on external part surfaces. Injection flow textures can be introduced at points in the mold cavity where the slip sharply changes speed or direction and where injection fronts

meet. A series of short-shots were used to establish the correct injection rate profile for the rotor hub. The profile established for the 4-blade pre-prototype tool was used for the RPD 20-blade prototype rotor without modification.

Two molding related defects were identified with the as-received tooling in initial testing: 1) a surface void defect on the peak of the balance stock, 2) a surface void defect on the inner diameter of the shaft. Both these defects were the result of inadequate venting. Defects were eliminated by adding vents to the tool in these areas. Venting at the balance stock and the inner diameter of the rotor shaft were subsequently incorporated into the design of the RPD 20-blade prototype rotor tooling. Representative prototype rotors were internally inspected by x-ray radiography. No internal defects were found.

All fired rotors were visually inspected using a 40 X optical microscope. Aside from green part handling defects on an occasional rotor surfaces of fired rotor parts were visually defect free. In the course of the process development, rotor handling procedures were modified to minimize the probability of a rotor being damaged via handling. Green part handling fixtures were used during all post drying procedures up to the time of firing, which minimized handling damage.

Several representative rotors were sectioned and polished for internal optical microscopic inspection. No internal voids, molding defects, or density gradients, were revealed in these observations. Representative fired RPD 4-blade

pre-prototype rotors were internally inspected by x-ray radiography. No internal defects were found. Sintered densities of RPD 4-blade pre-prototype rotor parts ranged from 3.235 g/cm$^3$ to 3.255 g/cm$^3$ which corresponds to 99.2% and 99.8% of theoretical density, respectively. Theoretical density for SRS-201 SiAlON is 3.26 g/cm$^3$. As stated previously, the average four-point flexure mechanical strength was 136.7 $\pm$ 11.7 Ksi (942.9 $\pm$ 80.4 MPa)

## 4.3 RPD 20-Blade Prototype Tooling

Design discussions for the RPD 20-blade prototype mold began in April 1993. An outside machine shop was selected to fabricate the prototype tooling early in May.

The design plan had a one step part design approval process based upon Allison's approval of a three-dimension model on a computer screen at the machine shop. The part design was approved by B. Riehle of Allison on July 28, 1993.

Fabrication of the tooling began in August. The RPD 20-blade prototype tooling was received in mid December of 1994. Balance stock and shaft venting concepts which were added to the pre-prototype tooling were incorporated in the design and fabrication of this mold. The prototype mold functioned as designed. Only a minor sprue modification was necessary to ensure proper

solidification in the Quickset™ injected components.

## 4.4 RPD 20-Blade Prototype Rotor Process Development

Pictures of green and fired RPD 20-blade prototype rotors are shown in Figure 10. Nearly 100 RPD 20-blade prototype rotors were molded in this program. Once modifications were made to the sprue no further process development work was required for the RPD 20-blade prototype rotor.

All RPD 20-blade prototype rotors were visually inspected after molding in the green state using a 40 x optical microscope. Despite taking extreme care, an occasional handling defect was observed. Process automation is required to completely avoid the potential for this problem. Candidate engine quality rotors were internally inspected by x-ray radiography. No internal defects were found.

Approximately 40 of the RPD 20-blade prototype rotors were fired. All fired rotors were visually inspected using a 40 X optical microscope. Fired surfaces of rotors were found to be visually defect free. No firing related part distortions were noted. The measured as-processed surface finish for the RPD 20-blade prototype rotor was 0.70 μm which was within the surface finish specification of better than 1.6 μm. The sintered densities of 20-blade prototype rotors ranged from 3.235 g/cm$^3$ to 3.254 g/cm$^3$ which corresponds to 99.2% and 99.8% of theoretical density, respectively. Theoretical density for SRS-201 SiAlON is 3.26 g/cm$^3$.

The room temperature and 1370°C flexure strength data for material machined from RPD 20-blade prototype rotor hubs are summarized in the Weibull plots shown in Figure 11 and Figure 12, respectively. Fourteen A-bars were tested at each temperature. Rotors tested were fabricated prior to the fabrication of candidate engine quality RPD 20-Blade prototype rotors. The average room temperature flexure strength was 138 $\pm$ 7.0 Ksi (953 $\pm$ 48 MPa) for A-bars. At 1370°C, the average flexure strength was 74.8 $\pm$ 4.6 Ksi (516 $\pm$ 32 MPa) for A-bars. The Weibull modulii calculated for room temperature and 1370°C were 22.3 and 18.7, respectively.

Fifty A-sized bulk test bars will be delivered to Allison Engine corporation for their evaluation.

Candidate engine quality fired rotors were internally inspected by x-ray radiography and micro-focus x-ray radiography. No internal defects were found by either technique. Several non-engine quality rotors were sectioned and polished for internal optical microscopic inspection. No internal voids, molding defects, or density gradients, were revealed in these observations. Non-engine quality rotors have been submitted for mechanical testing.

Outside hub diameters were measured on fired RPD 20-blade prototype rotors. Diameters were measured using an optical comparitor at a magnification of 40 X. Thirty rotors were

measured; comprising approximately ten rotors for three separate rotor fabrication lots. The average measured diameter for RPD 20-blade prototype rotors was with a range of $\pm$ 0.06 mm. The design tolerance range was .30 mm. The range of diameter values measured for these parts were within the specified tolerance values. Three candidate engine quality rotors have been selected for dimensional analysis measured by a coordinate measurement machine.

## 5.0 Conclusions

Low cost fabrication of structural ceramic material components are necessary for the success of advanced gas turbine heat-engines. To achieve this goal requires cost-effective fabrication techniques and cost-effective material choices. Ceramics Process Systems has made significant advances towards this goal throughout the ATTAP program.

The approach used by CPS to achieve this goal was to fabricate SRS-201 SiAlON RPD 20-blade prototype gasifier rotors using the CPS Quickset™ injection molding process. SRS-201 SiAlON, a duophase SiAlON material developed for high temperature heat engine applications, is densified by pressureless sintering. The Quickset™ process produces complex-shaped parts that have uniform sintered shrinkages and reproducible dimensional control allowing for near-net-shape fired component fabrication. Because the CPS approach

fabricates engine components to near-net shape by pressureless sintering, high cost fabrication processes such as Hot Isostatic Pressing and sintered component machining are eliminated.

In 1993, process refinements were made to improve the overall mechanical strength and reliability of near net-shape heat engine components. Elimination of process related defects resulted in an increase in the SRS-201 duophase SiAlON bulk mechanical strength to 119 Ksi (820 MPa) with a Weibull modulus of 13.1.

Additionally, the as-processed surface strength was improved for SRS-201 SiAlON. Prior to initiating the 1993 program, the as processed surface strength was measured to be 54 Ksi (372 MPa). In this program the as-processed surface strength was improved to 80.1 Ksi (552 MPa) and 69.2 Ksi (477 MPa) for room temperature and 1370°C, respectively; fracture toughness was 4.4 $MPa \cdot m^{1/2}$ (B-Bars).

Strength was characterized for RPD 20-Blade prototype rotors fabricated prior to the production of spin test rotors. The room temperature mechanical strength was measured to be 138 Ksi (953 MPa) as measured on A-bars. The Weibull modulus value was 22.3.

The RPD 20-blade prototype gasifier rotors are currently being prepared for spin testing in April 1994.

## 6.0 Bibliography

1) C.A. Sundback, G.V. Franks, R.R. Lee and B.E. Novich "Near Net Shape Fabrication of AGT-5 Ceramic Gas Turbine Rotors Using Quickset™ Injection Molding", in Proceedings of the Annual Automotive Technology Development Contractors Coordinators Meeting, Dearborn, MI, October 28-31, 1990, SAE International, P-256 (1992), 31-36.

2) B.E. Novich, C.A. Sundback, and R.W. Adams, "Quickset™ Injection Molding of High Performance Ceramics", in Ceramics Transactions: Forming Science and Technology for Ceramics, Vol 26, ACS (1992) 157-163.

3) C.A. Sundback, G.V. Franks, R.R. Lee, and B.E. Novich, "Cost Effective Fabrication of Heat Engine Components: Near Net-Shape SRS-201 Gas Turbine Rotors Using Quickset™ Injection Molding Process", in Proceedings of the Annual Automotive Technology Development Contractors Coordinators Meeting, Dearborn, MI, November 2 - 5 1992, SAE International, P-265 (1992) 329-337.

TABLE 1: A-BAR AND B-BAR MECHANICAL TEST SPECIMEN DIMENSIONS (MIL-STD 1942 (MR); 4-PT. LOADING)

| BAR | WIDTH (mm) | THICKNESS (mm) | LENGTH (mm) | LOAD SPAN (mm) |
|---|---|---|---|---|
| A | 3 | 1.5 | 25 | 20 |
| B | 6 | 3 | 45 | 40 |

TABLE 2: ROOM TEMPERATURE FLEXURAL STRENGTH VERSUS PROCESS IMPROVEMENT
B-BARS 4-POINT FLEXURE

| PROCESS IMPROVEMENT | STRENGTH LIMITING DEFECT REVEALED | ROOM TEMPERATURE 4-PT FLEXURE | WEIBULL MODULUS | BARS TESTED |
|---|---|---|---|---|
| BASELINE MATERIAL | VOIDS | 114.4 +/- 12.6 Ksi<br>788.8 +/- 86.9 MPa | 10.8 | 30 BARS |
| DISSOLUTION AND FILTRATION | SMALL VOIDS | 119.1 +/- 10.8 Ksi<br>821.0 +/- 74.8 MPa | 13.1 | 28 BARS |

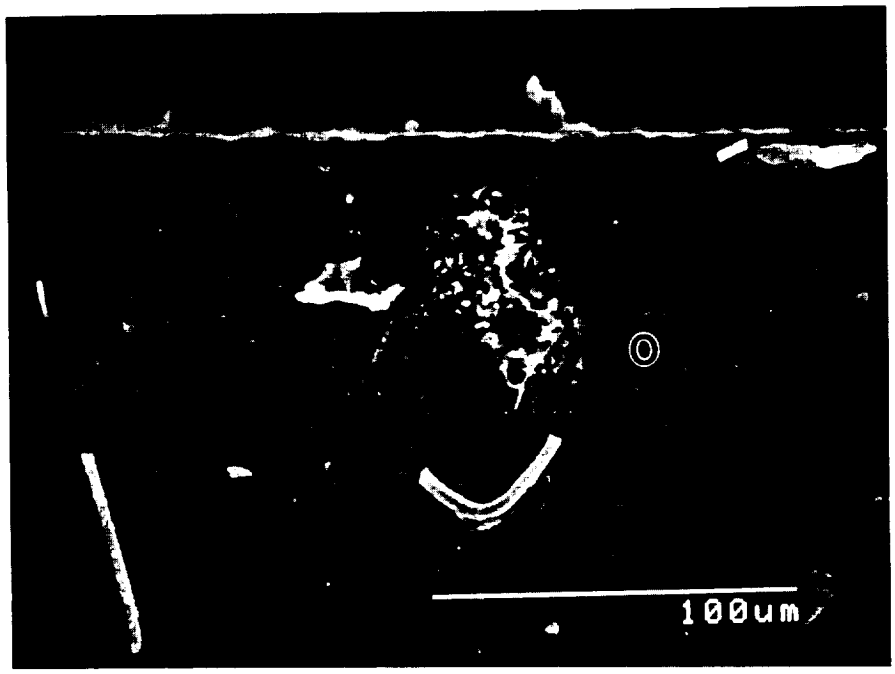


Figure 1 Void Defect in SRS-201 SiAlON Fracture Surface.

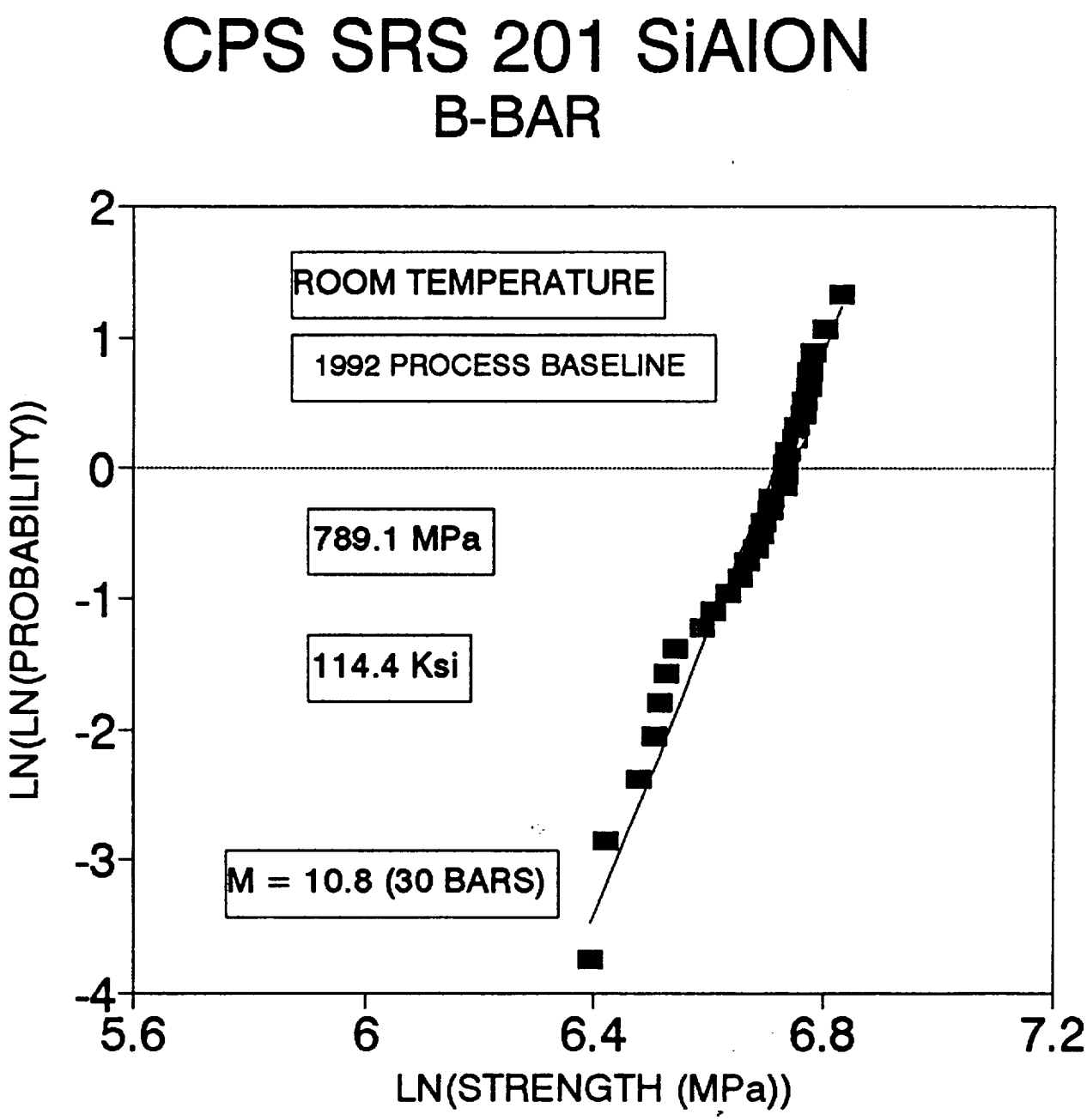


Figure 2 Weibull Plot of 4-Point B-Bar Flexural Data for Material Processed Before the Process Improvements

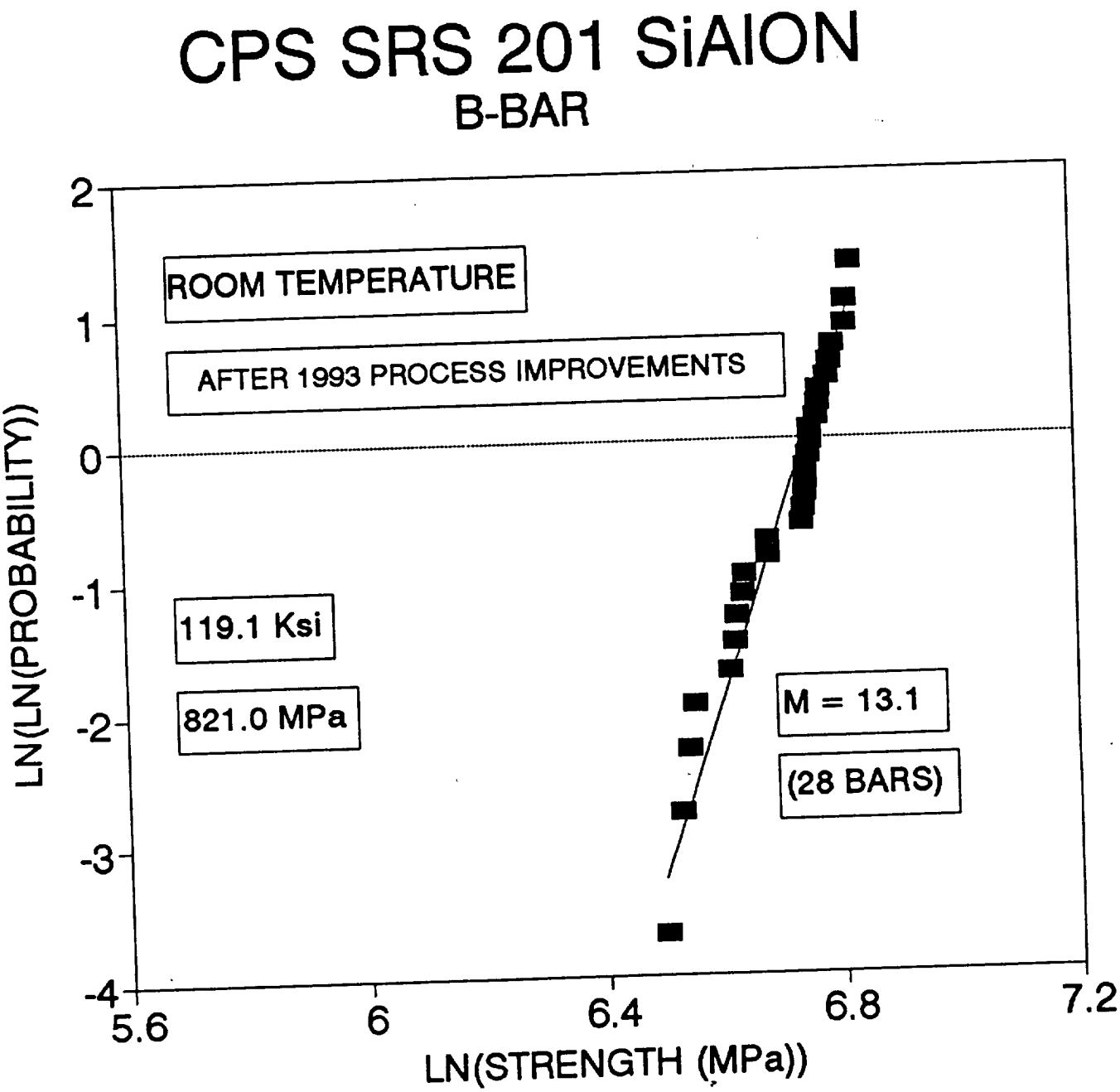


Figure 3 Weibull Plot of 4-Point B-Bar Flexural Data for Material Processed After the Process Improvements.

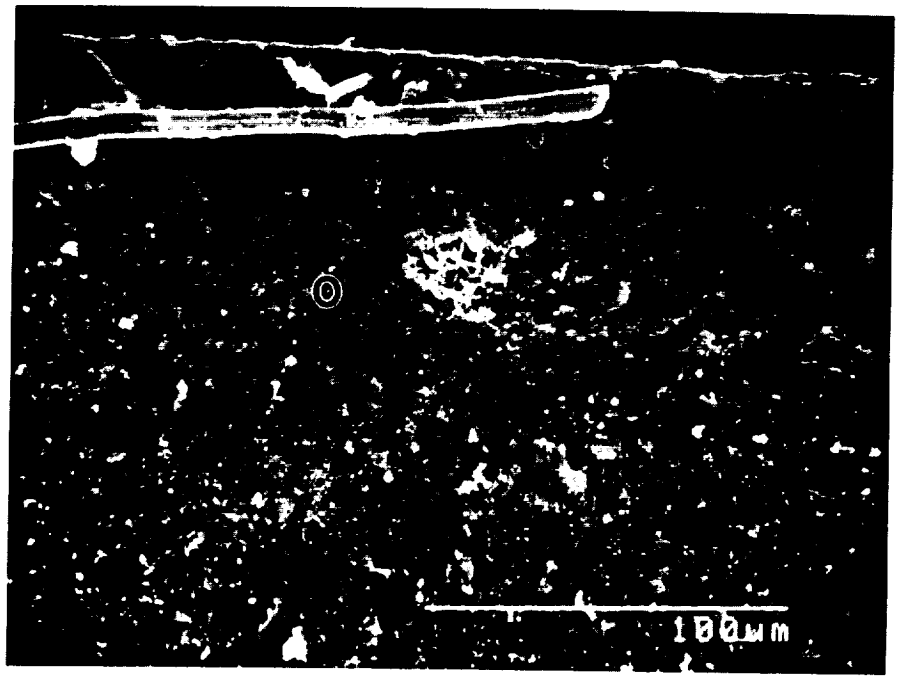


Figure 4 Burn-Out Void Defect in SRS-201 SiAlON Fracture Surface for Material Processed With the Process Improvements.

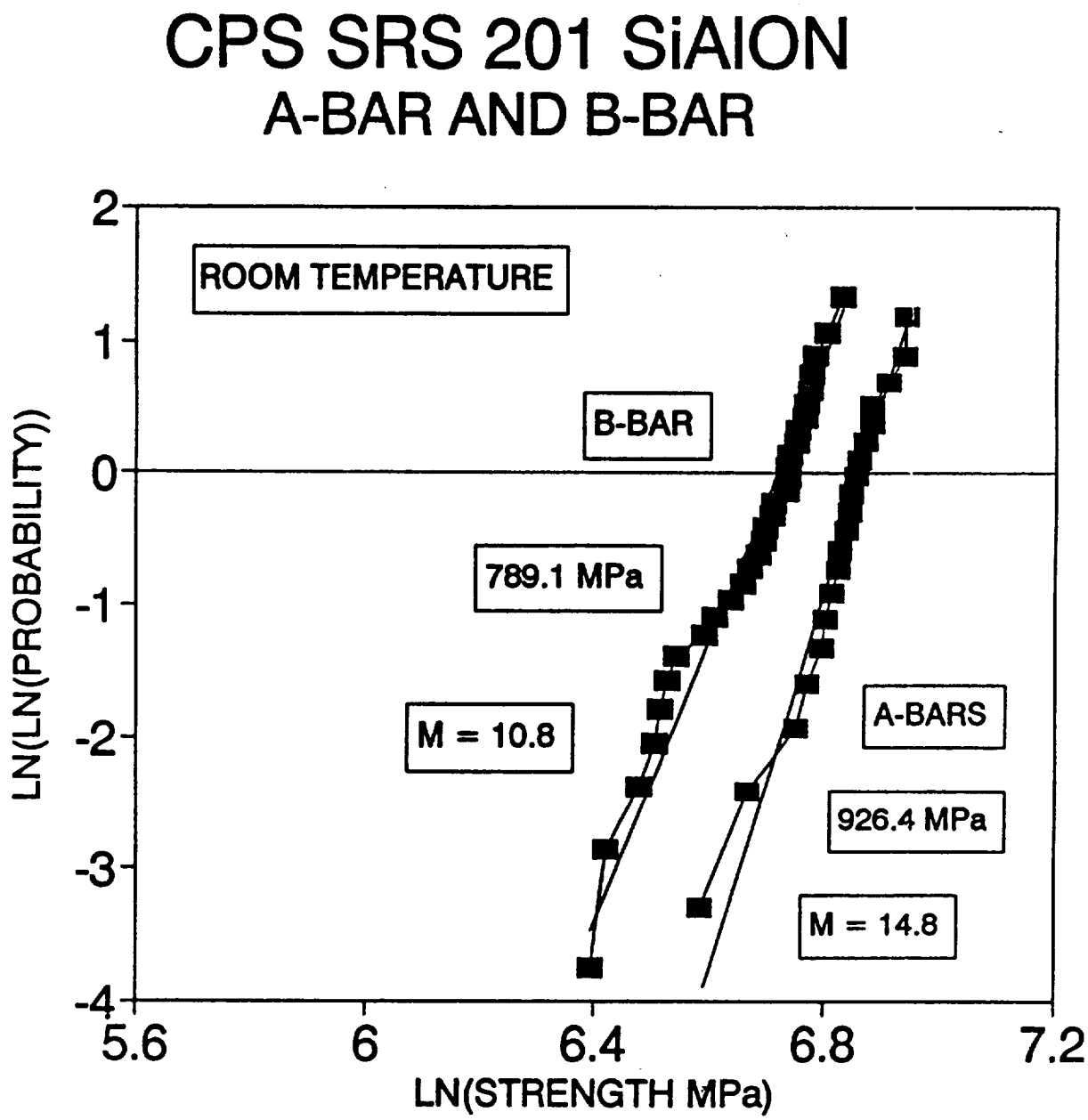


Figure 5 Weibull Plot Comparing 4-Point Flexure Data for A- and B-Bars Machined From Billets (Material Processed Prior to the Process Improvement).

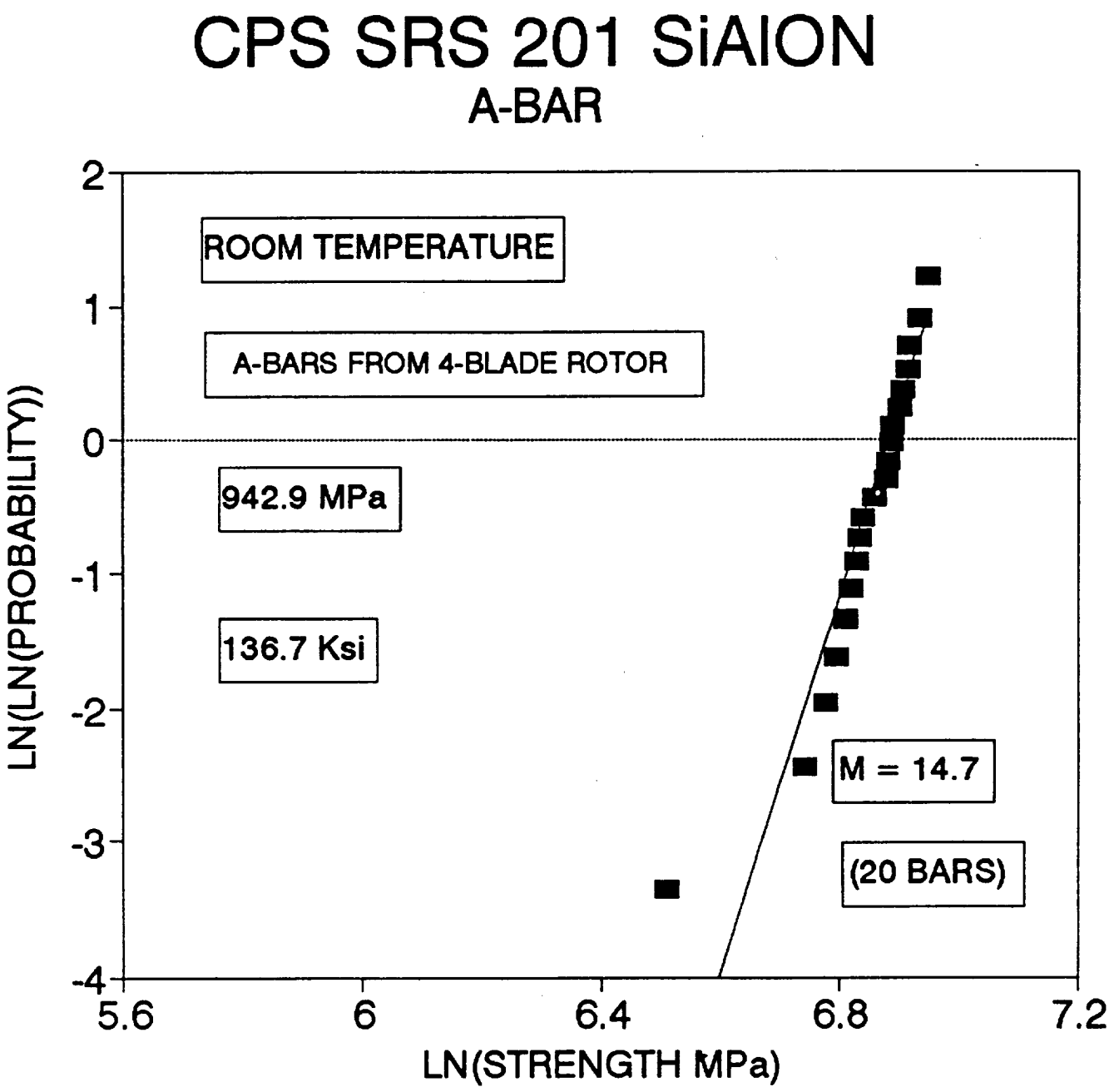


Figure 6 Weibull Plot Data for A-Bars (4-Point Flexure) Machined From 4-Blade Pre-Prototype RPD Rotors (Material Processed Prior to the Process Improvement).

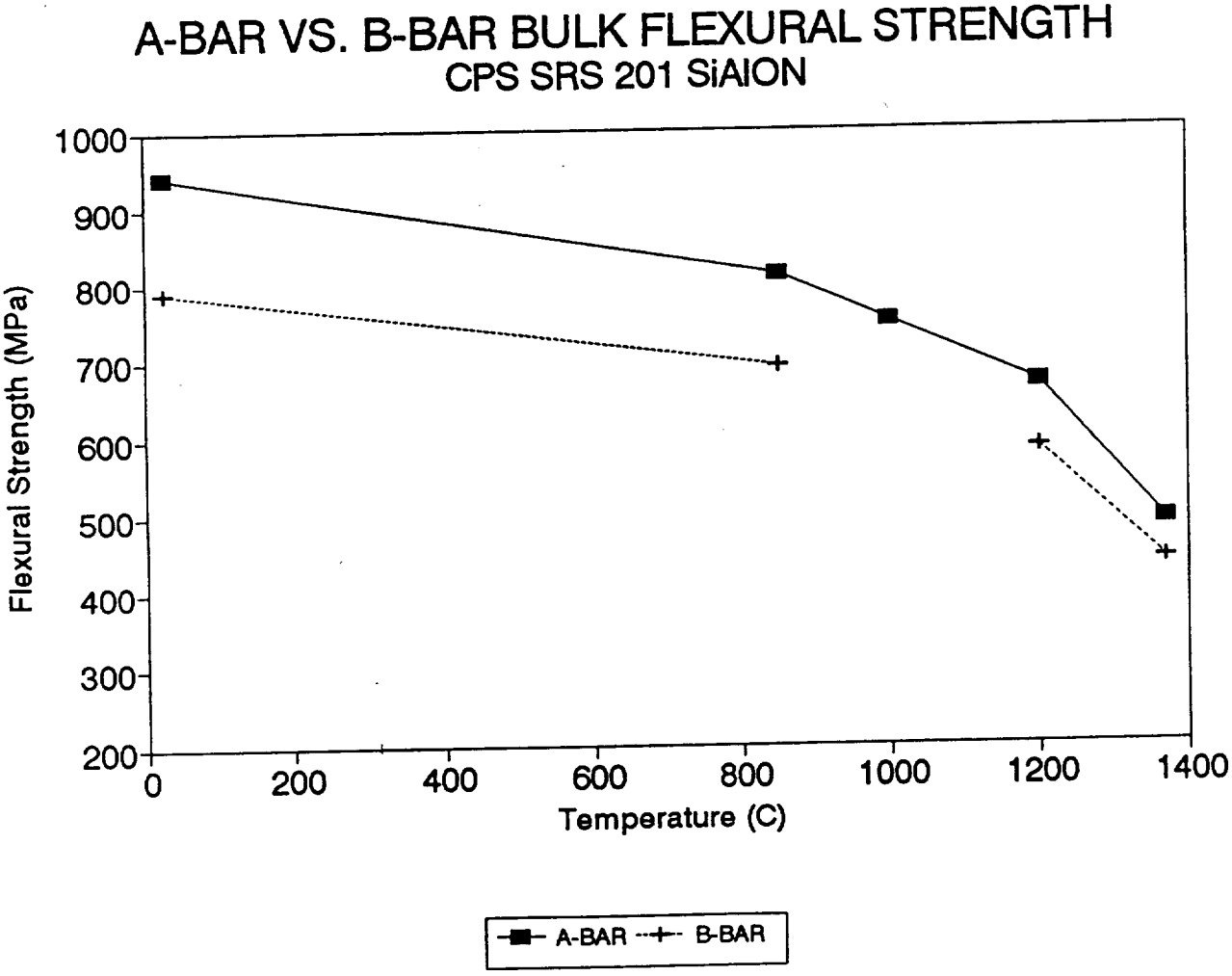


Figure 7 A- and B-Bar 4-Point Flexure Data for SRS-201 SiAlON as a Function of Test Temperature (Material Processed Prior to the Process Improvement).

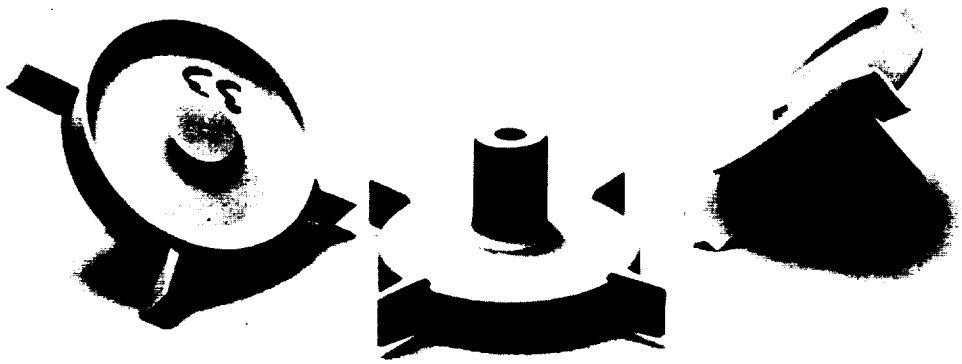

Figure 8 Fired 4-Blade Pre-Prototype RPD Size Rotor.

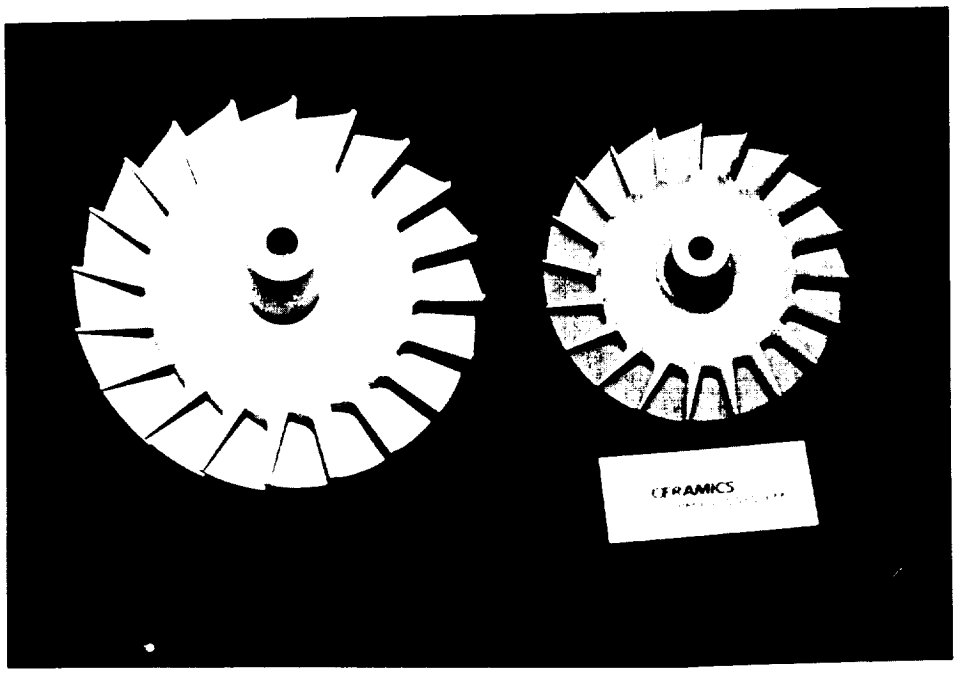


Figure 10 Green (left) and Fired(right)20-Blade Prototype RPD Size Rotors.

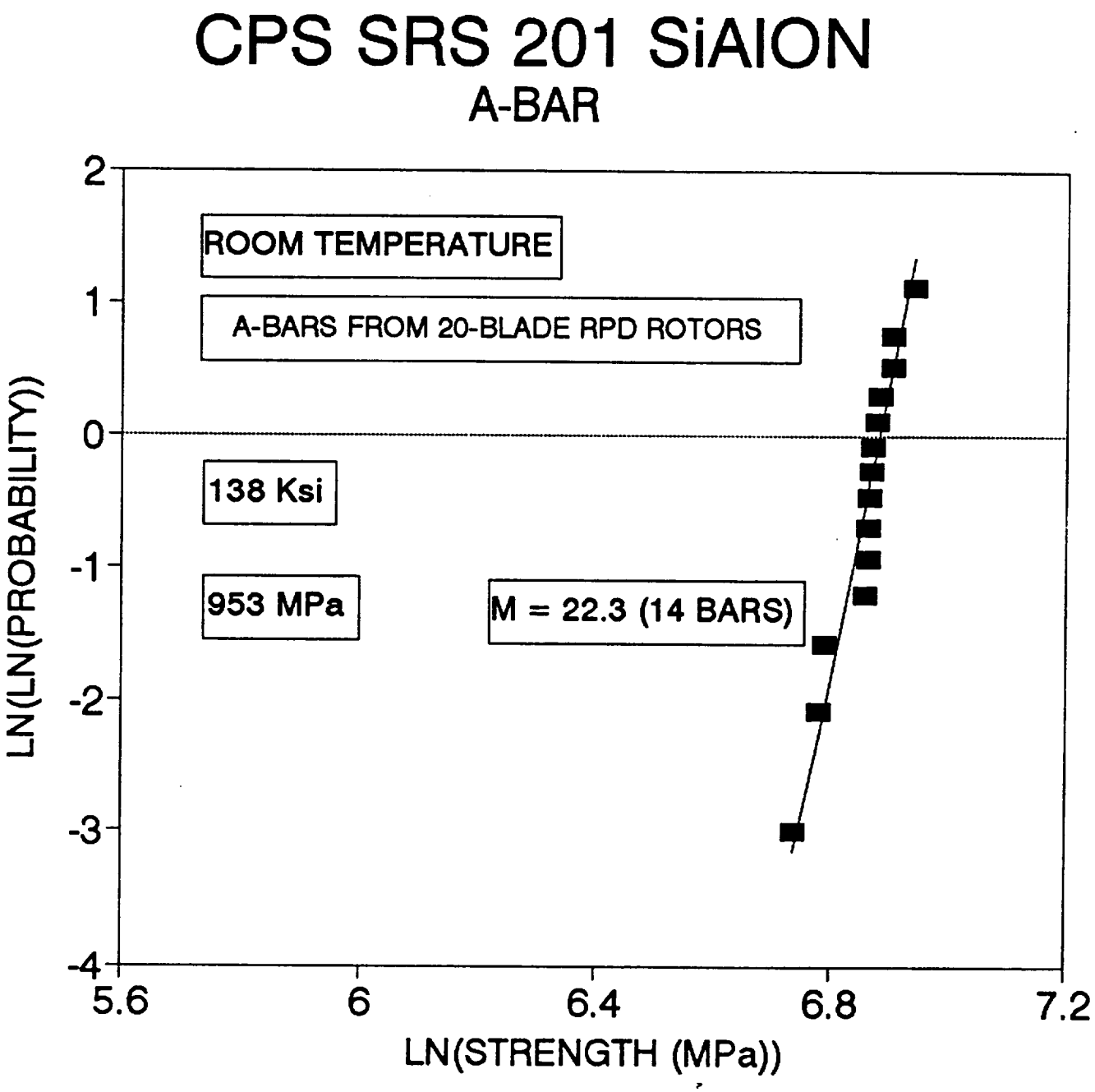


Figure 11 Weibull Plot of Room Temperature A-Bar 4-Point Flexural Data for Machined From 20-Blade Prototype Rotors Processed With the Process Improvement.

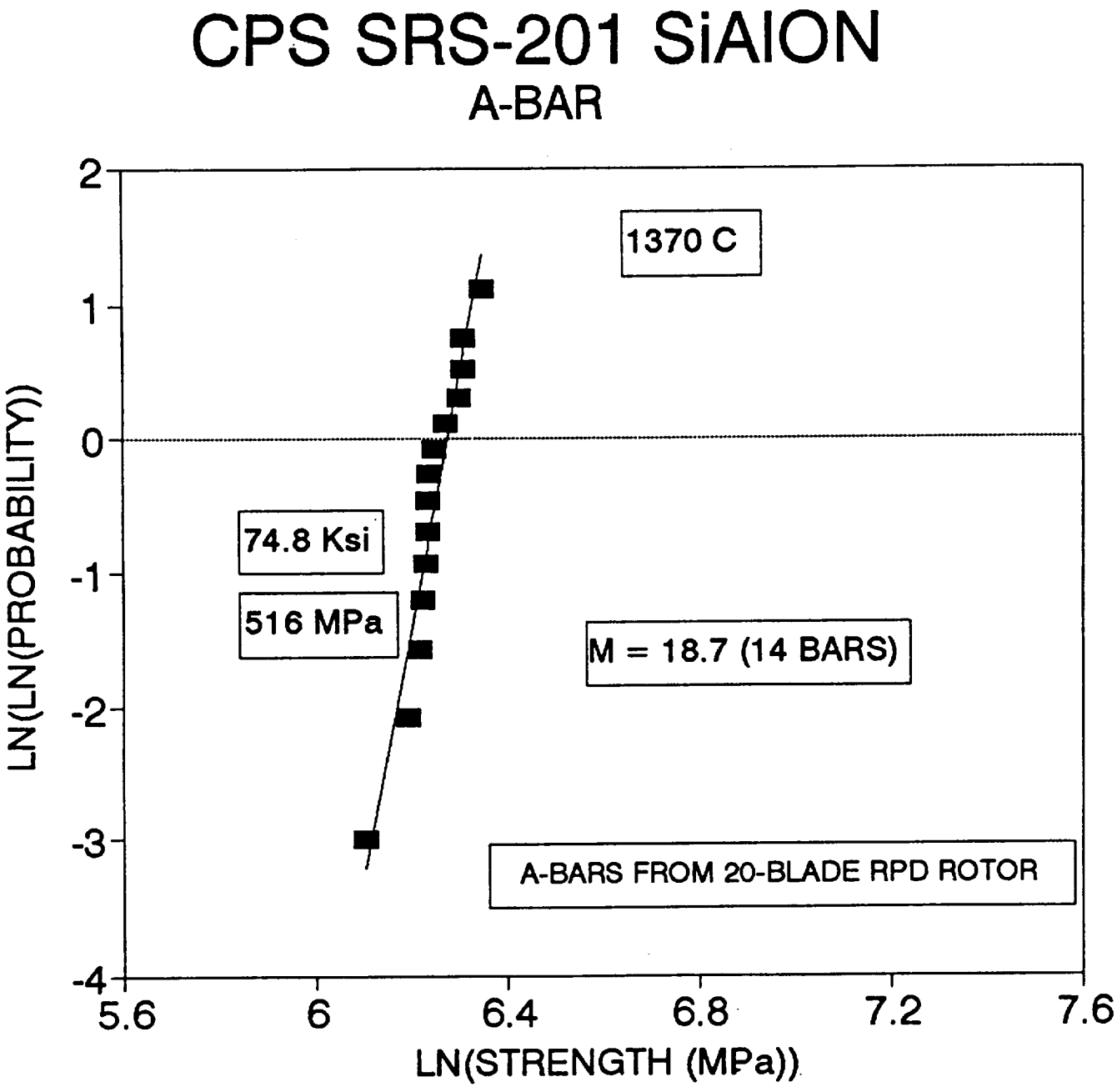


Figure 12 Weibull Plot of A-Bar 4-Point Flexural Strength at 1370°C for Machined From 20-Blade Prototype Rotors Processed With the Process Improvement.

# APPENDIX G

Norton Advanced Ceramics
1993

NOTE: INFORMATION SUBMITTED THAT IS DEEMED TO BE
PROPRIETARY IN NATURE
HAS BEEN DELETED.

# ADVANCED TURBINE TECHNOLOGY APPLICATIONS PROJECT

# COMPONENT DEVELOPMENT PROGRAMS FOR AGT-5 AND RPD GASIFIER ROTORS AND SCROLLS

Annual Report For The Period
January 1, 1993 through December 31, 1993

Work Performed Under Allison Gas Turbine Division
Purchase Order Nos. H321527 and H321526.

Prepared For:

ALLISON ENGINE COMPANY
Indianapolis, IN 46206

Submitted By:

NORTON ADVANCED CERAMICS
Northboro, MA 01532-1545

Report Prepared by:

Eric Bright
Steve A. Dynan

Report Date: January 18, 1995

## EXECUTIVE SUMMARY

Presented in this report are Norton Advanced Ceramic's (NAC) component development activities on AGT-5 and RPD-size rotors and scrolls completed during 1993. Work in 1993 focused on utilization of appropriate tooling, molds, and processes to develop production viable processes for rotors and scrolls. A summary of significant accomplishments for the year is given below.

AGT-5 and RPD Gasifier Rotor Component Development:

- The NT164 powder processing operation was scaled-up and optimized. The powder batch size was increased from 20 Kg to ≈ 60 Kg. The scale-up and optimization of the NT164 powder processing operation reduced the cost of NT164 powder by approximately 50%.

- Improvements to the NT164 slip formulation were explored for casting complex-shape components. A slip formulation containing a green body toughening additive was identified that exhibited stable rheological properties, casting rates 5 to 20 times greater than the current standard NT164 slip formulation, and improved capability to pressure cast, demold, and dry crack-free complex-shapes. This slip formulation, however, resulted in lower as-processed surface strength, and was dropped from further development efforts.

- A bladeless rotor hub mold was design and fabricated for use at high casting pressures up to 600 psi on NAC's Dorst pressure casting machine. Results from NT164 Dorst machine casting trials indicated that higher casting pressures in conjunction with a smaller average pore size in the porous plastic mold material produced NT164 hubs with the highest wet green strength and best shape retention.

- A mold for casting RPD rotors on NAC's Dorst machined was designed. This mold design incorporated concepts from the industrialized RPD rotor mold evaluated in benchtop casting trials.

- Work was performed to simplify and reduce the number of NT164 furnacing operations. It was determined that mechanical properties were at optimum levels when the crystallization and oxidation process steps are performed separately. Additional work was performed to optimize the as-processed surface strength of NT164 through a combination of presinter, HIP, and post-HIP furnacing treatments. Various encapsulant glass compositions and HIP time-temperature cycles were investigated. None of the experimental treatments resulted in improved as-processed surface strength compared to standard NT164 processing conditions.

- Abrasive flow machining (AFM) was evaluated as a means of removing material from NT164 as-processed surfaces. Material removal of up to 0.005" per surface was achieved resulting in a typical surface finish of less than 16 microinches. Results of an L9 optimization experiment revealed that as-processed surface strength was not improved for any of the AFM treatments.

- RPD rotors for Delivery Set No. 1 were pressure cast using an industrialized mold design, and were processed through dense casting inspection. Of a total of eight RPD rotors inspected, two passed NAC's engine quality rotor acceptance criteria. Surface defects and other discrepancies were traced back to the casting process. Mold and casting process modifications to minimize or eliminate the defects were identified and demonstrated.

- A process to finish machine RPD rotors was developed and demonstrated based on the previous AGT-5 rotor grinding technology.

AGT-5 Scroll Manufacturing Development:

- In support of developing a design data base for scrolls, room temperature tensile data was generated for NT230 Si-SiC. The characteristic room temperature tensile strength was measured to be 248 MPa with a weibull modulus of 5.1.

- Two AGT-5 Task 3.2 design scroll castings were machined, inspected and delivered to Allison. Eight Task 3.2 design scrolls were cast to make up a balance quantity of two deliverable scrolls.

- A linked experiment coupling the optimization of the NT230 slip formulation with simplification of downstream firing operations was completed. Based on a review of all of the response variables, the optimal slip formulation and firing process parameters for NT230 was identified.

- Benchtop pressure slip casting trials were conducted to demonstrate the AGT-5 to RPD-size "scale down" of NAC's NT230 scroll casting process. The standard NT230 slip formulation (ie, without a reinforcement additive) produced crack-free components upon demolding and drying.

- A preliminary demonstration of casting and processing NT154 RPD scrolls through HIP densification was completed. Sub-scale NT154 and NT164 AGT-5 Task 3.2 design scrolls were successfully cast as well. A number of sub-scale AGT-5 NT164 scrolls were successfully processed through HIP densification.

- A modified formulation of the Dorst/Laufen material was developed to reduce pore size and water volumetric flow rate. A water volumetric flow rate 20-40X lower than the standard Dorst/Laufen mold material was achieved. This mold material produced the highest scroll demolding yield and best shape retention results to date. Lower casting rates were observed for this mold material in tensile rod casting trials on the Dorst machine.

- Two porous plastic RPD scroll mold design iterations were evaluated on NAC's Dorst casting machine. Scroll casting trials using pressures up to 600 psi were performed. RPD scrolls were successfully cast in the range of 350 to 400 psi with a casting time of approximately 60 seconds. RPD scroll castings exhibited good mold release and shape retention, but a had a relatively poor inside drain surface due to pooling of slip and clumping around the reinforcement material. The second RPD scroll mold design

iteration incorporated a sub-assembly to allow for mold rotation to eliminate pooling of slip during the drain cycle.

This effort continued in each of the above areas in 1994. Work is scheduled to continue for the 1995 program year. The 1995 activity is focused on development of component specific cost effective manufacturing processes for NT164 rotors, scrolls, and combustors.

## INTRODUCTION

Commercialization of advanced structural ceramics requires development of reliable component manufacturing processes. The Advanced Turbine Technology Applications Project (ATTAP) addresses this requirement. The ATTAP is a DOE-sponsored, 5-year ceramic component development program which utilizes the AGT-5 gas-turbine engine as a functional test-bed. The goals of this program include: (1) The development and demonstration of reliable ceramic fabrication processes; (2) Production of the required ceramic components; and (3) Evaluation of these components in actual engine tests.

As a participant in ATTAP, and subcontractor to Allison Engine Company, Norton Advanced Ceramics (NAC) is developing ceramic fabrication processes for AGT-5 and RPD gasifier rotors and scrolls. NAC has performed this effort in accordance with separate Work Statements (SOW) for each component. NAC has simplified the scope of its component development efforts by evolving from three principal materials in 1992 (NT154 Silicon Nitride, NT164 Silicon Nitride, and NT230 Siliconized Silicon-Carbide) to two materials (NT164 Silicon Nitride, and NT230 Siliconized Silicon-Carbide) in 1993. An overview of these materials is as follows:

NT154 Silicon Nitride ($Si_3N_4$) - NT154 is a 4% $Y_2O_3$-doped composition densified by hot-isostatic pressing (HIP). HIPing is accomplished using glass encapsulation techniques. Assessment and characterization of this material has been conducted at NAC, Allison, other engine builders, and independent laboratories. NT154 possesses excellent flexural fast-fracture behavior up to 1370°C, accompanied by an acceptable Weibull Modulus. Failure origins have been associated with surface related machining flaws or internal impurities. Reported tensile strengths under fast-loading conditions parallel flexural tests. For tensile tests, principal failure origins were volume inclusions--generally identified as iron impurities. Under slow-loading conditions at elevated temperatures, creep and slow crack growth behavior have been characterized. NT154 exhibits creep through a cavity nucleation and growth mechanism. Failure occurs via cavity link-up. In comparison with other advanced materials, excellent durability has been noted.

NT164 $Si_3N_4$ - NAC has utilized the experience in processing NT154 to make several alternations within the material itself in an effort to improve its properties. NT164 was developed from NT154 through optimization of slight changes to the glass phase composition, along with adjustments of selected heat-treatment schedules. NT164 has equivalent room-temperature strength and fracture toughness to NT154. However, significant improvements are noted in high-temperature strength and creep resistance. NT164 has four times the expected creep life of NT154 at 1370°C. NT164 derives its enhanced high temperature strength and creep resistance from the fact that it has no intergranular phase at two grain junctions. Two grain junctions in NT154 possess a glassy phase which allows creep, cavity nucleation, and growth to occur. In NT164, the absence

of any discernible intergranular phase greatly enhances creep resistance. During 1993, NAC continued to increase its data base on NT164, and delivered various components and specimens to a number of engine builders including Allison.

NT230 Siliconized Silicon Carbide (Si-SiC) - NT230 siliconized silicon carbide (Si-SiC) was developed and introduced into the Scroll Program in 1991. This material has approximately double the strength of previous Si-SiC compositions. At elevated temperatures (up to 1370°C), its strength is nearly equivalent to NT154. NT230 Si-SiC was utilized in the scroll manufacturing development effort in 1993.

## AGT-5 AND RPD GASIFIER ROTOR COMPONENT DEVELOPMENT

In 1989-90, NAC developed and produced a number of 20 bladed NT154 gasifier rotors for Allison. Four of these components met spin test requirements and were delivered. One of the rotors has successfully completed cyclic durability rig testing in excess of 200 hours. Temperatures and stresses within this test parallel anticipated engine conditions. The remaining three rotors have also been successfully tested at Allison.

As a result of these successes, NAC was requested to propose a follow-on developmental program for Allison. The program, which was initiated in March of 1991, was originally comprised of four tasks. However, with the introduction of NT164, the program was expanded to include seven tasks: (1) Rotor Forming Development; (2) 20 Blade NT154 Engine Quality Rotor Production; (3) 20 Blade NT164 Engine Quality Rotor Production; (4) NT164 Test-Bar Production; (5) 26 Blade NT154 Engine Quality Rotor Production; (6) Cost Analysis; and (7) Project Management. During 1992, NAC completed all planned tasks required under the gasifier rotor component development program. Using an optimized casting mold from the 1991 effort, NAC fabricated and delivered to Allison a total of fourteen engine quality, proof tested AGT-5 gasifier rotors. Under Task 3.2, NAC spin tested a total of seven 20-blade, NT154 rotors. Four of these seven passed the 80 krpm spin test requirement. Two were purposefully burst above this proof level at 88 and 92 krpm. The remaining two were delivered to Allison for engine testing. The remaining three failed from known defects in the blades or hub. Under Task 3.3, NAC used its experience from Task 3.2 to improve the fabrication process prior to initiation of NT164 rotor production. Under Task 3.3, NAC spin tested a total of five 20-blade, NT164 rotors. All five passed the 80 krpm spin test requirement and were delivered to Allison for engine testing. Under Task 3.5, NAC designed and fabricated a casting pattern and molds for a 26-blade AGT-5 gasifier rotor. A total of nine 26-blade, NT154 rotors were proof tested. Eight of the nine passed the 80 krpm spin test requirement. NAC delivered seven of the proof tested rotors to Allison for engine testing. Using its experience from this rotor development program, NAC completed a cost analysis task for high volume production of gasifier rotors.

Based on the successful completion of the 1992 effort, a follow-on effort was funded by Allison for NAC to focus on process simplification and development of cost-effective production processes for gasifier rotors. NAC's 1993 rotor process development activities encompassed two major tasks: Task 1 - Process Simplification; and Task 2 - Prototype Production. Work performed under these tasks in 1993 is summarized as follows:

Task 1- Process Simplification. This task included the following sub-tasks: (1) Slip

Engineering; (2) Forming Development; (3) Firing Development; (4) Machining Development; and (5) Quality Assurance and Inspection.

Slip Engineering - Under this sub-task, the NT164 powder processing operation was scaled up and optimized. The batch size was increased form 20 Kg to ≈60 Kg. A Taguchi L9 experiment was performed, and optimal conditions for: (1) Powder Pre-Treatment, (2) Deflocculant Type, (3) Deflocculant Level, (4) Solids Content, and (5) Milling Time were selected. The scale-up and optimization of NT164 powder processing operation reduced the cost of processed NT164 powder by approximately 50%.

Utilizing the optimized NT164 processed powder, NAC conducted subsequent work to optimize the storage life of "ready to cast" NT164 slip. Evaluations were performed at both room temperature and low temperature. The slip formulation and storage techniques were optimized, resulting in stable rheological properties for two weeks at room temperature and four weeks at low temperature.

Concurrent with optimizing the slurry storage life, work was performed in an attempt to engineer the NT164 slip formulation for casting complex-shape components. The objective of this effort was to identify an NT164 slip formulation that exhibited long term rheological stability, a fast casting rate, and capability to produce crack-free complex-shapes upon demolding and drying. A linked designed experiment was performed to optimize the NT164 slip formulation. The first of two linked arrays was and L9 design to investigate the effect of green body reinforcement additives.

The reinforcement additive L9 experiment was linked with an L7 flocculation array. The factors in this array were: (1) Solids content; Flocculation agent type; and (3) Flocculation agent level. The response variables were: (1) Slip rheology; (2) Casting rate; (3) Green density; (4) Complex-shape formability; and (5) Mechanical properties. Results were analyzed and a set of optimal process parameter settings was determined. Characteristics of material fabricated from NT164 slip prepared under the optimal conditions are summarized as follows:

- Stable rheological properties for greater than two weeks at room temperature.
- Casting rates 5 to 20 times greater than the current standard NT164 slip formulation.
- Green densities comparable to the current standard NT164 slip formulation.
- Superior capability to pressure cast, demold, and dry crack-free complex-shapes.
- ≈30% lower as-processed surface strength at room temperature.
- Small but statistical significant decrease in bulk elevated temperature fast fracture strength and stress rupture performance.

Based on this result, it was decided to utilize the standard slip formulation in further "downstream" process optimization activity, including firing optimization, and RPD rotor deliverable set no. 2.

Forming Development - Work under this sub-tasked focused on: (1) Porous Plastic Mold Material Optimization; (2) Rotor Benchtop Casting Optimization, and (3) Semi-automated Rotor Casting Optimization and Verification.

Porous Plastic Mold Material Optimization - Screening trials were performed to optimize porous plastic mold materials for pressure casting NT164 rotors. A bladeless rotor hub mold was design and fabricated for use at high casting pressures (greater than 500 psi) on the Dorst pressure casting machine. This mold allowed for a variety of porous plastic mold materials to be evaluated in a standard test on the Dorst machine.

A similar trend was observed in NT230 Si-SiC Dorst machine casting trials. Sticking of the part in the mold increased with reduction in mold material pore size. Several mold coatings were identified that eliminated this effect. Based on these results, the porous plastic mold material formulation and processing conditions were fixed for both NT164 and NT230.

Rotor Benchtop Casting Optimization - An industrialized mold for casting RPD rotors at intermediate pressures (80-200 psi) was designed and fabricated. This mold was used in casting the prototype RPD rotors for Deliverable Set No. 1.

Semi-automated Rotor Casting Optimization and Verification - A mold for casting RPD rotors on NAC's Dorst machined was designed. This mold design incorporated concepts from the industrialized RPD rotor mold evaluated in benchtop casting trials. Fabrication of this mold was canceled due to Allison's direction to NAC to not continue manufacturing development on the RPD-size rotor.

Firing Development - The objective of this activity was to simplify and standardize NT164 furnacing conditions. This work included an evaluation of combining the crystallization and oxidation process steps. Material from NAC's standard NT164 slip formulation and casting process was utilized in these evaluations. A screening experiment was performed to determine if the crystallization step could be eliminated or combined with the oxidation process step. It was determined that mechanical properties were at optimum levels when the crystallization and oxidation process steps are performed separately. Additional work was performed to optimize the as-processed surface strength of NT164 through a combination of presinter, HIP, and post-HiP furnacing treatments. Various encapsulant glass compositions and HIP time-temperature cycles were investigated. None of the experimental treatments resulted in improved as-processed surface strength compared to standard NT164 processing conditions.

Machining Development - Work under this sub-task focused on evaluation and optimization of abrasive flow machining (AFM) of NT164 as-processed surfaces. An initial screening experiment was completed to demonstrate the AFM material removal technique. Material removal of up to 0.005" per surface was achieved resulting in a typical surface finish of less than 16 microinches. An L9 designed experiment was performed to optimize the AFM process conditions. Abrasive media type, media pressure, pre-treatment cycle time, and number of AFM cycles were evaluated at three levels each. Results of this L9 experiment revealed that as-processed surface strength was not improved for any of the AFM treatments. Despite removal of up to 0.005" per surface for select AFM treatments, KOH-etched fracture surfaces of as-processed surface test bars revealed "wormhole" appearing defects that were greater than 0.005" deep. Plans to conduct further AFM trials on rotors

were dropped in order to focus on elimination of these strength-limiting surface defects.

Quality Assurance and Inspection - Key process parameters were identified for SPC control for the NT164 RPD rotor prototype fabrication process. Control chart for these parameters were maintained and reviewed with Allison personnel on a periodic basis.

Task 2 - Prototype Production - Work performed under this task was limited to fabrication of RPD rotors using the current NT164 prototype process under the first sub-task - RPD Rotor Deliverables Set No. 1. RPD rotors were pressure cast using an industrialized mold design, and were processed through dense casting inspection. Of a total of eight RPD rotors inspected, two passed NAC's engine quality rotor acceptance criteria. Surface defects and other discrepancies were traced back to the casting process. Mold and casting process modifications to minimize or eliminate the defects were identified and demonstrated. It was decided to utilize the discrepant RPD rotor castings to complete development of the finish machining process. A process to finish machine RPD rotors was developed based on the previous AGT-5 rotor grinding technology. Upon demonstration of the RPD rotor finish grinding process, Allison directed NAC to put this activity on hold, including the balance of all planned RPD rotor prototyping activity.

Project Management - During the year, NAC held periodic review meetings with Allison at both NAC's and Allison's facilities. In addition, NAC prepared and delivered bi-monthly progress reports. A summary of NAC's work on the gasifier rotor development program was presented at the Annual Contractor's Coordination Meeting in Dearborn MI, in November of 1993.

## AGT-5 AND RPD SCROLL MANUFACTURING DEVELOPMENT

NAC's participation with Allison on prototype fabrication and manufacturing process development of scrolls produced from NT230 siliconized silicon-carbide is summarized within this section of the report. Building on technology developed under the prior year's ATTAP, NAC continued efforts to develop an automated pressure slip-casting process for NT230 scrolls. In 1992, automated pressure slip casting of scrolls was successfully demonstrated using porous plastic molds on NAC's Dorst pressure casting machine. Developments in mold fabrication technology, slip formulation, and casting procedure were identified which led to this result. In addition to work in automated pressure slip casting development, NAC produced and delivered in 1992 five engine quality scrolls using a benchtop casting process utilizing plaster molds.

Based on the successful completion of the 1992 effort, a follow-on effort was funded by Allison for NAC to continue the development of a cost-effective manufacturing process for NT230 gasifier scrolls. The following work tasks comprised this follow-on effort: (1) Phase I - RPD Scroll Prototype Fabrication; (2) Phase II - RPD Scroll Production Process Development; (3) Phase III - Production Process Proof Demonstration, and (4) Project Management and Reporting.

Phase I - RPD Scroll Prototype Fabrication.

Fabrication and Delivery of Tensile Specimens - In order to establish a tensile strength data

base for NT230 scrolls, NAC fabricated a batch of 34 tensile rods for delivery to Allison. Final inspection of these tensile rods revealed silicon-filled veins in the buttons and shanks in approximately 10-15 of the finished rods. These defects were determined to originate from thermal gradients present in thick cross sections (≥ 0.5") during the silicon metal freezing reaction. To check for adequacy of testing specimens with these defects, a total of 8 representative tensile rods with silicon-filled veins in at least one button and/or shank was tested at room temperature by the Norton Analytical Group. The tensile testing results are summarized in Table I. A weibull plot of this tensile data compared to co-processed material flexural data is shown in Figure 3. None of the specimens failed from silicon-filled veins.

AGT-5 Task 3.2 Design Scroll Machining - The purpose of this sub-task was to machine four additional Task 3.2 design AGT-5 scrolls. A total of four siliconized scroll castings from NAC's 1992 effort were processed through dense casting inspection and qualified for machining. One casting was inadvertently chipped in the first machining operation and was pulled from the machining process. A second scroll was fully machined, and was found to have out of specification slot widths (.001",.004", .008") due to an improper machining and wheel dressing setup. The balance of two scroll castings were machined, inspected and delivered to Allison (Reference letter-reports dated 8/25/93 and 9/20/93 respectively).

Table I - NT230 Si-SiC Flexural Strength vs. Tensile Strength Comparison

| NT230 Si-SiC Material Description | Room Temperature Flexural vs Tensile Strength Comparison | | | | |
|---|---|---|---|---|---|
| | Flexural MIL-STD 1942 Size B | | Tensile ORNL Cylindrical Buttonhead | | Flexural-Tensile Difference (%) |
| | Characteristic Strength (MPa) | Weibull Modulus | Characteristic Strength (MPa) | Weibull Modulus | |
| Standard AGT5 Scroll Process (Slip Batch No. 395, Siliconization Date 8/4/93) | 365 | 6.7 (n=20) | 248 | 5.1 (n=8) | - 32 % |

A batch of eight (8) Task 3.2 design scrolls was cast to make up the balance of two deliverable scrolls. A total of four of the eight scrolls were siliconized and processed through dense casting inspection. Two of these castings passed NAC's dense casting acceptance criteria, and were processed through machining. Cracks were detected in these two finished scrolls at final inspection. The type, location, and size of the crack in each of the two components was nearly identical. The cause of these cracks has been traced to one of two machining operations where part holding and/or grinding pressure are operator-dependant parameters. Siliconization and machining of the balance of two AGT-5 scrolls was pushed back to NAC's 1994 scroll manufacturing development effort.

Phase II - RPD Scroll Production Process Development.

Materials Development - This objective of this internally funded sub-task was to qualify a reaction-sintered $MoSi_2$-SiC composite, designated NTX-002-008, for the scroll manufacturing development effort. Initial $MoSi_2$-SiC infiltration screening trials were performed, in which full infiltration of thick cross sections was achieved. Flexural strength of this material was determined to be equivalent to NT230 at room temperature, but not as high as NT230 at 1370°C. Polished sections of NTX-002-008 confirmed complete infiltration of $MoSi_2$, but revealed grain growth and the presence of an unknown phase. Based on the initial screening trials, no further work was performed on $MoSi_2$-SiC materials development.

Slip Engineering - A linked experiment coupling the optimization of the NT230 slip formulation with simplification of downstream firing operations was completed. A summary of the linked optimization experiment design is as follows:

Slip Matrix:

| Trial No. | Grain Purity | Percent Addition Ultra-Fine SiC Powder | Green Body Toughening Additive Type | Green Body Toughening Additive Amount |
|---|---|---|---|---|
| 1 | 1 | 1 | 1 | 3 |
| 2 | 2 | 3 | 3 | 3 |
| 3 | 2 | 3 | 1 | 1 |
| 4 | 2 | 2 | 3 | 1 |
| 5 | 2 | 2 | 2 | 3 |
| 6 | 1 | 2 | 2 | 1 |
| 7 | 1 | 2 | 1 | 2 |
| 8 | 2 | 1 | 2 | 2 |

Firing Matrix:

- Carbon Impregnation (On vs. Off).
- Prefire (On vs. Off).

RPD scrolls, test tile, and tensile rods were cast using each of the L8 matrix slip formulations. The components cast from each experimental slip were equally divided up into four subgroups of material and processed through each of four firing matrix treatments. The acid treatment employed in the standard NT230 process was not used in any of the experimental treatments. Test components were made from the standard NT230 slip formulation and were processed through the firing matrix treatments for comparison. A modified siliconization cycle (alternate time-temperature schedule) was kept constant for all treatments in the experiment.

Response variables included: Slip viscosity; pH; specific gravity; Cast body shape retention; Wet green strength; Mold release; Cast body surface quality; Green density; Cast body trace

metal impurity concentrations; Siliconized density; Siliconized material trace metal impurity concentrations; and Mechanical properties.

Results and conclusions of the experiment are summarized as follows: (1) All treatments utilizing more than 10 weight percent of fine particle size SiC resulted in a lower green density and siliconized density; (2) The standard NT230 slip formulation processed using the modified one-step siliconization cycle achieved a siliconized density equivalent to the standard two-step NT230 process.

Mechanical properties of select treatments from this experiment are summarized as follows:

| NT230 Si-SiC Material Description | Flexural Strength (Bulk-Ground Surface) | | | |
|---|---|---|---|---|
| | Room Temperature | | 1370°C | |
| | Average (MPa) | Weibull Modulus | Average (MPa) | Weibull Modulus |
| AGT5 Scroll Benchtop Casting Process (All Batches Combined) | 359 ± 41 | 9.3 (n = 126) | 427 ± 48 | 12.1 (n = 59) |
| Slip Formulation: Standard NT230 Firing : Prefire/Carbon Impregnation | 424 ± 48 | - (n = 6) | 476 ± 106 | - (n = 5) |
| Slip Formulation: Treatment No. 1 Firing: No Prefire/No Carbon Impregnation | 377 ± 67 | - (n = 6) | 437 ± 27 | - (n = 5) |
| Slip Formulation: Treatment No. 1 Firing: No Prefire/Carbon Impregnation | 410 ± 70 | - (n = 6) | 478 ± 30 | - (n = 5) |
| Slip Formulation: Treatment No. 8 Firing: No Prefire/No Carbon Impregnation | 331 ± 45 | - (n = 6) | 438 ± 43 | - (n = 5) |
| Slip Formulation: Treatment No. 8 Firing: Prefire/No Carbon Impregnation | 356 ± 24 | - (n = 9) | 519 ± 52 | - (n = 5) |

Based on a review of all of the response variables, the optimal slip formulation/firing process parameters were determined.

Follow-up confirmation trials were performed in 1994 to confirm casting of scrolls and to verify mechanical properties.

Automated Pressure Slip Casting Development

Benchtop Pressure Slip Casting Trials - The following is a summary of benchtop scroll

casting trials:

- Demonstrated AGT-5 to RPD-size "Scale Down" of NAC's NT230 scroll casting process. The standard NT230 slip formulation (ie, without a reinforcement additive) produced crack-free components upon demolding and drying.
- Completed a preliminary demonstration of NT154 RPD scrolls through HIP densification.
- NT154 and NT164 AGT-5 Task 3.2 design scrolls were successfully cast. Acceptable quality inside drain surface and wall thickness uniformity was achieved, however, the mold insert that forms the inner vane caused sticking and minor "tearing" of the shroud OD. AGT-5 NT164 scrolls were HIP'ed to demonstrate the densification process.

Porous Plastic Mold Design, Fabrication, and Optimization

Porous Plastic Mold Material Optimization - An alternative mold material was evaluated and compared to the Dorst/Laufen material. This activity was dropped due to inability to fabricate the alternative mold material in to complex-shape molds. A modified formulation of the Dorst/Laufen material was developed to reduce pore size and water volumetric flow rate. A water volumetric flow rate 20-40X lower than the standard Dorst/Laufen mold material was achieved. This mold material produced the highest scroll demolding yield and best shape retention results to date. Lower casting rates were observed for this mold material in tensile rod casting trials on the Dorst machine over a range of casting pressures.

RPD Scroll Mold Design, Fabrication and Optimization - The first of two planned porous plastic RPD-scroll molds was fabricated in June of 1993. This porous plastic RPD scroll mold was installed on NAC's Dorst casting machine, and initial casting trials were performed. RPD scrolls were successfully cast in the range of 350 to 400 psi with a casting time of approximately 60 seconds.

The RPD scroll castings exhibited good mold release and shape retention, but a had a relatively poor inside drain surface due to pooling of slip and clumping around the reinforcement material.

A second porous plastic RPD scroll mold was fabricated using the modified fine pore porous plastic formulation. This mold incorporated a sub-assembly to allow for mold rotation to eliminate pooling of slip during the drain cycle. A tensile rod blank mold of the same alternate formulation porous plastic mold material was fabricated as well. Initial casting trials were completed in the November-December 1993.

Firing Development - An evaluation of experimental conditions linking the optimization of single step firing with slip formulation is summarized under the slip engineering sub-task.

Project Management - During the year, NAC held periodic review meetings with Allison at both NAC's and Allison's facilities. In addition, NAC prepared and delivered bi-monthly progress reports. NAC presented a summary of the NT230 scroll manufacturing development program at the Annual Contractor's Coordination Meeting in Dearborn MI, in November of 1993.

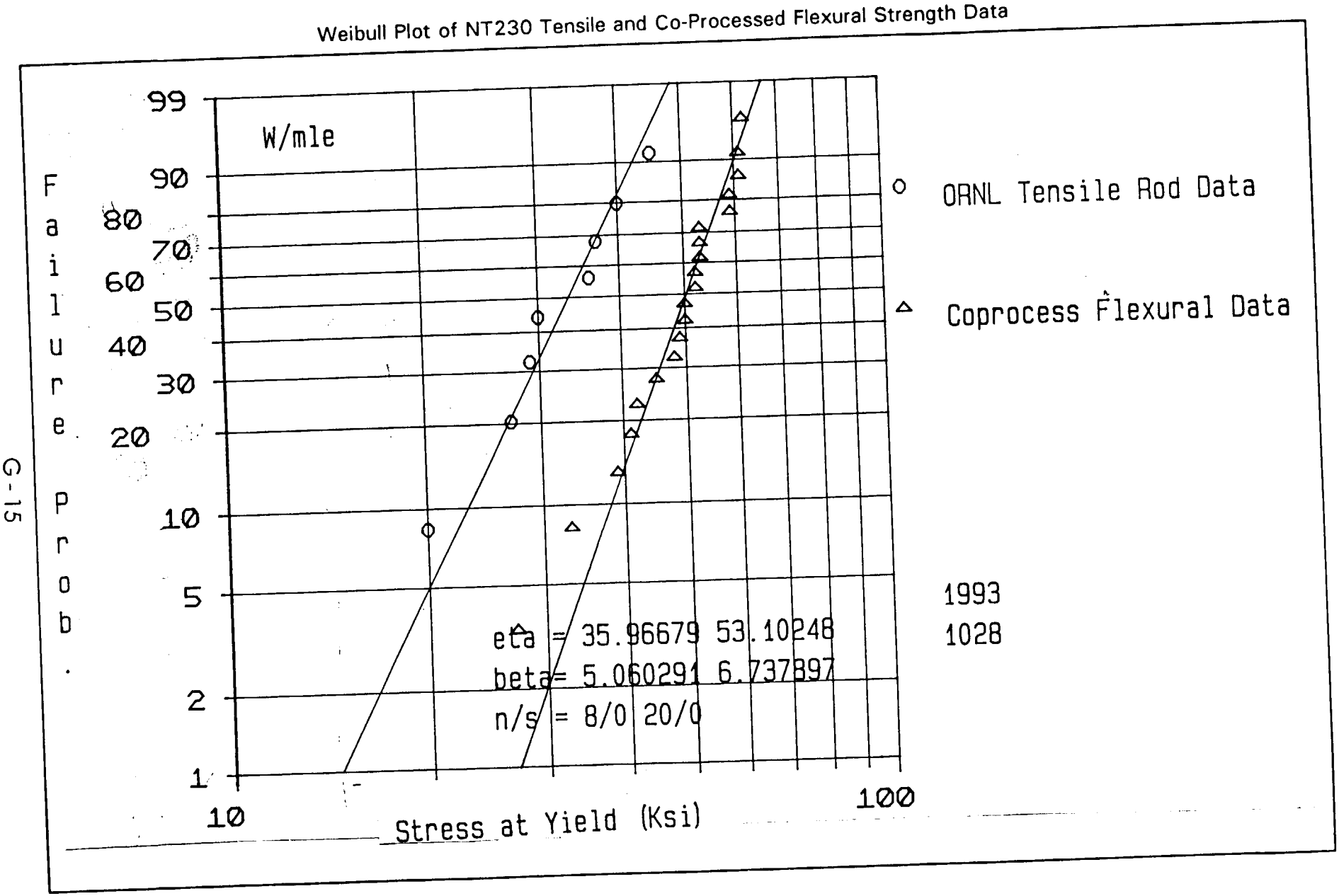
Weibull Plot of NT230 Tensile and Co-Processed Flexural Strength Data
W/mle
Failure Prob.
99
90
80
70
60
50
40
30
20
10
5
2
1
10
100
Stress at Yield (Ksi)
ORNL Tensile Rod Data
Coprocess Flexural Data
1993
1028
eta = 35.96679 53.10248
beta= 5.060291 6.737897
n/s = 8/0 20/0

# APPENDIX H

Norton Advanced Ceramics
1994

NOTE: INFORMATION SUBMITTED THAT IS DEEMED TO BE
PROPRIETARY IN NATURE
HAS BEEN DELETED.

# ADVANCED TURBINE TECHNOLOGY APPLICATIONS PROJECT
# COMPONENT DEVELOPMENT PROGRAM

for

# COMBINED ROTOR AND SCROLL MANUFACTURING DEVELOPMENT

Annual Technical Progress Report
for the period
January 1, 1994 through December 31, 1994
under
Allison Gas Turbine Division Purchase Order No. H416208 and H416209

Prepared For:
ALLISON COMPANY
Indianapolis, Indiana 46206

Submitted by:
Vimal Pujari
Northboro Research and Development Center
Saint-Gobain/Norton Industrial Ceramics Corporation
Goddard Road
Northboro, MA 01532-1545

## 1.0 INTRODUCTION

This report summarizes technical progress made during the reporting period on the Advanced Turbine Technology Applications Project. As a subcontractor to Allison Company, Norton Advanced Ceramics (NAC) is responsible for process development of the Scroll, and Rotors.

### 1.1 Objective

The objective of this program is to develop and demonstrate manufacturing processes for ceramic turbine engine components. Manufacturing will be demonstrated by producing engine-quality scrolls and rotors and delivering them to Allison for experimental use in the AGT-5 gas turbine engine.

### 1.2 Scope

This effort encompasses processing, fabrication, and characterization of AGT-5 silicon nitride rotor and scrolls, and delivery of selected quantities of these components to Allison for experimental use in the AGT-5 gas turbine engine.

This is a combined rotor and scroll manufacturing development report.

Effort was focused mainly towards the development of a robust NT164 processing and forming methodology which is applicable to both the rotor and scroll components. In this ATTAP follow-on program, all components are needed to be fabricated from high strength silicon nitride. However, under Task 1, fabrication and finish machining of two NT230 scrolls (leftover from Phase I program) is described.

## 3.0 TECHNICAL PROGRESS SUMMARY

The rotor and scroll fabrication efforts have been divided into following four sub-tasks respectively:

Rotor
i. Rotor Prototype Fabrication
ii. Hybrid Fabrication Development
iii. NT164 Cost Effective Process Development and
iv. Project Management and Reporting

Scroll
i. Scroll Prototype Fabrication
ii. Scroll Production Process Development
iii. Hybrid Component Fabrication Development
Project Management and Reporting

## 3.1 Rotor and Scroll Prototype Fabrication

### 3.1.1(a) AGT-5 Rotor Fabrication

Under task 3.3 (NT164 Engine Quality Rotor Production) effort of Phase I, program, 19 rotors were cast. Out of these, eight NT164 rotors were kept on hold for future engine tests and evaluation. These rotors were fabricated using SOP established for NT164 processing. After casting, these rotors were processed through presinter stage. Two out of these eight rotors have now been HIP'ed and currently undergoing post HIP inspection and evaluation. Density measurement on these rotors suggest full densification. Additional three rotors will also be HIP'ed using the same heating cycle. Subsequent to HIP, the rotors will be crystallized, finish machined and oxidized prior to delivery to Allison Company.

### 3.1.1 (b) AGT-5 Scroll Fabrication

Four AGT-5, NT230 scrolls fabricated following the established SOP were kept on hold from Phase I of the ATTAP program. These scrolls are now being finish machined as a part of deliverables due in April 1995.

### 3.1.2 AGT-5 Size/GEN 1 Design Prototype Fabrication

Activities within this task was planned to focus on the development of an improved casting method and tooling/mold design above and beyond the established fixed NT164 process employed during Phase I of this program. More specifically the process improvements included:

- Establishment of NT164 composition range. Screening experiments were also performed to evaluate alternative approaches to oxygen control and compare the results with the base line process.

- Implementation of a contamination free closed loop powder processing methodology developed in a separate DOE funded program titled "Processing for Reliability". The closed loop processed NT164 silicon nitride slip will be utilized for all prototype casting trials of both the rotor and the scroll.

3.1.3 Pattern Design and Fabrication

Lithographic plastic patterns of the rotor and scroll were received from Allison Company (around the middle of November) as a preliminary part drawing to help establish the casting procedures and the resultant shrink factor to be applied to the hard tooling pattern. Multi-segmented porous plaster based molds were fabricated for both the rotor and the scroll prototype casting trials. A limited casting trials, so far, have been performed. Both the rotor and the scroll molds were fabricated based on design procedures established during Phase I of the ATTAP program.

Both molds have rough casting surfaces due to the rough finish on the plastic patterns. Considerable difficulty, therefore, was encountered during the demolding operation due to sticking. Corrective actions were taken to minimize the sticking problem by providing a coating on the surface of the patterns.

### 3.2 Robust Forming Development.

#### 3.2.1 Pressure Casting development

The significant challenge in the current pressure casting process for fabricating complex shape turbine components is the elimination of cracking during de-molding and during drying. Possible causes for this cracking phenomenon is as follows:

a) De-molding stress,
b) Low wet green strength and
c) Drying stress.

In this effort these three factors were examined in detail, with a goal to first understand and subsequently define suitable corrective solutions as described below.

**3.2.1.1 De-molding stress.** Stresses arise when de-molding complex shaped components that have thin curved elements (as in fins or blades) or when parts stick in the mold. This is especially true in the case of rotors and vanes. Forming a component with a rotor mold requires placement of impervious rubber inserts between the blades during casting. Removal of the inserts after casting has to be carried out with precision as there is little clearance between blades.

Mechanical de-molding. This operation would therefore seem suited to mechanization, where the angles and displacements during removal of the inserts can be carefully calculated. These can then be coded into a mechanical procedure and repeated for every piece. Replacing manual de-molding by mechanical de-molding should increase yields, if the primary cause for rejects is high/uneven stress caused by manual de-molding. The automated casting process will incorporate mechanical removal of inserts from the rotor mold if the current forming method is maintained.

Sticking. Wetting of impervious (non filtration) surfaces of the molds by the slurry/component and subsequently the suction caused during the de-molding operation causes parts of the component to stick in the molds. Mold release agents are needed to prevent wetting of the mold surfaces and therefore to reduce the force required to demold a component. A method was developed to examine surface tension reducers. For mold release agents, a drop of slurry is placed on a metallic surface that has previously been treated with the release agent. The angle of contact between the drop of slurry and the flat surface is measured using an optical comparator at approximately 60x magnification (Figure 1.). The agents that result in the largest contact angle are noted as possible candidates. A number of mold release agents have been screened using this method with 2

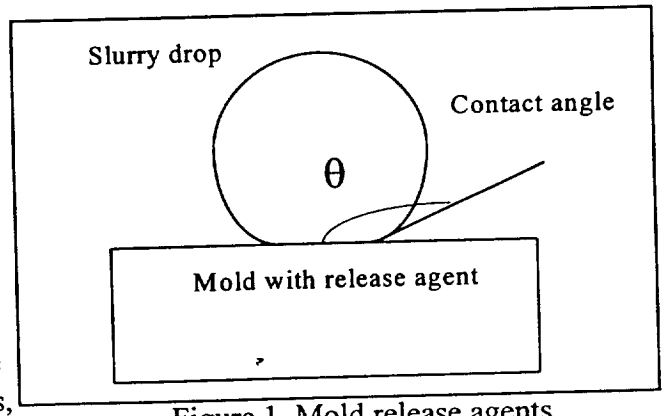

Figure 1. Mold release agents

different slurry systems and the results presented in Table 1. The "best" system D4 was independently confirmed using an actual cast component. This release agent is presently being used for cast components.

**Table 1. Contact angles between surface and droplet.**

| De-molding agent | NT154 | N02 | DI Water |
|---|---|---|---|
| D1 | 35 | 24 | 24.5 |
| D2 | 167.5 | 176 | |
| D3 | 52 | 42 | |
| D4 | 174 | 175 | |
| D5 | 90 | 84 | |
| D6 | 90 | 90 | |
| D7 | 96 | 79 | |
| D8 | 21 | 15 | |
| No Coating | 73 | 57.5 | |

### 3.2.1.2 Wet green strength.

A component which has been pressure cast and is being demolded is slightly plastic. This is because it is supersaturated - having a moisture content greater than its pore volume when its particles are in contact. During drying the component goes from a supersaturated state, through a saturated state - when it loses its plasticity as particle contact increases, to a dry state - when pores are depleted of moisture, - with accompanying shrinkage[1]. Shrinkage results in an increase in strength due to increased particle-to-particle contact in the green body[2]. An experiment was conducted to examine the relationship between the control variables casting pressure and drying and the performance variables strength and ductility of the green body. Half inch by three inch cylindrical specimen were cast and bi-axially flexure tested. This test provides a relative strength measurement calculated from the formula :

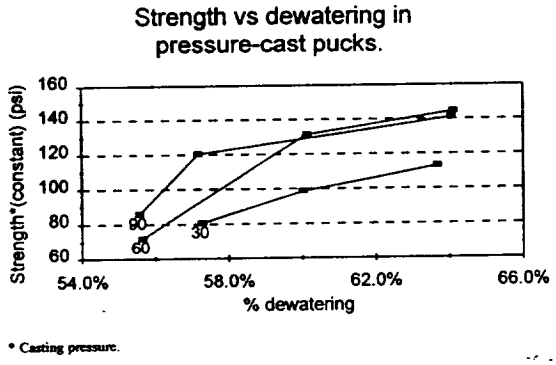


Figure 2. Strength vs dewatering

$$\text{Strength} = K * (\text{load at failure}) / (\text{thickness of puck})^2, \quad \text{(for some constant K)}.$$

As expected, strength of the component increased with increased dewatering and ductility (measured by the strain to failure) decreased. The strength of the components doubled over approximately 10% loss in moisture level (Figure 2.)

A method of decreasing the effect of the de-molding stress is by increasing the wet green strength by binder additions. Ten of the most promising binder systems have been evaluated for

as cast green strength using biaxial flexure tests in Figure 3.

In general none of the 10 binders that were evaluated gave much improvement in wet green strength over pucks made without binders. The pucks made from slips without binders had bi-axial flexure strengths of ~ 60 psi at similar moisture levels. Addition of these binders did not improve the wet green properties and may in fact have reduced them.

(Note: All the binders gave substantially higher strengths after drying)

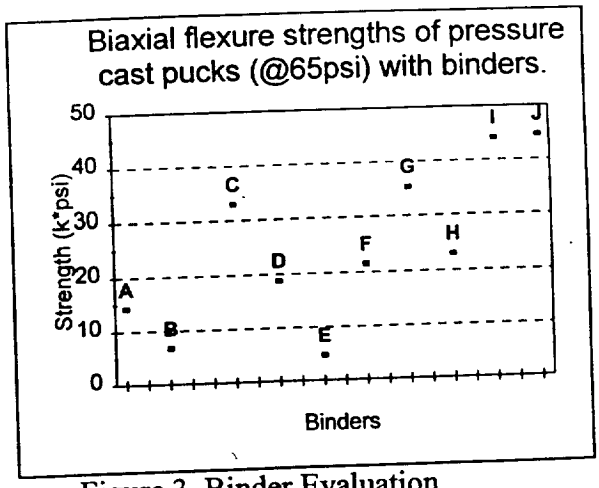

Figure 3. Binder Evaluation

### 3.2.1.3 Drying stress.

Stresses during drying are related to the loss of liquid from within the pores of the component. To prevent exposure of the solid body during drying (which would lead to a higher solid/vapor interfacial energy), liquid spreads from the volume of the body to maintain a lower energy liquid/vapor interface[3]. As the liquid volume is reduced, the meniscus must become curved to stay in contact with the solid skeletal network (Figure 4.). The tension in the liquid (opposite in sign to tension in the solid) is given by;

$P = -2\gamma_{LV} / r$ where, $\gamma_{LV}$ = liquid/vapor interfacial energy
and $r$ = radius of curvature of the meniscus.

The maximum pressure occurs when the radius of the meniscus fits within the pore i.e. when the radius of the meniscus is at a minimum.

For a cylindrical pore of radius $a$,

$r = a / \cos(\theta)$ where, $\theta$ is the contact angle.

For the whole body which has a surface to volume ratio of the pore space given by $S_p/V_p$, the tension can be written as;

$$P = \gamma_{LV} \cos(\theta).S_p/V_p$$

The surface to volume ratio of the body is related to the specific surface area $S$ by;

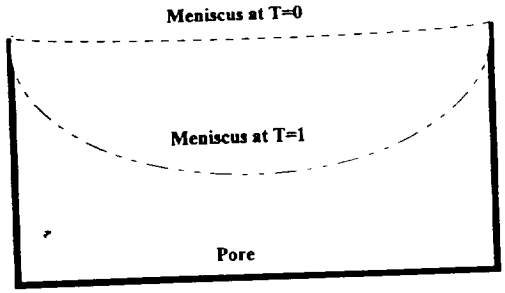

Figure 4. Receding meniscus.

$$S_p/V_p = S\,\rho_s\,\rho\,/\,(1-\rho)$$ where $\rho$ is the relative density and $\rho_s$ is the skeletal density.

This implies that the stress in the body caused by capillary pressure is;

$$P = \gamma_{LV}\cos(\theta)\,.\,S\,\rho_s\,\rho\,/\,(1-\rho)$$

This capillary pressure in the pores results in shrinkage of the pores, and therefore in shrinkage of the body (if not relieved by cracking) Shrinkage during drying increases inter-particle contact of the green body which increases green strength. This is desirable as long as the drying stresses are uniform and less than the wet green strength at that stage. Non-uniform drying or non-uniform pore sizes may lead to cracking in larger pores that have been depleted of liquid by neighboring smaller pores (whose walls then shrink away from the larger pore).

Drying related cracking of the green component may be reduced by i) ensuring a uniform pore size distribution prior to drying, ii) reducing overall shrinkage by having a high green density, and iii) increasing the wet green strength.

**Pore size Distributions**

Standard slurries. In the casting process, particle packing and the interstitial pores are a function of the particle size distribution, and the packing rate (casting rate). For components cast from as-milled slurries, the pores are *not* of a uniform size but follow a *uni-modal* distribution Figure (5.a). This usually results in cracking as the larger pores are depleted and the smaller pores then shrink away from the larger pores. For components made with standard slurries non-uniformly distributed pore sizes is unavoidable

Agglomerated slurries. A component cast from an agglomerated slurry results in a bi-modal pore size distribution with a finer intra-agglomerate pore , and a larger inter agglomerate pore (figure 5b). The size and strength (degree of cohesion) of the intra-agglomerate pore is dictated by the agglomeration/calcining conditions prior to introduction into a slurry. These agglomerates undergo very quick drying (95% weight percent of the moisture is removed in approximately 2-3

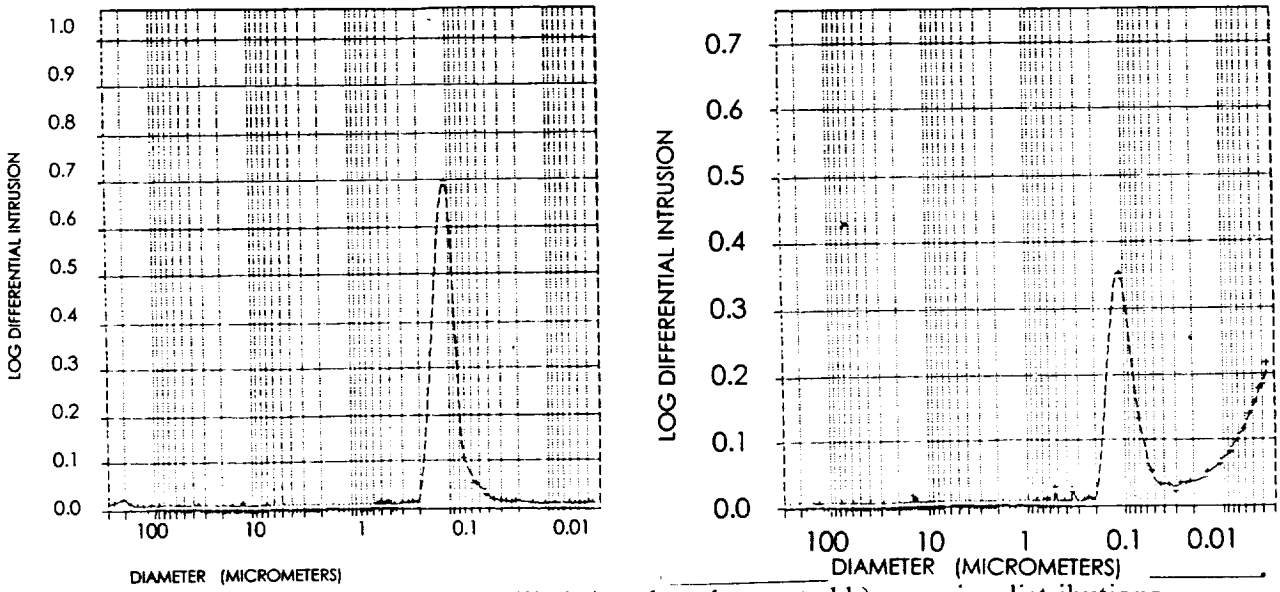


Figure 5. Comparison of as-milled a) and agglomerated b) pore size distributions.

H -

seconds), and are not compressible after the calcining process retaining their features through casting. The inter-agglomerate pore size is very similar to the pore size in the standard slurry, and is dictated by the agglomerate size distribution and casting kinetics (slower casting results in better packing of the agglomerate). The liquid meniscus recedes from the larger pores to the smaller as drying proceeds.

If the shrinkage that results as liquid is drawn from the large to the smaller pore is too great the component cracks. However spherical agglomerates (Figure 6.) are less restricted by neighboring agglomerates than a high aspect ratio agglomerates or particles would be . It is surmised that if the part does not crack during the initial drying period when the meniscus recedes into the agglomerate, the result is a crack-free component. In general casting a component from an agglomerated slurry will lessen the cracking during drying and result in higher green densities. In addition these components have more uniform cake densities relative to the distance from the filtration surface. It is interesting to note that the inter-agglomerate pore in the component made from the agglomerated powder is of the same magnitude as the inter-particle pore of the component made with the "as-milled" slip while the intra-agglomerate pore is an order of magnitude finer. This explains the higher densities achieved by the agglomerated system.

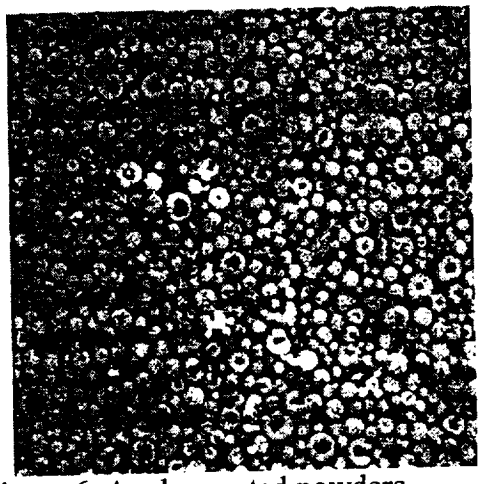

Figure 6. Agglomerated powders.

### 3.2.2 Gel-Suspension/Casting Development.

The casting of gel suspensions may be achieved in two ways:

1. Pressure-assisted drained gel casting in which the slurry is cast on a porous surface, the solids loading is increased by filtration to approximately 61% by volume and the remaining 39% liquid/monomer mix retained in the body is then gelled.
2. Undrained gel casting in which the ceramic/liquid/monomer mix is introduced into an impervious mold and the liquid/monomer mix (usually at approximately 52% by volume) is then gelled,

The benefit of the second approach is that the logistics can be kept fairly simple (no pressure equipment) and depending on the number of molds available, many components can be formed in a short period and then processed for gelling. The drawback of this approach is that the green density of the component subsequent to removal of the gel is low , which results in a low green strength. The benefit of using the drained gel casting approach is that higher green densities can be achieved having good green strengths after removal of the gel. The drawback of this approach is that pressure casting of large cross-section components requires substantial casting time (typically a 1" cross-section requires >1 hr at 100 psi), control of the moisture content at the component surface is not repeatable and the process is prone to all the other drawbacks of the non-gel pressure casting process. (Note: Ensuring no loss of moisture from the surface is important to achieve gelling and smooth surfaces.)

**Summary:**

**Short term goals**
Complex shape components will continue to be manufactured using the pressure casting approach even though the yields to date have been lower than desirable. Some of the drawbacks of this approach will be addressed by increasing the solids loading of the slurries from 76% to approximately 80%. In addition reproducible methods of manufacturing and calcining the agglomerates are under investigation.

**Long term goals**:
Future work will be geared toward further developing the gel system in the following direction;

1. Mold material development will examine materials which enhance the gelling process.
2. Non-contaminating agglomeration/calcining techniques from above will be incorporated.
3. De-airing procedures for high solids and high viscosity slurries are being investigated.
4. .Automated mold filling, gelling. de-molding.
5. Controlled drying procedures.

---

[1] R.C.Chiu and M.J.Cima. "Drying of Granular Ceramic Films: II" June 1993.
[2] K. Kendall, N. McN Alford and J.D. Birchall. "The Strength of Green Bodies."
[3] G.W.Scherer. "Theory of drying". Journal of the American Ceramic Society, Volume:73, Issue:01. Pg 3-14.

# APPENDIX I

Acronym List

## GLOSSARY/ABBREVIATIONS/ACRONYMS LIST

| | |
|---|---|
| °C | degrees Celcius |
| °F | degrees Fahrenheit |
| μSiC | μ-phase silicon carbide |
| AES | Advanced Engineering Staff |
| AGT | automotive gas turbine/Advanced Gas Turbine |
| APU | auxiliary power unit |
| AS800 | ASCC silicon nitride |
| ASCC | AlliedSignal Ceramic Components |
| ATTAP | Advanced Turbine Technology Applications Project |
| BU | build up |
| CAD | computer aided design |
| CFDC | Combined Federal Driving Cycle |
| CO | carbon monoxide |
| CPS | Ceramics Process Systems |
| CTAHE | Ceramic Technology for Advanced Heat Engines |
| DoE | Department of Energy |
| FOD | foreign object damage |
| g/cc | grams per cubic centimeter |
| GM | General Motors Corporation |
| hp | horsepower |
| HTML | High Temperature Materials Laboratory |
| HVTE-TS | Hybrid Vehicle Turbine Engine - Technology Support |
| Hybrid | Hybrid Vehicle Propulsion System Program |
| I.D. | inside diameter |
| KICC | Kyocera Industrial Ceramics Corporation |
| Kpa | kiloPascals |
| ksi | kilopounds per square inch |
| LAS | lithium-aluminosilicate |
| $lb/in^2$ | pounds per square inch |
| lb/sec | pounds per seconds |
| LeRC | NASA Lewis Research Center (LeRC) |
| m | Weibull modulus |
| MAS | magnesium-aluminosilicate |
| MIL-STD | military standard |
| Mpa | megaPascals |
| mpg | miles per gallon |
| N1 | gasifier speed |
| NAC | Norton Advanced Ceramics |
| NASA | National Aeronautics and Space Administration |
| Nb | number of blades |
| NDE | nondestructive evaluation |
| No. | number |
| $Nox$ | oxides of nitrogen |

| | |
|---|---|
| NT154 | Norton silicon nitride |
| NT164 | Norton silicon nitride |
| NT230 | Norton siliconized silicon carbide |
| NZP | zirconium phosphate |
| O.D. | outside diameter |
| ORNL | Oak Ridge National Laboratory |
| P/N | part number |
| POS | probability of survival |
| psi | pounds per square inch |
| psid | pounds per square inch delta (pressure differential) |
| RIT | rotor inlet temperature |
| RPD | reference powertrain design |
| rpm | revolutions per minute |
| S/N | serial number |
| SEM | scanning electron microscopic |
| $Si_3N_4$. | silicon nitride |
| Sialon | CPS silicon nitride |
| SiC | silicon carbide |
| SN252 | Kyocera silicon nitride |
| SRS201 | CPS sialon |
| T4 | turbine inlet temperature |
| temp | temperature |
| TIT | turbine inlet temperature |
| UHC | unburned hydrocarbons |
| ULEV | ultra low emissions vehicle |
| VPI | Virginia Polytechnic Institute |
| WBS | work breakdown structure |

# REPORT DOCUMENTATION PAGE

Form Approved
OMB No. 0704-0188



| 1. AGENCY USE ONLY (*Leave blank*) | 2. REPORT DATE | 3. REPORT TYPE AND DATES COVERED |
|---|---|---|
| | March 1996 | Final Contractor Report |

**4. TITLE AND SUBTITLE**

Advanced Turbine Technology (ATTAP) Applications Project
1993 - 1994 Annual Report

**5. FUNDING NUMBERS**

WU-778-32-21
DEN 3-336

**6. AUTHORS**

Allison Engine Company

**7. PERFORMING ORGANIZATION NAME(S) AND ADDRESS(ES)**

Allison Engine Company
P.O. Box 420
Indianapolis, Indiana 46206-0420

**8. PERFORMING ORGANIZATION REPORT NUMBER**

E-10160
EDR 17625

**9. SPONSORING/MONITORING AGENCY NAME(S) AND ADDRESS(ES)**

National Aeronautics and Space Administration
Lewis Research Center
Cleveland, Ohio 44135-3191

**10. SPONSORING/MONITORING AGENCY REPORT NUMBER**

NASA CR-198466
DOE/NASA 0336-6

**11. SUPPLEMENTARY NOTES**

Prepared under Interagency Agreement DE-AI01-90CE50300. Project Manager, Paul T. Kerwin, Propulsion Systems Division, NASA Lewis Research Center, organization code 2701, (216) 433-3409

**12a. DISTRIBUTION/AVAILABILITY STATEMENT**

Unclassified - Unlimited
Subject Category - 02, 07, 27

**12b. DISTRIBUTION CODE**

**13. ABSTRACT (*Maximum 200 words*)**

The Advanced Turbine Technologies Application Project (ATTAP) is in the seventh year of a multi-year development program to bring the automotive gas turbine to a state at which industry can make commercialization decisions. Commercialization decisions in industry have led to the program redirecting focus to support the development of technologies for turbogenerators used in hybrid propulsion systems, thus ATTAP has become the Hybrid Vehicle Turbine Engine Technology Support (HVTE-TS) program. Test-bed engine design and development continued with the analysis and design of poppet valve premixing combustors and the associated controls system. Ceramic and associated ceramic/metal component design activities included the continuing effort for designing a gasifier turbine rotor. Material characterization efforts continued and have yielded additional information on two new material systems. Ceramic component process development and fabrication continued with several subcontractors. Component rig activities focused upon the transfer of assets and capabilities from the General Motors Tech Center to facilities at Allison. Total test time during the 1993-1994 time period was 603 hours, of which 241 hours were engine testing and 362 were hot rig testing.

| 14. SUBJECT TERMS | 15. NUMBER OF PAGES |
|---|---|
| small gas turbine; ceramic components; automotive APU; emissions | 177 |
| | 16. PRICE CODE: A09 |

| 17. SECURITY CLASSIFICATION OF REPORT | 18. SECURITY CLASSIFICATION OF THIS PAGE | 19. SECURITY CLASSIFICATION OF ABSTRACT | 20. LIMITATION OF ABSTRACT |
|---|---|---|---|
| Unclassified | Unclassified | Unclassified | |